THE EXTRACTION OF AUDITORY AND SOMATOSENSORY EVOKED POTENTIALS FOR USE IN DEPTH OF ANAESTHESIA MONITORING

Brent Vivian Potgieter

Submitted to the Faculty of Medicine at the University of Cape Town in partial fulfilment of the requirements for the degree of Master of Science in Medicine in the field of Biomedical Engineering.

Cape Town, 1995

DECLARATION

I, ***BRENT VIVIAN POTGIETER***, hereby declare that the work on which this thesis is based is my original work (except where acknowledgements indicate otherwise) and that neither the whole work nor any part of it has been, is being, or is to be submitted for another degree in this or any other University.

I empower the University to reproduce for the purpose of research either the whole or portion of the contents in any manner whatsoever.

Signed

Signature

.....

Date

ABSTRACT

The importance of adequate monitoring during surgical anaesthesia has increased with the need for safety and reliability. In particular, adequate depth of anaesthesia (DOA) is needed to prevent patient awareness during surgery. The use of modern anaesthetic agents and neuromuscular blockers may result in the occurrence of awareness during surgery. Assessment of anaesthetic depth has traditionally relied on the observation of physical signs. These are however subjective indicators. The monitoring of evoked potential (EP) signals has been proposed as a means of obtaining an objective measure of DOA. Various changes in the characteristics of EP signals take place during the administration of anaesthesia reflecting changes in corresponding neural pathways. These changes have been shown to correlate with DOA.

EP signals are of low amplitude and require special signal processing techniques to separate them from the "background" electroencephalogram (EEG) and other electrical noise and interference. The EP signals are usually time-varying during the administration of anaesthesia and conventional synchronous time averaging (AVE) techniques are often inadequate. Various adaptive algorithms including the adaptive impulse correlated filter (AICF) and the Fourier series model (FSM) have been proposed for the extraction of time-varying EP's.

A study which compared the performance of the AICF, FSM and AVE algorithms in extracting EP's was conducted. The software for a PC-based evoked potential extraction system (EPES) was designed and implemented. This system allows for the extraction of auditory evoked potential (AEP) and somatosensory evoked potential (SSEP) signals using the AICF, FSM and AVE algorithms within a user-friendly environment. The EPES provides a user-friendly interface which is menu-driven and supports a mouse as a pointing device. Data was collected from a commercial evoked potential monitoring system and recorded onto magnetic tape. The EPES was used to extract EP signals from this data off-line.

A simulation study which investigated the performance of the AICF, FSM and AVE algorithms was also executed. Data obtained with the EPES was used in the simulation study. The stimulation study was performed by testing the algorithms using different types of interference combined with both stationary and non-stationary AEP and SSEP signals. The interference signals were of four types, viz. "background" EEG, band-limited random noise, 50-Hz interference and a combination of the latter two. Each type was divided into three graded levels defined as low, medium and high. Each of the algorithms was tested with the various interfering signals added to the EP signals. Parameters used to measure the performance of the algorithms included the signal to noise ratio (SNR). A total of 336 simulations was performed, each running for 1000 trials. ANOVA statistical analysis was conducted on these parameters.

The EPES performs well and satisfactorily extracted EP and EEG signals off-line for use in the simulation study. The results of the simulation study suggest that the FSM algorithm tends to provide faster initial extraction of the EP signals compared to the AICF algorithm. The FSM algorithm also has a greater ability to adapt to changes and track these changes. However, the FSM algorithm is sensitive to dominant periodic interference signals. The AICF algorithm has typically a bell-shaped SNR response and thus shows a decline after a certain number of trials.

ACKNOWLEDGEMENTS

The help of the following people is acknowledged with gratitude:

Mladen Poluta, Department of Biomedical Engineering, UCT, for his support and guidance as thesis supervisor and mentor.

Professor MFM James and Dr Patrick Musto, Department of Anaesthetics, Groote Schuur Hospital, for their clinical contribution and acting as clinical supervisors.

Jan Topp, Department of Neurology, Groote Schuur Hospital, for his assistance in obtaining data using the Medelec Commercial Evoked Potential Monitoring system.

The staff and fellow students, Department of Biomedical Engineering, UCT, for their contribution and constructive critique.

The staff of the Postgraduate Scholarship Office at UCT, for managing my financial assistance during the execution of this project. Special thanks to Mrs Paula Foley for her interest and helpfulness.

The German Academic Exchange Service (DAAD), Foundation for Research Development (FRD) and SmithKline Beckman donors for their financial assistance during the execution of this project. This support is greatly appreciated.

My parents, family and friends, for their undying support and encouragement.

TABLE OF CONTENTS

		Page
DECLARATION		ii
ABSTRACT		iii
ACKNOWLEDGEMENTS		v
TABLE OF CONTENTS		vi
LIST OF FIGURES		ix
LIST OF TABLES		xii
LIST OF ABBREVIATIONS AND SYMBOLS		xiii
GLOSSARY		xiv
1.	INTRODUCTION	1
2.	DEPTH OF ANAESTHESIA AND CEREBRAL MONITORING	3
2.1	Introduction	3
2.2	Use of the Electroencephalogram in DOA Monitoring	6
2.2.1	Introduction	6
2.2.2	Signal Processing Techniques	8
2.3	Use of Evoked Potentials in DOA Monitoring	15
2.3.1	Introduction	15
2.3.2	Signal Acquisition	17
2.3.3	Signal Extraction Techniques	20
2.3.4	Signal Classification	26
3.	MATERIALS AND METHODS	28
3.1	Introduction	28
3.2	Evoked Potential Extraction System	28
3.2.1	Hardware Considerations	28
3.2.2	Software Design and Implementation	33
3.2.3	Sources of Clinical Data	40

Page

3.3 Simulation Study 41

3.3.1 Algorithms Evaluated 42

3.3.2 Simulation Design 43

3.3.3 Generation of Evoked Potential Signals 46

3.3.4 Generation of Interference Signals 48

3.3.5 Figures of Merit 51

3.3.6 Statistical Analysis 53

4. RESULTS 54

4.1 Typical Results 54

4.1.1 Typical Extracted Time Domain Signals 54

4.1.2 Typical SNR Responses 57

4.2 Results of Study 60

4.2.1 Auditory Evoked Potentials 66

4.2.2 Somatosensory Evoked Potentials 71

5. DISCUSSION 76

5.1 Evoked Potential Extraction System 76

5.2 Simulation Study 78

5.2.1 Relative Performance of Algorithms 78

5.2.2 Use of the FSM and AICF in DOA Monitoring 81

6. CONCLUSIONS AND RECOMMENDATIONS 83

6.1 Conclusions 83

6.2 Recommendations for Future Development 84

REFERENCES 86

		Page
SELECTED BIBLIOGRAPHY		93
APPENDIX A	CLINICAL SIGNS AS INDICATORS OF DOA	A-1
APPENDIX B	DEFINITION AND ORIGIN OF EEG	B-1
APPENDIX C	DEFINITION AND ORIGIN OF EVOKED POTENTIALS	C-1
APPENDIX D	SYNCHRONOUS TIME AVERAGING	D-1
APPENDIX E	ADAPTIVE ALGORITHMS AND THE LMS ALGORITHM	E-1
APPENDIX F	ADAPTIVE IMPULSE CORRELATED FILTER	F-1
APPENDIX G	FOURIER SERIES MODEL	G-1
APPENDIX H	ANALYSIS OF VARIANCE	H-1

LIST OF FIGURES

Figure		Page
2-1	Typical power spectrum	9
2-2	Compressed spectral array	10
2-3	Amplitude histogram	11
3-1	Data acquisition hardware interactions	29
3-2	Schematic of EP extraction using the CEPMS and data recorder	31
3-3	Schematic of EP extraction using the front-end	32
3-4	Flow chart of EP extraction using data recorder configuration	34
3-5	Flow chart of EP extraction using front-end configuration	35
3-6	Photograph of EPES display showing menu and command bars	37
3-7	Photograph of EPES display showing a pull-down menu	37
3-8	Photograph of EPES display showing a dialogue box	38
3-9	Photograph of EPES display showing the graphical plotting screen	39
3-10	Electrode configuration for extracting SSEP's	41
3-11	Electrode configuration for extracting AEP's	41
3-12	Summation of EP and interference signals	44
3-13	Time domain plots of the AEP signals	47
3-14	Time domain plots of the SSEP signals	47
3-15	Time domain plots of typical interference signals	49
3-16	Accumulated power spectral density of the interference signals	50
3-17	Time domain plots of different levels of interference signals	51
4-1	Time domain plots of extracted EP signals vs. increasing trial number	54
4-2	Time domain plots of typical extracted EP signals	55
4-3	Time domain plots of extracted EP signals from different interferences	55
4-4	Time domain plots of extracted EP signals from different levels of random interference	56
4-5	Time domain plots of extracted EP signals from different levels of EEG Interference	56

Figure		Page
4-6	Plots of typical SNR responses for stationary EP's	57
4-7	Plots of typical SNR responses for non-stationary EP's	57
4-8	Plots of AICF SNR responses - different convergence factors	58
4-9	Plots of FSM SNR responses - different convergence factors	59
4-10	ANOVA plot of interactions of interference by algorithm (AEP)	62
4-11	ANOVA plot of interactions of interference by algorithm (SSEP)	63
4-12	ANOVA plot of interactions of level by algorithm (AEP)	64
4-13	ANOVA plot of interactions of level by algorithm (SSEP)	65
4-14	SNR - random interference (AEP)	66
4-15	ΔSNR - random interference (AEP)	66
4-16	SNR - 50-Hz interference (AEP)	67
4-17	ΔSNR - 50-Hz interference (AEP)	68
4-18	SNR - combined interference (AEP)	68
4-19	ΔSNR - combined interference (AEP)	69
4-20	SNR - EEG interference (AEP)	69
4-21	ΔSNR - EEG interference (AEP)	70
4-22	SNR - random interference (SSEP)	71
4-23	ΔSNR - random interference (SSEP)	72
4-24	SNR - 50-Hz interference (SSEP)	72
4-25	ΔSNR - 50-Hz interference (SSEP)	73
4-26	SNR - combined interference (SSEP)	73
4-27	ΔSNR - combined interference (SSEP)	74
4-28	SNR - EEG interference (SSEP)	74
4-29	ΔSNR - EEG interference (SSEP)	75
A-1	The stages of anaesthesia	A-2
B-1	The International 10-20 system	B-1
B-2	Time domain EEG activity of different frequency bands of EEG	B-2
C-1	Illustration of EP recording paradigm	C-2

Figure		Page
C-2	The brain stem pathway of the auditory signal	C-3
C-3	Nomenclature used to name peaks and troughs of the EP waveform	C-5
C-4	Extraction of EP's using repeated stimuli	C-7
E-1	Block diagram of time-varying digital system	E-1
E-2	Elements of the basic adaptive system	E-1
E-3	MSE performance surface for one-coefficient filter	E-3
F-1	Block diagram of the AICF algorithm	F-1
G-1	The Fourier series model	G-1
G-2	Block diagram of the adaptive FSM algorithm	G-2

LIST OF TABLES

Table		Page
3-1	Convergence factors for the AICF algorithm	43
3-2	Convergence factors for the FSM algorithm	43
3-3	Nomenclature for interference amplitude levels	51

LIST OF ABBREVIATIONS AND SYMBOLS

A/D	analogue to digital
A/D-D/A	analogue to digital / digital to analogue
AEP	auditory evoked potential
AICF	adaptive impulse correlated filter
AICF1	adaptive impulse correlated filter (convergence factor = $1x10^{-6}$)
AICF2	adaptive impulse correlated filter (convergence factor = $5x10^{-6}$)
AICF3	adaptive impulse correlated filter (convergence factor = $1x10^{-5}$)
ANOVA	analysis of variance
AVE	synchronous time averaging
CSA	compressed spectral array
CEPMS	commercial evoked potential monitoring system
D/A	digital to analogue
DOA	depth of anaesthesia
DSP	digital signal processor
ECG	electrocardiogram
EEG	electroencephalogram
EMG	electromyogram
EP	evoked potential
EPES	evoked potential extraction system
FFT	fast Fourier transform
FIR	finite impulse response
FSM	Fourier series model
FSM1	Fourier series model (convergence factor = $1x10^{-5}$)
FSM2	Fourier series model (convergence factor = $5x10^{-5}$)
FSM3	Fourier series model (convergence factor = $1x10^{-4}$)
IBM	International Business Machines
LMS	least mean square
MF	matched filter
MMSE	minimum mean square error
MSE	mean square error
PC	personal computer
SNR	signal to noise ratio
ΔSNR	rate of change in signal to noise ratio
SSEP	somatosensory evoked potential
WFM	Walsh function model
au	arbitrary unit (custom-defined unit of voltage)
dB	decibel
∇	gradient
Hz	hertz (cycles per second)
msecs	milliseconds
Ω	ohm (unit of electrical resistance)
μV	microvolt
μ	convergence factor, mu

GLOSSARY

convergence factor	Refers to the parameter μ used by the LMS algorithm to control how an adaptive system adapts to changes in the incoming signal.
kurtosis	A measure of the relative peakedness or flatness of a distribution.
latency	The time interval between the onset of the stimulus and a specific point on the EP waveform, typically a peak or a trough.
notch filter	A filter used to reduce the signal power in a very narrow frequency band.
raw signal	Unprocessed EEG-type signal derived during the recording of EP's
skewness	Refers to the symmetry of a distribution. If the skewness factor is zero then the distribution is symmetrical.
stationary	Refers to signals which do not exhibit changing statistical characteristics with time. Non-stationary refers to the opposite conditions.
trial	Refers to the fixed-length time signal recorded after each stimulus elicited during EP studies. Equivalent to *sweep*.

CHAPTER 1

INTRODUCTION

The importance of adequate monitoring during surgical anaesthesia has increased with the recognised need for safety and reliability. Adequate *Depth Of Anaesthesia* (*DOA*) is needed to prevent patient awareness during surgery. A patient aware of surgical stimulation (e.g. the cutting of tissue with a scalpel) would typically be unable to respond to the pain stimulus because of neuromuscular blockers used during surgery. In addition, the use of modern totally intravenous anaesthetic agents provide for rapid recovery on discontinuing the agent and lack side effects. This compounds the problem because these very qualities of the modern anaesthetic agents may result in the occurrence of awareness during surgery.

Assessment of anaesthetic depth has traditionally relied on the observation of physical signs. These may include the absence/presence of various reflexes and the size of the pupils of the eyes. These are however subjective indicators.

The monitoring of *evoked potential* (EP) signals has been proposed as a means of obtaining an objective measure of DOA. Various changes in the characteristics of EP signals take place during the administration of anaesthesia reflecting changes to corresponding neural pathways. These changes have been shown to correlate with DOA.

EP signals are of low amplitude and require special signal processing techniques to separate them from the "background" *electroencephalogram* (EEG) and other electrical noise and interference. In addition to this, the EP signals are usually time-varying during the administration of anaesthesia and conventional *synchronous time averaging* (AVE) techniques are often inadequate. Various adaptive algorithms including the *adaptive impulse correlated filter* (AICF) and the *Fourier series model* (FSM) have been proposed for the extraction of time-varying EP's.

A study which compared the performance of the AICF, FSM and AVE algorithms in extracting EP's was conducted. The software for a PC-based *evoked potential extraction system* (EPES) was designed and implemented. This system provided a user-friendly and mouse-driven environment and allowed for the extraction of EP's using the above-mentioned algorithms.

A simulation study which investigated the performance of the AICF, FSM and AVE algorithms was also executed. Data obtained with the EPES was used in the simulation study. The simulation study was performed by testing the algorithms using different types of interferences combined with both stationary and non-stationary *auditory evoked potential* (AEP) and *somatosensory evoked potential* (SSEP) signals. Selected *signal to noise ratio* (SNR) parameters were extracted and were used to perform *analysis of variance* (ANOVA).

Chapter 2 presents a review of the literature describing the use of cerebral monitoring (either spontaneous electrical activity or EP's) for use in depth of anaesthesia monitoring. Various signal processing techniques are also described with more detailed discussions presented in the appendices. Chapter 3 begins by describing the implementation of the EPES. This is followed by a description of the simulation study and its execution. Results from the simulation study are presented in Chapter 4. A description of results produced by the ANOVA analysis is also briefly presented. The PC-based EPES and the results of the simulation study are discussed in Chapter 5. The simulation study results are discussed separately for both the AEP and SSEP signals in relation to each type of interference. A discussion of the AICF and FSM algorithms for use in DOA monitoring is also presented. Finally, Chapter 6 provides conclusions and recommendations.

CHAPTER 2

DOA AND CEREBRAL MONITORING

2.1 Introduction

A heightened awareness of the effects of anaesthesia on various systems of the human body has resulted in an increased focus on the importance of monitoring the anaesthetised patient. The general purpose of monitoring patients is to obtain information that will:

1. enable the anaesthetist to ascertain whether physiological homeostasis is present under anaesthesia;
2. alert the anaesthetist to undesirable changes in the patient status so that therapeutic intervention may be initiated;
3. adequately assess the efficacy (or lack thereof) of therapeutic intervention

(Blitt, 1985).

Within this context, monitoring of anaesthetic depth is essentially used to:

1. prevent patients' perception of pain, awareness, and recall;
2. judge autonomic status and prevent unfavourable effects of excessively light or deep anaesthesia;
3. minimise stress and its manifestations; and
4. facilitate prompt emergence when indicated.

The need for establishing a sufficient DOA is particularly evident when one reviews cases of awareness and recall under apparent anaesthesia *(Grantham and Hameroff, 1985).*

The introduction of balanced anaesthetic techniques involving the use of neuromuscular blocking drugs such as beta-blockers, anticholinergic and hypotensives has made the assessment of the DOA more difficult, because respiratory patterns and

spontaneous movement are no longer available as signs of inadequate DOA (see Appendix A). Assessment of the DOA was being carried out by monitoring autonomic responses to surgery, but this was not wholly satisfactory as demonstrated by the incidence of awareness during surgery *(Sebel et al., 1985; Grantham and Hameroff, 1985)*. The problem is also compounded by the use of modern intravenous anaesthetic agents. The use of these agents is appealing because they show a lack of side effects and rapid recovery on discontinuing the drug. It is because of these very appealing qualities that unrecognised awareness may occur *(Jones, 1988)*.

It is perhaps more useful to define DOA in terms of desirable depth for surgery. In 1957, Philip Woodbridge *(cited by Grantham and Hameroff, 1985)* recognised the problems inherent in contemporary use of diverse anaesthetic agents and developed a system which conceptually has good application to the modern anaesthetic situation. According to Woodbridge, satisfactory "general anaesthesia" comprises the following four components:

- sensory block, or blocking of afferent impulses;
- motor block, or blocking of efferent impulses;
- blocking of reflexes (respiratory, circulatory, gastrointestinal); and
- mental block, or production of sleep.

Woodbridge coined the word "nothria" to describe depression of these four components, and he related signs of DOA to each component. The selection of anaesthetic agents determines to what degree motor, sensory, reflex, and mental functions are each depressed. The anaesthetic can be tailored to the condition and needs of the patient, the type of surgery, and the requirements of the surgeon.

Heneghan et al. *(1987)* states that the characteristics of an ideal index of DOA should include the following:

- the index must be graded, so that the approach of awareness can be detected at its onset;
- it should be applicable to all anaesthetic agents, and to mixtures of agents; and
- it should be unaffected by non-anaesthetic drugs such as neuromuscular blocking drugs.

Sebel et. al *(1985)* also state that the indicator should be easily quantified, readily interpreted, and be unaffected by routine operating theatre interference such as electrocautery.

The concept of DOA has not been associated with an explicit definition. This is mainly due to the fact that a complete understanding of its mechanism is still lacking. In turn, this is partly due to the unavailability of a quantitative method for assessment of the cerebral effects of anaesthesia *(Bankman and Gath, 1987)*. This brings us to the use of cerebral monitoring in DOA assessment.

Spontaneous electrical activity from the brain was first noted in animals by Richard Caton in 1875 *([Caton, 1875] cited by Donegan, 1985)*. Not long after, spontaneous cortical activity in animals was also recorded by Adolf Beck who published his findings in 1890. However, the pioneer work in human electroencephalography was performed by Hans Berger in the 1920s and 1930s. He was the first to successfully record the EEG from scalp electrodes in humans in 1929. Berger's work was at first received with scepticism, and it was not until some time after his initial publications that his findings were confirmed by Adrian and Matthews in 1934 *([Adrian and Matthews, 1934] cited by Donegan, 1985)*.

Various relationships between brain electrical activity and DOA have been identified by numerous workers. Thornton et al. *(1988)* presented the following definition in which they attempt to conceptually link DOA and neural electrical activity: "DOA implies a state of the central nervous system resulting from a balance between the depression caused by anaesthetic drugs and arousal caused by surgical or other stimuli."

In this chapter, each of the EEG and EP's are discussed in succession. For each of these, their relationship with DOA and the associated signal processing techniques are discussed. More detailed descriptions of the EEG and EP's can be found in Appendices B and C respectively.

2.2 Use of the EEG in DOA Monitoring

2.2.1 Introduction

As early as 1934, Adrian and Matthews *([Adrian and Matthews, 1934] cited by Donegan, 1985)* noted that one of the characteristics of the electrical activity from the cortex was that lower frequency components became more prominent with increasing DOA and that sensory stimulation during light anaesthesia attenuated the lower frequency components and accentuated the higher frequency components. Berger also showed that changes in the EEG pattern could be demonstrated in patients anaesthetised with chloroform *([Gloor, 1969] cited by Payne and Ingram, 1979)*. It has since become generally accepted that the amplitude and frequency of scalp EEG signals vary consistently with changes in anaesthesia. Typically there is an increase in the amplitude in the lower frequency components and a decrease in the amplitude of the higher frequency components of the spontaneous EEG with an increase in the administration of an anaesthetic agent. At deep levels of anaesthesia there is total suppression of the EEG signal *(Payne and Ingram , 1979)*.

A particular spectral parameter, the spectral edge frequency (SEF) has been tried as an indicator of DOA. In a power versus frequency histograph the SEF is the frequency which has 95% of the area of the power histograph below it. It can also be regarded as the highest frequency component of the EEG visible in the particular spectrum. However, the variable effects of different drugs on the SEF, and the lag on recovery that it displays, suggest that it may be a poor indicator of DOA *(Donegan, 1985; Jones, 1988)*.

Another frequency related indicator is that of the median frequency and as the name suggests is the middle frequency component in the power spectrum of the EEG. Some evidence has suggested that the median frequency derived from the EEG power spectrum might be a preferable index of DOA because it shows dose-related changes with changing DOA induced by a number of commonly used general anaesthetic agents. However, it has been suggested that the median frequency method may not be a completely satisfactory

approach because it reduces all the complex information contained in the EEG to one number - the median frequency *(Jones, 1988)*.

A particular problem experienced with the EEG in anaesthesia is the "burst suppressions" which are experienced. These burst suppressions can be described as repeated short periods of activity followed by periods of suppression. They are characteristic of deeper planes of anaesthesia with many anaesthetic agents. They can cause confusion in that they might be interpreted as a lightening of the DOA *(Payne and Ingram, 1979)*.

Silbert et al. *(1989)* evaluated the use of the Lifescan™ to monitor the EEG of a patient during carotid artery surgery. The system used aperiodic analysis (see later) and responded well to increasing DOA by volatile agents.

The use of processed EEG as a guide for the DOA has been controversial because early analysis techniques did not allow for adequate clinical analysis and interpretation *(Payne and Ingram, 1979)*. Rampel and Laster *(1992)* also indicate that a meaningful use for monitoring DOA has proven elusive. Although changes in the EEG with changing anaesthetic dose or concentration have been noted for 60-odd years, it has been difficult to demonstrate a reliable, quantitative correlation between the EEG and other physiological measures of DOA. In their work, Rampel and Laster tried to correlate several quantitative EEG measurements in rats, including average amplitude, spectral edge frequency, and burst suppression ratio, with the movement response onset of supramaximal noxious stimulation. They found no difference in any parameter between rats that responded and those that did not respond to stimuli at a given concentration of isoflurane.

The EEG has been broadly investigated but has generally been found unsatisfactory because changes are agent specific, difficult to interpret, and show wide inter-patient variations. Methods such as the cerebral function monitor, compressed spectral arrays, power spectral edge and aperiodic analysis (discussed in the next section) have

received interest but that they suffer from the shortcomings as described above *(Sebel et al., 1985)*.

2.2.2 Signal Processing Techniques

The visual analysis of the EEG recordings on paper has traditionally been the most common EEG analysis technique used. This has disadvantages and various methods of continuous automatic analysis have been developed typically providing a simple video display of the most relevant EEG features with time-domain and/or frequency information *(Glaria and Murray, 1983)*. In general, the EEG has a characteristic waveform with variations in amplitude, frequency, phase, and other parameters. Any single analysis procedure (e.g. Fourier analysis) cannot simultaneously provide information regarding all these variables. Consequently, the selection of any one analytic technique will emphasise changes in one or more selected parameters at the expense of the others. This observation is extremely important if one is to properly interpret the results obtained by any analytical technique *(Bronzino, 1984)*.

This section describes a number of the more popular techniques used to analyse the EEG signal.

Power Spectra:

Spectral analysis involves the transformation of the EEG signal from the time domain to the frequency domain. Power spectral analysis, i.e. based on measurements of the frequency spectra, provides a quantitative measure of the frequency distribution of the EEG. With the introduction of the fast Fourier transform (FFT), rapid computation of the power spectrum of the EEG became commonplace.

Power spectral analysis not only provides a summary of the EEG in convenient graphic form (see Figure 2-1), but also facilitates statistical analysis of effects on the EEG of different anaesthetic agents which may not be evident on simple visual inspection of the records. It provides a method of reducing selected EEG segments to a convenient

quantitative summary so that two spectra can be compared by measuring differences in power over any set of frequency bands. However, information such as the amplitude distribution and information about specific patterns of the EEG are lost *(Bronzino, 1984; Donegan, 1985; Cohen, 1986).*

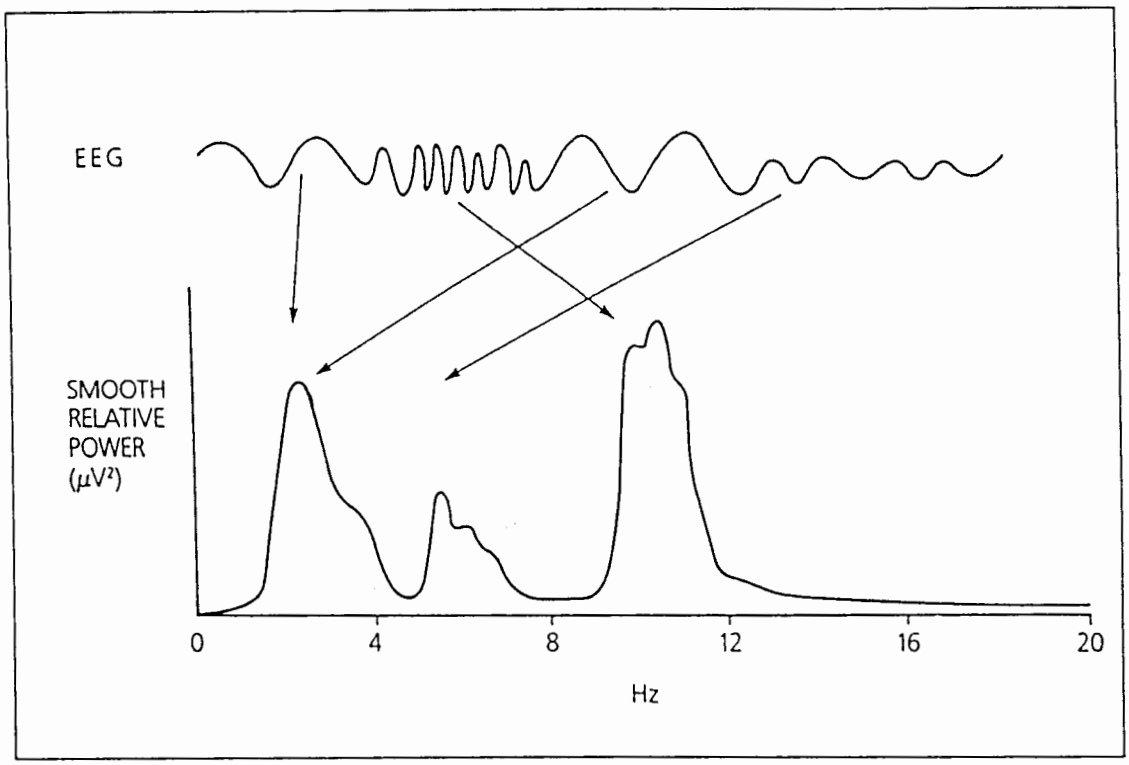

Figure 2-1: Typical power spectrum. (Adapted from *Jones, 1988*).

Parameters such as the spectral edge frequency and median frequency discussed earlier in this chapter are derived from the power spectrum of the EEG.

Compressed Spectral Arrays:

The compression of EEG data by isometric power spectral plots was introduced by Bickford et al. *([Bickford et al., 1971] cited by Donegan, 1985)* and are called compressed spectral arrays (CSA's). Power spectra of the EEG data are typically computed at fixed intervals. This is accomplished by digitising the data and then performing Fourier analysis to separate the EEG signal into its frequency components. The Fourier analysis is usually implemented in the form of the FFT *(Donegan, 1985).* This is an effective method of displaying EEG data where frequency shifts and amplitude changes in the power spectrum can easily be seen. In this way conventional

EEG traces covering hundreds of feet of paper can be summarised on a single sheet. The EEG is analysed in epochs of 2-20 seconds, and each spectrum appears behind the previous analysis to give a three dimensional effect *(Jones, 1988)*.

An example of such a CSA plot is shown in

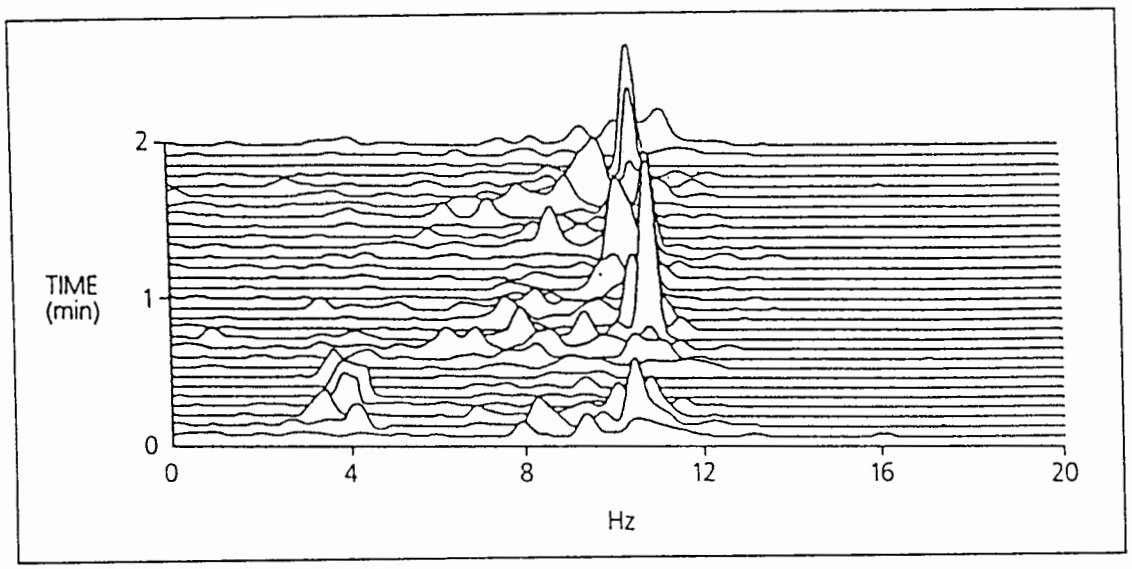

Figure 2-2: Compressed spectral array. (Adapted from *Jones, 1988*).

Figure 2-2. The CSA has been particularly useful for computing and representing EEG spectra over long periods of time *(Bronzino, 1984)*. It is also one of the most frequently-used methods of displaying the spectral properties of the EEG *(Donegan, 1985)*.

Aperiodic Analysis:

Aperiodic analysis could be regarded as an extension of CSA's. The aperiodic analysis method maps each waveform in relation to its frequency, amplitude and time of occurrence and then presents the signal subdivided into frequency and amplitude components *(Jones, 1988)*. The low frequency (0.5 - 8 Hz) and higher frequency (8 - 30 Hz) components are detected differently. The low frequencies require the presence of zero level crossings between highest peaks and lowest valleys of the raw EEG signal. The higher frequencies require only consecutive peaks and valleys. The algorithm thus avoids the use of averaging as used in Fourier analysis. The amplitude

scale is a direct representation of the raw EEG in contrast to the average power spectrum as used in Fourier analysis *(Silbert et al., 1989)*.

Amplitude Histograms:

In addition to the frequency content of the EEG, there has been interest in the computation of amplitude distributions of the EEG. In order to employ this technique,

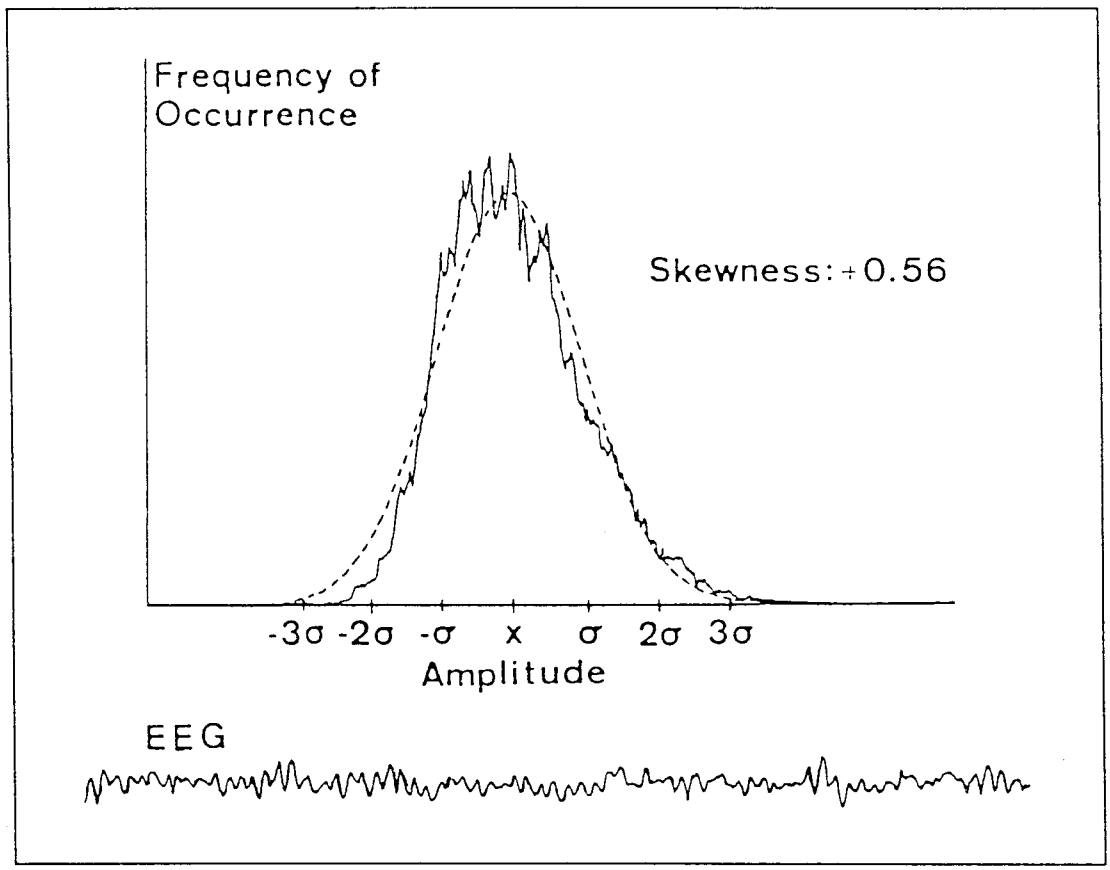

Figure 2-3: Amplitude histogram. (Reproduced from *Dumermuth, 1973*).

successive EEG amplitudes must be measured and ordered into specific amplitude classes or "bins". The amplitude histogram (as illustrated in Figure 2-3) that results from this process is often an asymmetrical, essentially Gaussian distribution.

The primary characteristics of the Gaussian distribution are summarised by simply specifying its mean and standard deviation, since the higher central moments of the distribution, such as skewness and kurtosis are equal to zero. However, in non-Gaussian distributions, the measures of skewness and kurtosis assume nonzero values and can be used to characterise the particular amplitude distribution *(Bronzino, 1984)*.

Cerebral Function Monitor:

One of the first fully functional EEG monitors was the "cerebral function monitor" or CFM *([Maynard et al., 1969] cited by Glaria and Murray, 1983).* The CFM measures the average amplitude of the rectified EEG in a selected frequency band in the range 2 to 15 Hz but contains no specific frequency information *([Maynard et al., 1969; Prior et al., 1971] cited by Payne and Ingram, 1979).* A development of the CFM, the "cerebral function analyser monitor" or CFAM *([Maynard, 1977, 1979] cited by Glaria and Murray, 1983)* provided both frequency and time-domain information: a continuous detailed analysis of amplitude trends and frequency distribution of the weighted EEG signal derived from a single pair of surface electrodes *(Wark et al., 1986).* This technique does not avoid the problem of different patterns of EEG activity with different anaesthetics. Furthermore, this approach does not provide information about localisation of action of these drugs in different parts of the brain *(Jones, 1988).*

Walsh Analysis:

Walsh functions *([Walsh, 1923] cited by Dzwonczyk et al., 1984)* are a set of periodic orthogonal functions which are rectangular in nature and are analogous to the sinusoidal functions which are used in Fourier analysis. The periodicity of Walsh functions is described in terms of sequency or generalised frequency. The definition of sequency coincides with that of frequency when applied to sinusoidal functions, thus the terms can be used interchangeably for either sets of functions.

Dzwonczyk et al. *(1984)* performed a study comparing the Walsh and Fourier analysis of the EEG for tracking the effects of anaesthesia. In this study, the quantitative and dynamic differences between the results of Walsh and Fourier analysis were evaluated statistically. The parameters included lower and upper corner frequencies, algebraic and geometric means, median frequency, actual and normalised bandwidths, and total power. Their results confirmed that Walsh power spectra are more diffuse, less peaked, and generally less detailed than Fourier spectra. There is essentially no difference between the dynamics of the Walsh- and Fourier-derived sets of parameters with the exception that the Walsh-derived parameters were slightly sensitive to changes in the EEG signal in comparison to the Fourier-derived parameters. The results have shown

that there are quantitative differences between corresponding estimates, but that the estimates are dynamically equivalent, both showing essentially the same changes in the background EEG signal with the administration of anaesthesia.

Slope Descriptors:

Normalised slope descriptors *([Hjorth, 1970] cited by Bankman and Gath, 1987)* have also been used to describe EEG signals. Three of the seven normalised slope descriptors are defined as:

activity = s_a^2

mobility = s_d / s_a

complexity = $(s_{dd}/s_d)/(s_d/s_a)$

where s_a is the signal standard deviation, s_d is the standard deviation of the first derivative and s_{dd} is the standard deviation of the signal's second derivative. The normalised slope descriptors are also known as the Hjorth parameters. These are theoretically well-founded and have shown to provide essential information about the EEG *([Hjorth, 1970; 1972] cited by Bankman and Gath, 1987).*

The method described by Bankman and Gath *(1987)* was aimed at monitoring those EEG changes which are correlated with relevant pharmacological and physiological variables during surgical anaesthesia in real-time. They used adaptive segmentation during the extraction of the signal and sequential fuzzy clustering for the classification. The adaptive segmentation process essentially produced quasi-stationary epochs of EEG signals. The power in each of six frequency bands and the three Hjorth parameters were calculated and a vector of 9 features for each window period was created.

The approach which seemed best suited for dealing with classification of the EEG during anaesthesia was clustering in a fuzzy environment *([Bellman and Zadeh, 1970]; [Gath and Bar-on, 1980] cited in Bankman and Gath, 1987)*. The sequential (time dependent) fuzzy clustering system classified the segments in a nine-dimensional space using the descriptive features described earlier. Each analysis window produced one heavy (principal) cluster, representing the main trend in the EEG state, and two to

three small (secondary) clusters , describing short-term fluctuations in the EEG state. The Hjorth parameters conveyed relevant information on the EEG state during anaesthesia. The essential advantages of the system were the adaptive technique and the efficient data reduction. This allowed for on-line, quantitative evaluation of the EEG changes on a relatively slow computer.

Multiparametric Methods:

Thomsen et al. *(1991)* introduced a multiparametric method to monitor the EEG and so provide a simple display and decision support system in the operating theatre. The digitised dual EEG signal was divided into fixed 2-second segments using a rectangular window function. The length of the window had to be much greater than 1/4 of the wavelength of the lowest frequency, and short enough to ensure stationarity within the window. A window length of 1 to 5 seconds was suitable, but 2 seconds was preferred. From each of these segments, ten normalised autocorrelation coefficients together with the root mean square (RMS) amplitudes were extracted. These features were transformed to amplitude or power spectra by autoregressive modelling using the Durbin algorithm (see *Cohen, 1986*). Feature vectors were extracted and unsupervised off-line learning was performed using hierarchical clustering. It was shown that the three different anaesthetic agents used modified the EEG in such a way that specific amplitude/frequency classes were found at the same level of anaesthesia. Another important finding was that the common learning set based on 5 patients could be used for patients outside the learning set. This demonstrated that general anaesthetic tends to decrease the interpatient variability of the EEG. It was also shown that the clustering method of classification is as sensitive to outliers (patient features which deviate significantly from the mean values) as many other parametric statistical methods such as linear regression. This result emphasises that it is essential to remove insignificant outliers when reference material is collected. The performance of single parameter methods (e.g. median frequency or spectral edge frequency) was shown to be poor compared to the multiparametric method implemented by Thomsen et al. *(1991)*.

2.3 Use of Evoked Potentials in DOA Monitoring

2.3.1 Introduction

One of the first demonstrations of the potential application of evoked potentials in monitoring DOA was performed by Uhl and his colleagues in 1980 *([Uhl et al., 1980] cited in Sebel et al., 1985)*. They showed that increasing concentrations of halothane resulted in graded increases in the latency of the first major peak of the cortical visual evoked response. Sebel and various colleagues suggested the use of SSEP's as an indicator of DOA *(Sebel et al., 1984; Sebel et al., 1985)*. A more optimal index may need to be a function of both latency and amplitude of EP's *(Sebel et al., 1985)*. Generally, increasing concentrations of anaesthetics are accompanied by reductions in EP amplitudes and increasing latencies *(Sebel et al., 1986; Heneghan et al., 1987)*.

Heneghan et al. *(1987)* performed studies where the effects of isoflurane were compared with halothane and enflurane and found no differences in the effects of the three agents on the amplitudes of the early cortical (middle latency) waves, although significant differences between the effects of the three were shown for the long latencies. They concluded that the consistent dose-related effect on the amplitude of the middle latency cortical waves implies that the AEP could be used to provide a promising index of DOA.

According to Pfurtscheller et al. *(1987)*, reliability and sensitivity can be improved when different evoked responses are monitored simultaneously. Maresch et al. *([Maresch et al., 1983] cited by Pfurtscheller, 1987)* introduced simultaneous EEG and AEP monitoring in which EEG spectra, SSEP's and AEP's are displayed in a compressed form. The EP stimulations were interweaved: the SSEP was generated every 200 ms and the AEP every 100 ms. The EEG samples were taken every 10 milliseconds. This technique was applied successfully more than 30 times intra-operatively. An important aspect of this type of intra-operative monitoring is to obtain the signals as quickly as possible and optimised digital filtering has to be applied to

improve the SNR of the EP's. Applications of such a technique could include the investigation of the influence of systemic changes, drug levels, and DOA.

Sebel et al. *(1988b)* indicated that the problem with EEG monitoring of anaesthetic depth is that each anaesthetic agent produces a different EEG pattern. Single derivatives, therefore, have limitations in assessing anaesthetic depth. On the other hand, the effects of all anaesthetic agents on cortical EP's appeared to be similar.

Thornton et al. *(1988)* concluded from various studies that the amplitudes of cortical waves in the AEP are sensitive not only to anaesthetic concentration but also to surgical stimulation. It was shown by Sebel et al. *(1988a)* that the stimulus of surgery had an activating effect (increase in amplitude) on the SSEP. Thorton et al. *(1988)* and others *(Heneghan et al., 1987; Magatani et al. 1985)* suggest that the AEP may provide a useful index of DOA.

Liberati et al. *(1991)* investigated the problem of enhancing selective responses from the central nervous system when two (or more) sensorial responses are simultaneously elicited from a patient. In their study they considered a combination of visual and somatosensory stimulation and developed a parametric model of signal and noise interaction for the processing of the evoked responses. They defined the term "bipotential" which refers to the combined EP while the term "unipotential" refers to each response singly elicited. From their observations they hypothesised that the simultaneous presence of the somatosensory stimulus produces not only a transmission spread of electrical activity on the skull over the visual cortex, but also a direct neural interference to the visual cortex itself. They also suggested that the visual cortex shows itself to be more sensitive to somatosensory stimulation than the somatosensory cortex is to the visual stimulation. The occipital cortex is shown to be less specific to just visual stimulation than the central cortex is to the somatosensory stimulation. According to the model, if the two stimuli are not simultaneously present, inhibition of the cortico-cortical interactions occurs: the unipotential actually elicited is present without modification at the output. When the two stimuli are simultaneously present,

the cortico-cortical interaction is enhanced. Further studies of these interactions were to be performed.

In contrast to Liberati et al. *(1991)*, Keirn and Aunon *(1990)* found that an additive model of the simultaneous EP described the actual bimodal response quite well. In order to compare the actual bimodal response to the theoretical additive model, they calculated correlation coefficients between the averaged bimodal response (N=50) and the waveform obtained by simple superposition of the individual averaged evoked responses with appropriate time shifts.

2.3.2 Signal Acquisition

This section gives a brief description of some of the signal acquisition aspects to be considered in the acquisition of EP's. Detailed descriptions and methodologies can be found in references such as Nuwer *(1986)* and Chiappa *(1990)*, which considers the monitoring of EP's in the operating environment specifically.

Electrodes:

For most applications, it is not feasible to measure the evoked response directly in the cerebral cortex, and measurements are made by means of surface bio-potential electrodes attached to the scalp. Because of the intervening skull structure, there is substantial attenuation of the cortical response and typical signal levels are on the order of tens of microvolts. Also, because the electrodes are located an appreciable distance away from the primary response centres, they tend to pick up other brain activity with equal and often greater magnitude than that of the desired EP's *(McGillem and Aunon, 1977)*. Reliable measurements (especially suitable for prolonged testing) are achievable using cup electrodes and collodion. The electrode is held in place on the skin, and collodion is applied around the rim and dried rapidly. Conductive gel is then injected from a syringe into the cup *(Chiappa, 1990)*. Alternatively, use is made of Ag-AgCl (silver - silver chloride) disposable electrodes typically used for *electrocardiogram* (ECG) recordings.

Amplification:

The amplifiers must have a high-input resistance so that connecting electrodes to the amplifier does not affect the recorded signal. Most commonly this resistance is on the order of 10 MΩ. Basically the amplifier maintains a high degree of discrimination between unwanted *common mode* signals, which are *in phase* on both of a pair of electrode leads, and wanted *differential mode* signals which are *out of phase (Donegan, 1985)*.

Amplification in reasonable steps up to a gain factor of 500 000x is usually necessary, subject to reduction if there is preamplification and/or amplification in the signal processing unit. The amount of amplification used in a given situation depends on the amplitude of the signal of interest and the voltage resolution capabilities of the input A/D converter of the signal processing unit *(Chiappa, 1990)*.

Filtering:

Appropriate filtering of the signal prior to digitisation can shorten the signal processing time but incorrect filtering can distort the waveform, resulting in erroneous amplitudes and latencies. Approximate values of 1, 5, 10, 25, 100 and 300 Hz should be available as low cut-off (high pass) and 100, 250, 500, 1000 and 3000 Hz should be available as high cut-off (low pass) filters *(Chiappa, 1990)*.

Mains Interference Artefact:

A common problem experienced in EP monitoring is that of mains frequency (50 Hz or 60 Hz, hereafter referred to as *50-Hz*) interference. A mains frequency notch filter is often useful, but since that frequency is usually included in the range of interest for some EP's, its use is often limited *(Chiappa, 1990)*. The 50-Hz notch filter can also cause an actual increase in the amount of 50-Hz artefact present in some records. This comes about in a somewhat subtle manner as a result of the steep roll-off in notch filters. This phenomena is called "ringing" or paradoxical 50-Hz artefact. When a quick pulse (such as a calibration pulse) is put through a 50-Hz notch filter, the resulting filter signal has a brief oscillation. EP stimuli such as the SSEP stimulus in itself presents an electrical signal that resembles a calibration pulse and this can result in the

same sort of oscillatory ringing. This can be particularly confusing in the operating room where such oscillatory ringing could be confused for real EP's *(Nuwer, 1986).*

The 50-Hz noise can be reduced in several ways. The obvious approach is to reduce the number of nearby devices that are emitting 50-Hz interference. The worst culprits are usually exposed unshielded power cables running to electrical lights and devices. Unnecessary lights and equipment should be left unplugged. Cables can generate 50-Hz artefact even if the power is off. Another approach to reducing the effect of 50-Hz interference is to keep the recording electrode impedances at about 2000Ω and well matched among all electrodes since 50-Hz artefact is greater when recording electrodes have a relative imbalance of impedances (e.g. 800Ω versus 3000Ω). Impedances can be brought down by regelling or reapplying electrodes, or by slightly abrading the underlying skin. However, overly aggressive skin abrasion can result in impedances which are too low, increasing the relative imbalance of impedances and thus aggravating the artefact problem. Other tricks for reducing 50-Hz interference include keeping the recording electrode wires bundled together, braiding the wires with each other, and keeping the wires away from other electrical cords or devices. The shorter the electrode wire, the better. The final way of dealing with 50-Hz noise is to use a notch filter. This should always be the last choice for the reasons discussed earlier. It is generally better to eliminate the source of the 50-Hz artefact rather than to use the notch filter *(Nuwer, 1986).*

Very often harmonics of the mains frequency appear as interference. These harmonics are most common when the stimulation repetition rate is set at a simple ratio of the mains frequency. For example, a stimulus rate of 10 per second will result in considerable artefact, whereas just slightly altering that rate to 10.1 or 9.9 per second can eliminate or average out the artefact *(Nuwer, 1986).*

Artefact Rejection:

Potentials arising from the patient other than those related to the EP signal also occur. The sources of these potentials include eye movements, movement of the head and neck, respiration and the electrical potentials generated by the electrical conduction

system of the heart. Artefacts due to muscle movement and the ECG are not so easily eliminated, but simultaneous recording of the ECG and an *electromyogram* (EMG) of the muscles involved will aid in differentiating these from the electrical activity associated with the EP signal *(Donegan, 1985)*.

Some of these artefacts which have sharp spikes are removed using automatic artefact rejection. Most systems use a voltage threshold value and if any sample in a particular trial (sweep) exceeds this, then the trial is rejected as containing artefact *(Chiappa, 1990)*.

The most modern amplifier systems have all their gain, filter, and input electrode channel selection under computer control and this diminishes operator errors *(Chiappa, 1990)*.

2.3.3 Signal Extraction Techniques

EP recording requires separation of the nervous system's responses from accompanying noise. As mentioned in the previous section, the most commonly encountered noise includes EMG activity, environmental electrical noise, ECG, and EEG. The SNR for conventional EP signals is on the order of 1:1 to 1:100 *(Yu and McGillem, 1983)*. Apart from the potential problems with data acquisition, extraction of the EP has been shown to be difficult because of the poor SNR and can only be accomplished by employing special signal extraction techniques *(McGillem and Aunon, 1977)*. The latter pare of Appendix C describes the basic principle of EP extraction using repeated stimuli.

Traditional methods of EP signal extraction are discussed first in this section. This is followed by a discussion of the techniques which have been suggested for extracting the EP signal during the administration of anaesthesia in the surgical environment.

2.3.3.1 Traditional Synchronous Time Averaging

The most widely used method for estimating the EP is that of "synchronised time averaging" (AVE) also known as "ensemble averaging."

AVE is a well known signal processing technique which has been used for extracting EP's since the 1960's. The basic assumptions of conventional AVE are that the signal is time locked to the stimulus and is the same for each stimulus repetition (see Appendix C), and that the on-going EEG activity or noise is additive and uncorrelated with either the signal or the noise from another stimulus cycle. Under these assumptions, the summation of N single evoked responses due to N repetitions of a stimulus will cause the signal power to increase by a factor of N^2, while the noise power will increase by a factor of N. Thus, the average evoked response will have a power SNR directly proportional to N (see Appendix D for derivation) *(Aunon and Sencaj, 1978; Furst and Blau, 1991; Davila and Mobin, 1992).*

In classical AVE the improvement of the SNR increases indefinitely as the number of averages increases *([Rompelman , 1986] cited by Laguna et al., 1992)*. Implicit in the use of signal averaging is the assumption that the response of the nervous system is stable over the measurement interval and that the noise is stationary, uncorrelated to the stimulus, and has zero mean. *(Pfurtscheller and Cooper, 1975; Sgro et al., 1990).* The ensemble average gives a good estimate of the EP when the EP morphology and latency variations over the ensemble of responses are small *(Al-Nashi, 1986).*

Davila and Mobin *(1992)* introduce a method of weighted averages of EP's. Each single EP trial is weighted prior to averaging. The use of these weights is shown to maximise the SNR of the resulting estimate. A number of simplifying assumptions about the signal and noise correlation matrices are made which result in an efficient method of approximating the maximum SNR weights. Davila and Mobin produced experimental results using actual AEP data which demonstrated that the resulting weighted average had estimated SNR's that are up to 21% greater than the conventional AVE SNR.

However, the AVE method as a whole has a number of drawbacks. One serious shortcoming is the large number of trials required to obtain a suitable EP estimate. For example, brainstem AEP's measurements often require several thousand sweeps. This measurement can thus take up to several minutes resulting in unwanted artefacts being included in the average *([Aminoff, 1980 ; Woodworth et al., 1983] cited by Davila and Mobin, 1992).* In general, 500 to several thousand trials must be averaged in order to obtain a satisfactory EP signal or recording *(Sgro et al., 1990).* Serious errors in the EP estimation may also result when the variations in the EP signal, especially latency, are significant *([Brazier, 1964] cited by Al-Nashi, 1986).*

Pfurtscheller and Cooper *(1975)* proposed a system whereby selected trials which seemed to be artefact-free were used for the extraction of the EP signal using the AVE technique. They indicated that the distortion in the EP signal that can be introduced by not using selected trials for averaging can be considerable.

If some of the above assumptions of stability of the evoked response and stationarity of the noise are not valid, the conventional average will not be an optimum representation of the signal. In particular, if the signal characteristics change as a function of the stimulus application, the conventional average will be a distorted representation of the signal or it may even totally disappear *([Brazier, 1964; Ciganek, 1969] cited in Aunon and Sencaj, 1978).*

In addition, certain types of noise are poorly removed by AVE. For example, AVE has little effect on noise correlated with the stimulus (e.g. stimulus artefact, or a continuing response to a previous stimulus). Similarly, periodic noise (e.g., 50 or 60 Hz power line interference) is difficult, if not impossible, to remove using constant frequency stimulation *(Sgro and Emerson, 1985; Strackee and Peper, 1992).* Although individual transients are attenuated in proportion to the number of trials, high amplitude transients can require many trials to achieve the desired SNR. For example, a single 50 μV transient, such as that resulting from movement by a subject, would require

averaging 500 transient trials to achieve a SNR of 10:1 with a 1 μV EP signal *(Sgro et al., 1990)*.

2.3.3.2 Alternative Signal Extraction Techniques

Techniques other than AVE are discussed in this section. These techniques have been proposed for more rapid extraction of the EP signal as well as for tracking changes in the EP signal, as would be required in the surgical environment.

Autoregressive Model:

Cerutti and co-workers have proposed a parametric method of identification of EP's on a single trial basis using an ARX (AutoRegressive with eXogenous input) algorithm *(Cerutti et al. 1988)*. The basic estimation of the information contained in the single trial is taken from an average carried out on a sufficient number of trials, while the noise sources, EEG and electrical ocular activity (EOG signal), are characterised as exogenous inputs in the model. However, a model of the statistical behaviour of these signals is required in order to implement an optimal stochastic filter to perform the extraction of the useful signal from the composite signal. They show that their simulation and experimental results confirm the capability of the model of drastically improving the SNR in each single trial and satisfactorily identifying the contributions of signal and noise in the overall recording.

Adaptive Walsh Estimation:

The adaptive Walsh Function Model (WFM) considers the time-varying EP signal as a linear combination of Walsh functions. An adaptive algorithm is used to estimate the coefficients or weights of the individual Walsh functions. Walsh functions *([Walsh, 1923] cited by Dzwonczyk et al., 1984)* were described earlier in this chapter. Adaptive Walsh estimation *(Guo and Thakor, 1990)* using the WFM was found to be comparable to the adaptive FSM discussed below. Guo and Thakor showed that the WFM performs satisfactorily in detecting and tracking time-varying EP signals in high levels of noise.

Adaptive Fourier Series Model:

Thakor et al. *(1991)* presented a new approach for the analysis of time-varying EP's, called adaptive Fourier series modelling. This system is based upon the Fourier linear combiner proposed by Vaz and Thakor *(1989)*. Here the dynamic changes in the magnitudes of the Fourier coefficients are analysed for diagnostic purposes. This technique is evaluated in this study.

The EP signal is seen as a coherent waveform and is modelled by a dynamic Fourier series. The signal itself recurs with each stimulus. Therefore advantage can be taken of both recurrence and spectral properties. The Fourier coefficients are adapted using the *Least Mean Square* (LMS) algorithm (see Appendix E) to minimise the *mean square error* (MSE) between successive trials and the model therefore adapts to time-varying changes in the EP signal. This technique of adaptive FSM does not require *a priori* knowledge of the spectral or statistical properties of signal or noise. It is discussed in detail in Appendix G.

Earlier approaches of adaptive filtering techniques *(Thakor, 1987)* required that a low noise AVE-estimated EP signal be available as a reference to the LMS algorithm. Another problem experienced with the LMS algorithm in these earlier approaches was that disparate eigenvalues of the autocorrelation matrix of the reference signal resulted in a slow and non-uniform convergence.

The adaptive FSM technique overcomes principal limitations of earlier approaches: (a) a low noise reference signal is not required; and (b) since the eigenvalues of the Fourier coefficients are identical, the convergence of all the coefficients is uniform and rapid *(Thakor et al., 1991)*.

Thakor et al. *(1993)* performed an experimental study comparing the Fourier and Walsh models. The results show how the selection of model order and the adaptation rate of the estimator affect the SNR. The FSM results in a somewhat higher steady-state SNR than does the WFM; however, the WFM is computationally less complex than the FSM. They indicate that the reduced computational load may be important in

real-time monitoring. In addition, an indirect benefit of EP signal modelling is data compression because at each sweep only the model coefficients need to be saved and not all the individual sample values. They also indicate that periodic components of mains electrical interference (and its harmonics) will not be cancelled by the FSM and WFM methods. It was suggested that this type of interference be eliminated prior to data processing by analogue notch filtering, or by an adaptive noise canceller *(Thakor et al., 1993)*

Adaptive Impulse Correlated Filter:

Laguna et al. *(1992)* presented a technique applicable to signals that are time-locked to a stimulus. This adaptive impulse correlated filter (see Appendix F) estimates the deterministic component of the signal and removes the noise uncorrelated with the stimulus, even if the noise is coloured (band-limited) as in the case of EP's. This points to use in EP extraction from background EEG noise. As for the FSM, the LMS algorithm is used to adjust the weights of the AICF.

It is shown that the SNR for the AICF reaches a plateau. However, in AVE the SNR increases indefinitely as the number of trials increases *([Rompelman, 1986] cited by Laguna et al., 1992)*. They also show that the AICF filter tracks dynamic changes in the signal better than classical AVE or moving window averaging. On the other hand, when the signal characteristics remain constant, the different techniques obtain comparable results.

Segmented Matched Filter:

Lange et al. *(1995)* described a method which they claim offers a significant SNR improvement for single trial EP's. This is shown in both simulation and experimental studies. Their method could be described as a segmentation-based Matched Filtering process which becomes fast and simple once the parameters of the algorithm have been set and a reference signal constructed. The Matched Filters (MF's) can be viewed as a multi-bandpass filter bank, matched to the varying spectral contents of a predefined template.

The reference signal or template is obtained via AVE of N (typically 50) trials and defined to be a sum of K consecutive time segments. The Fourier transform for each of the K time segments are computed. A bank of K filters is constructed, each with a frequency response matched to the respective segment. A single trial estimate of the EP is obtained by filtering the segmented single trial through the filter band, and rejoining the filtered segments. Finally the rejoined waveform may be smoothed with a low-pass filter.

The simulation and experimental studies showed that the MF algorithm improves the SNR of EP signals significantly. The MF bank remained adequate as long as the trials remained stationary, or at least kept a similar contour. In such cases, they suggested that the filtering can be implemented on-line in real-time, provided that the template and filter bank are constructed on *a priori* knowledge. However, if drastic variations in the characteristics of the EP signal are expected, the template should be updated dynamically, resulting in a time-varying MF bank. The MF's estimated the deterministic components of the signal, allowing for variation of latency and amplitude from trial to trial.

2.3.4 Signal Classification

For sake of completion, two techniques for the classification of EP signals or their parameters are also presented.

Fourier Descriptors:

Clarson and Liang *(1989)* proposed an algorithm for the automated classification of normal and abnormal EP waveforms into clinically significant classes.

They proposed an application of a newly proposed approach to pattern recognition in which there are no restrictions upon the form of the features selected to represent the patterns. Thus, the advantages of the structural description of patterns may be incorporated in the classification procedure. An advantage of this method is that the training sample size does not need to be large.

Fourier descriptors (FD's) are used to characterise each waveform and are obtained by means of the FFT. Since the feature sets of FD's contain information about the shape of the waveforms, they are used in the structural stage of the algorithm. In this stage discriminant analysis is used to measure the dissimilarity between pairs of waveforms. Only the resulting interdistance matrix is preserved in the construction of the vector representation, making the dissimilarity measure crucial to the success of the remainder of the procedure.

This approach has considerable merit especially since the choice of features can be enhanced. Feature selection using vectors of waveform amplitudes combined with inter-peak latencies could be used to develop an interdistance matrix that would fully describe relative distance between waveforms.

Unsupervised Clustering of EP's by Waveform:

Geva and Pratt *(1994)* presented a procedure for clustering and classifying EP's according to their waveform. The clustering is performed without *a priori* selection of basis waveforms , the number of base waveforms, or the number of clusters. EP's are typically quantified by latency and amplitude measures of peaks and troughs along the curve, all other features of the record being ignored. The proposed method uses the *principal component analysis* (PCA) coefficients *(McGillem and Aunon, 1987; [Gonzales and Wintz, 1987] cited by Geva and Pratt, 1994)* of EP records as features for unsupervised optimal fuzzy clustering *([Zadeh, 1965; Bezdek and Castelaz, 1971; Bezdek 1981; Gath and Geva 1989] cited by Geva and Pratt, 1994).* In PCA, a set of basis waveforms (principal components) common to all records are computed and arranged in decreasing order of their contribution to reconstruction of all records in the set. Each record can be exclusively reconstructed by a linear combination of the basis waveforms and each can be multiplied by an appropriate weight, or reconstruction coefficient. These reconstruction coefficients are used by the clustering procedure as the features of each record for its clustering. The adaptive and machine-learning nature of unsupervised clustering by waveform is particularly suited for an evolving database. Classification is thus improved and refined with the growing experience of the machine-based learning system.

CHAPTER 3

MATERIALS AND METHODS

3.1 Introduction

The execution of this project was divided into two stages, viz. the implementation of an EPES and a simulation study to evaluate the performance of pre-determined algorithms. The EPES was designed and implemented to acquire and process data off-line as well as controlling and acquiring data from a custom designed multi-channel amplifier. The off-line data was recorded onto magnetic tape from a commercial evoked potential monitoring system (CEPMS). The implementation of the EPES required the development of software that could interface with the system hardware and provide a user-friendly operator interface. The simulation study was executed using data obtained from the first stage of the project.

3.2 Evoked Potential Extraction System

The EPES was developed so as to be used with existing hardware. The developed software provided for an interface with the various hardware components, the extraction of the EP signals and the storing and display of the results.

3.2.1 Hardware Considerations

Hardware used included:

- an IBM-compatible, Intel 80486 microprocessor-based personal computer (hereafter referred to as the *computer*);
- a LabMaster A/D-D/A interfacing card (hereafter referred to as the *interfacing card*) manufactured by Scientific Solutions Incorporated (USA);

- a 6-channel biosignal amplifier system (hereafter referred to as the *front-end*) designed and constructed by technical staff in the Department of Biomedical Engineering at the University of Cape Town;
- a MYSTRO Programmable Electrophysiological System (hereafter referred to as the *commercial evoked potential monitoring system (CEPMS)* manufactured by Medelec Limited (UK); and
- a TEAC (Japan) R-61 Cassette Data Recorder (hereafter referred to as the *data recorder*).

The interfacing card and the computer together constituted the EPES hardware. The interaction between the computer and the other hardware components was facilitated by the interfacing card.

The EPES was required to interface with both the front-end and the data recorder. Figure 3-1 broadly illustrates the various interactions that existed between the various

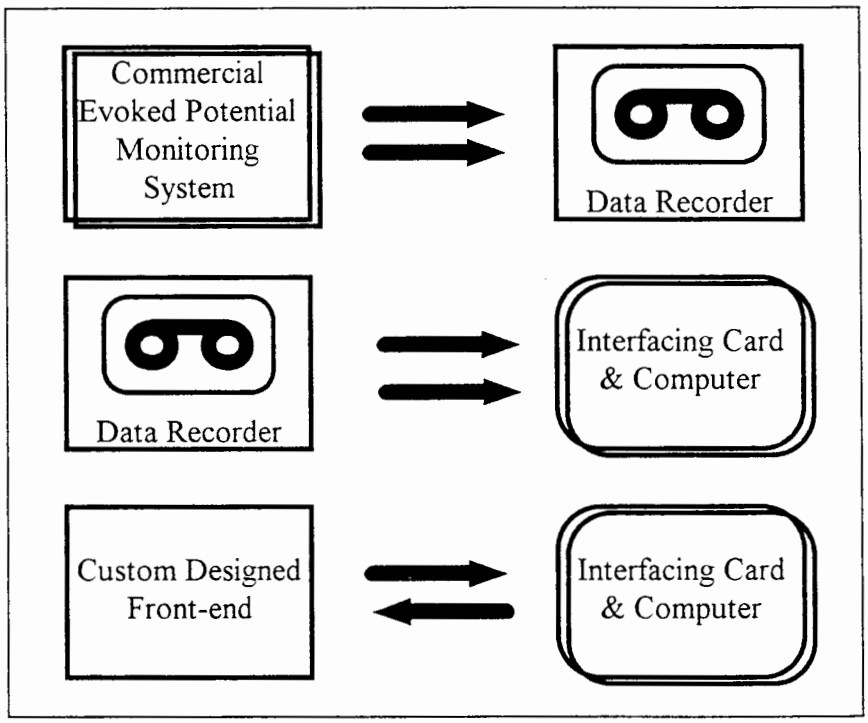

Figure 3-1: Data acquisition hardware interactions.

hardware components. All raw data obtained using the CEPMS was recorded onto

magnetic tape using the data recorder. This raw data could then be played back to the EPES at some later stage where the EP signals could then be extracted. This configuration was used mainly to obtain data in a controlled environment using the CEPMS.

The front-end used with the EPES was aimed at obtaining data in the surgical environment with the administration of anaesthesia to patients. This required a two-way interaction between the EPES and the front-end. The computer would control parts of the front-end while simultaneously collecting data from the front-end.

The data recorder was used mainly with the data recorder and CEPMS configuration but can be used with the front-end configuration as well. The TEAC cassette data recorder is able to record analogue signals onto 4 channels. These channels have two modes of recording, viz. direct (DR) mode and FM mode. Direct mode has a bandwidth of 20 to 8 000 Hz while FM mode provides for a bandwidth of DC (0 Hz) to 625 Hz.

(a) Data Recorder Configuration

Figure 3-2 illustrates the EPES used in conjunction with the data recorder and CEPMS in more detail. The CEPMS is normally used for clinical EMG and EP measurements with the option of using 2 to 5 recording channels. The system is controlled via an integrated microprocessor system providing software controlled operation. The MYSTRO provides a display of extracted EP's as well as hard disk storage and a printing facility. The MYSTRO was used in combination with the ST10 Stimulation Unit (also manufactured by Medelec Limited). The ST10 provides auditory, visual and somatosensory stimulation triggering to a patient during EP studies. The MYSTRO provided an analogue raw signal (unprocessed EEG-type signal) output while the synchronised trigger signal was obtained by tapping off from the connection between the MYSTRO and the ST10. Both the raw signal and the synchronised trigger signal were recorded onto magnetic tape. The recorded data could then be digitised by the EPES and the EP signals could be extracted off-line. The CEPMS was housed in a

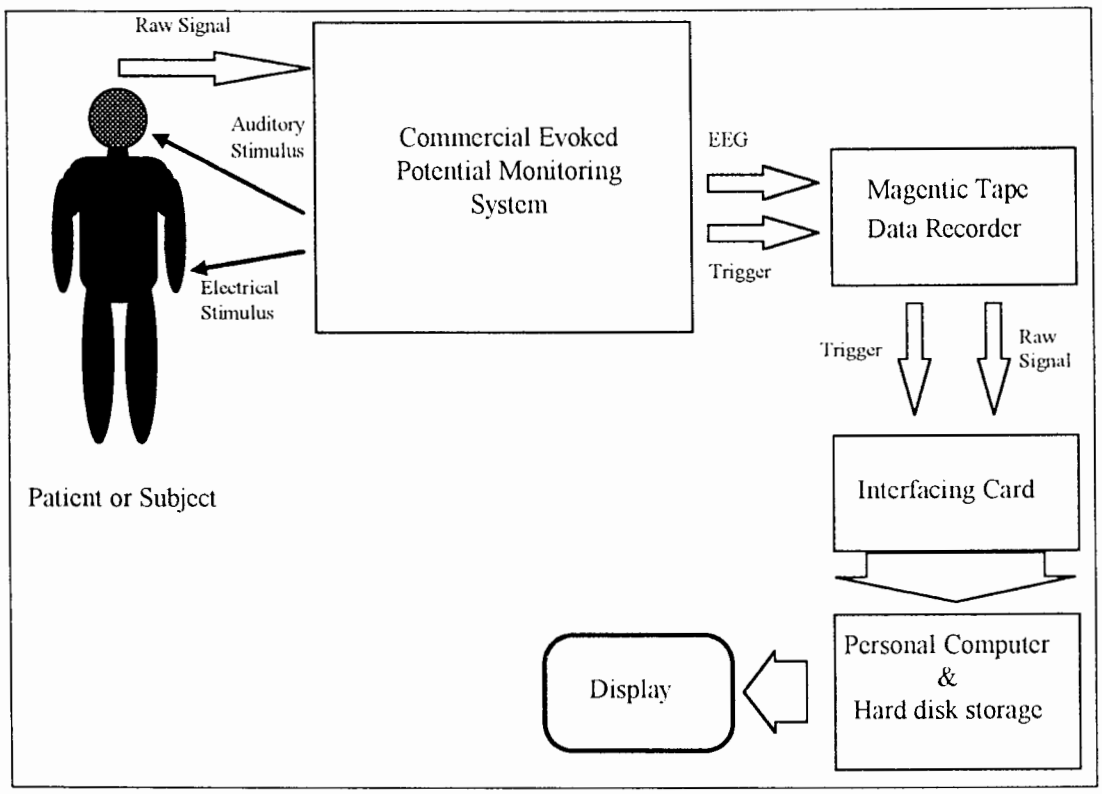

Figure 3-2: Schematic illustrating EP extraction using the CEPMS and data recorder.

special Faraday Cage type room which effectively reduced the effect of external electric fields and thus provided a controlled and relatively interference-free environment.

(b) Front-end Configuration

The front-end is a 6 channel biosignal amplifier system that had previously been designed as a general purpose unit and built specifically to obtain biosignals (ECG and EEG) from human subjects. Optocoupling devices protect the subjects against possible electrical shock by electrically isolating them from the rest of the measuring equipment. The system provides for very high gain amplification up to the order of 100 dB (100000 times). The original bandwidth specifications was 0.05 Hz to 200 Hz. This was not adequate for EP monitoring and necessitated the modification of two of the channels with bandwidths of 10 Hz to 3000 Hz. In addition to the signal channels, the

front-end also provided for an auditory click stimulator and electrical stimulator trigger through electrically isolated buffers.

Figure 3-3 illustrates the set-up for extracting EP signals using the front-end and the EPES. The front-end buffers provide the electrical isolation for the patient both from the amplification stages as well as the stimulation trigger stages. A portable battery operated constant current peripheral nerve stimulator manufactured by Fisher & Paykel

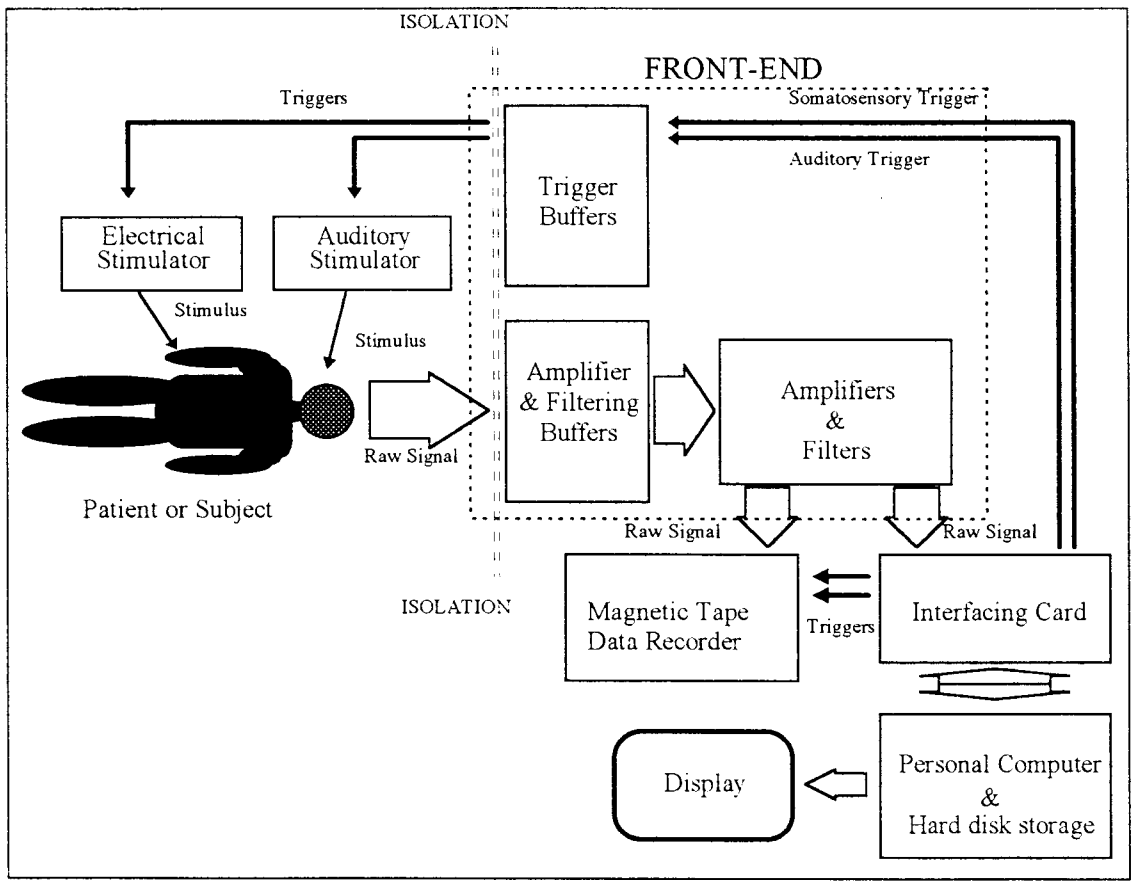

Figure 3-3: Schematic illustrating EP extraction using the custom-designed front-end amplifier system.

(New Zealand) was used as an external electrical stimulator. The nerve stimulator was modified so as to be triggered by the front-end which in turn was controlled by the EPES. The nerve stimulator was used to send an electrical impulse to the median nerve of a subject via skin electrodes and in so doing evoke a somatosensory evoked response. The auditory evoked response stimulator took the form of an amplifier unit

sending a "click" to earphones. The earphones were placed over the patient's ears and the volume could be adjusted.

Raw signals from the front-end could be directly processed by the EPES and then be saved permanently on hard disk. The same data could also be recorded on magnetic tape together with the synchronised trigger signal from the evoked potential extraction system for later off-line processing.

3.2.2 Software Design and Implementation

The code for the EPES software was developed in the C++ programming language using the Borland C++ ® version 3.1 compiler. The software allows for the system to be used with both the *data recorder configuration* as well as the *front-end configuration*. These configurations each require different approaches in terms of data acquisition and control. The data recorder configuration requires only a one-way interaction between the EPES and the data recorder while the front-end configuration requires a two-way interaction between the EPES and the front-end.

The LabMaster interfacing card provides A/D conversion, D/A conversion as well as digital timing. The A/D converters are used to sample the raw signals for both the data recorder and front-end configurations. The digital timers are used to control the timing of the stimulation triggers in the front-end configuration system.

The software provides for the control of the activities on the interfacing board, extraction of EP's from digitised raw signals, storage of all data to disk and the display of the various sets of data on the computer screen, as well as a user-friendly interface. The AVE, AICF and FSM algorithms are implemented for the extraction of the EP signals from the digitised raw signals. Each trial may be saved to disk as an individual file and the trial number incorporated into the filename for a given sequence of trials. Information about the trial number, time and algorithm used is included in each file header.

(a) Data Recorder Configuration

The basic operation of the EPES using the data recorder configuration is illustrated in Figure 3-4. The execution commences with the setting of various parameters of the EPES. These parameters include the channels to be sampled, sampling frequency required by the A/D converters, timing of trigger signals, period of sampling, display settings and others.

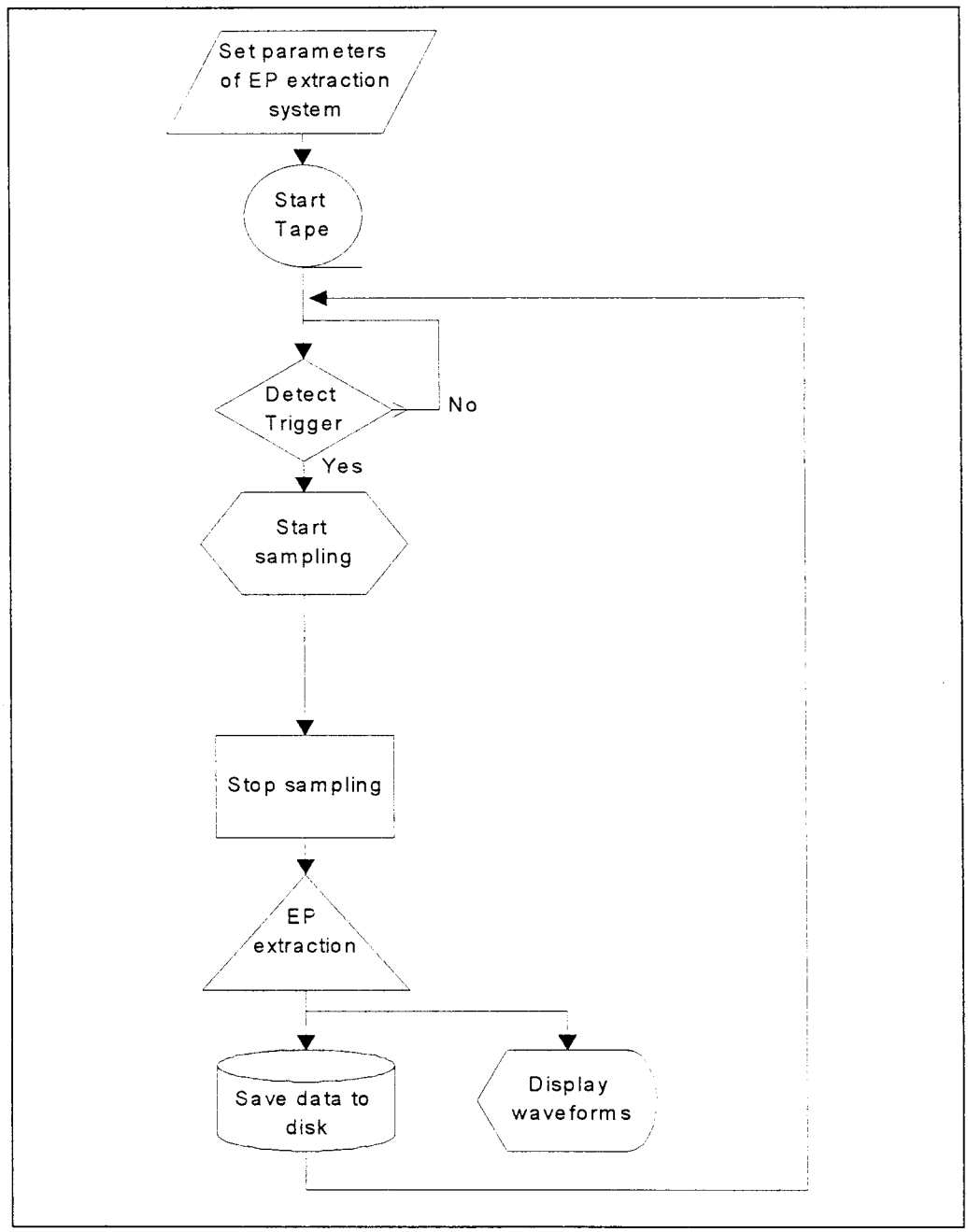

Figure 3-4: Flow chart of EP extraction using the cassette data recorder configuration.

The system waits for a trigger signal corresponding to the moment of occurrence of the stimulation from the data recorder. As soon as the trigger is detected, the signals are digitised for a fixed period of time called a *trial* (see last section of Appendix C).

Automatic artefact rejection in the form of a threshold level detector rejects any trials that have any sample values beyond predetermined upper and lower threshold limits. The accepted trials of data are then utilised by the extraction algorithms and may be saved to disk. The current extracted EP signals estimates may then be displayed at this stage. This procedure is repeated as the system again waits for the next trigger signal.

(b) Front-end Configuration

The procedure used in the front-end configuration is illustrated in Figure 3-5 and is

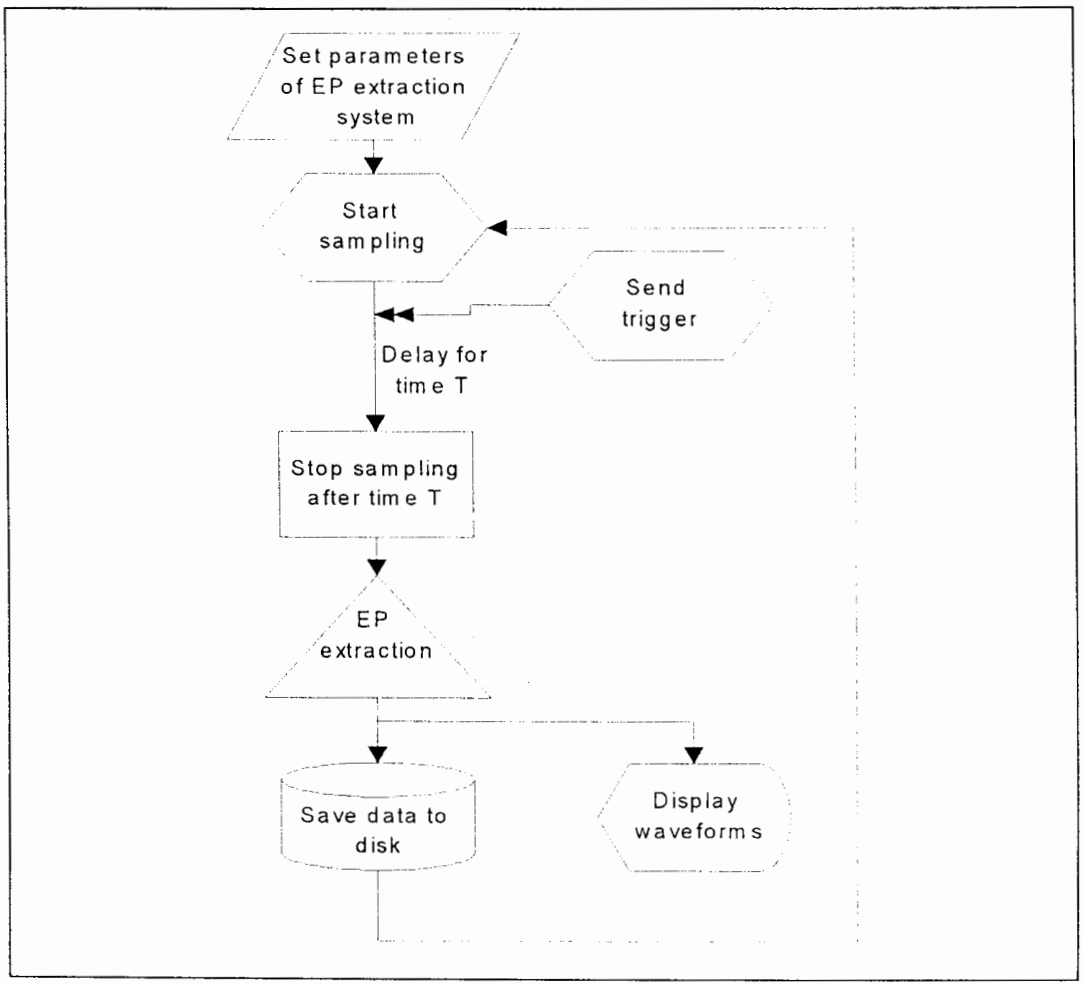

Figure 3-5: Flow chart of EP extraction using the front-end configuration.

essentially the same as for the data recorder configuration except for the following important differences. The front-end configuration is meant for on-line measurement for which the EPES has to control the stimulators as well as record the raw signals from the front-end. In this case the EPES provides the trigger signal. The system allows for pre-stimulus data to be recorded by commencing the sampling before the stimulus is triggered. The stimulus is thus triggered at a fixed period after sampling has commenced. Again the extracted EP signals may be stored and displayed.

(c) User Interface

The EPES has been designed with a user-friendly interface. It is menu-driven and supports the use of a mouse as a pointing-device. The main means of communication between the user and the system is through selecting commands on the *command bar*, setting or selecting options in *dialogue boxes* and adjusting certain parameters in the graphical plotting screen. Using the dialogue boxes, the user is able to select the sampling frequency, channels to be digitised, channel gains, trigger channel, algorithm traces to be displayed, initial graphical display amplitude and time scale values, pre-stimulus times and saving options. Default parameters are set automatically.

Menu and command bars:

The **Command bar** is a single bar at the bottom of the screen (see Figure 3-6). It provides the user with commands to control the main activities of the EPES. These commands include opening the graphical plotting window and reading data from the hard disk, activating data capture from the cassette recorder, controlling data capture using the front-end, capturing EEG signals in free run mode (no triggering), and exiting the EPES.

The **Menu bar** provides access to the menu commands or options. The bar consists of a single bar at the top of the screen (see Figure 3-6) providing the user with menu titles which open to menu commands or options. A **pull-down menu** is opened by choosing a menu title on the menu bar. The pull-down menu shown in Figure 3-7 is a window containing a list of options which either executes a command or opens a dialogue box.

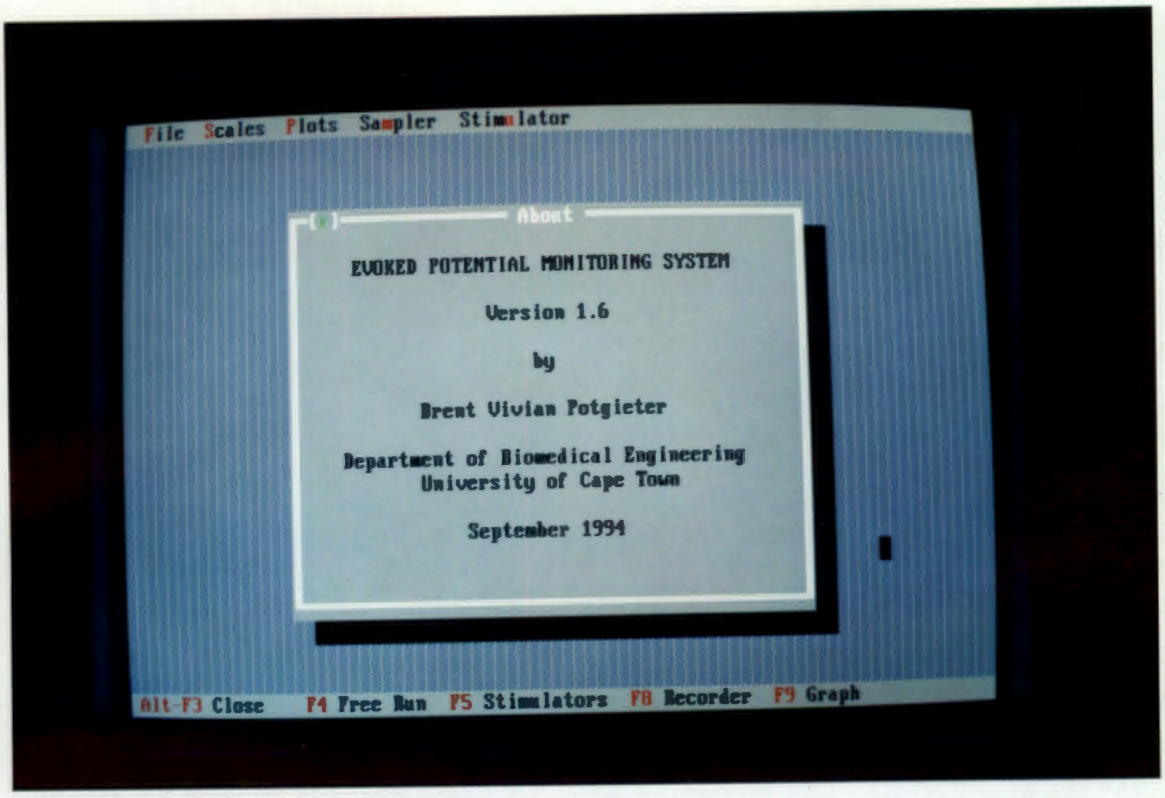

Figure 3-6: Photograph of EPES display screen showing menu and command bars. The "About" dialogue box is also shown.

Figure 3-7: Photograph of EPES display showing a pull-down menu.

Hot-keys are available for accessing menu options or executing commands. Thus a single keystroke performed using the keyboard can open a particular dialogue box without going through the process of opening a pull-down menu from the menu bar. Menu titles and command bar commands can also be selected using hot-keys. The hot-keys are displayed alongside the menu titles or menu options in the pull-down menus as shown in Figure 3-7.

Dialogue boxes:

Dialogue boxes shown in Figure 3-8 are windows that allow the user to enter or select parameters which control the system. These parameters are controlled by the user through the use of check boxes, radio buttons, input boxes and action buttons. **Check**

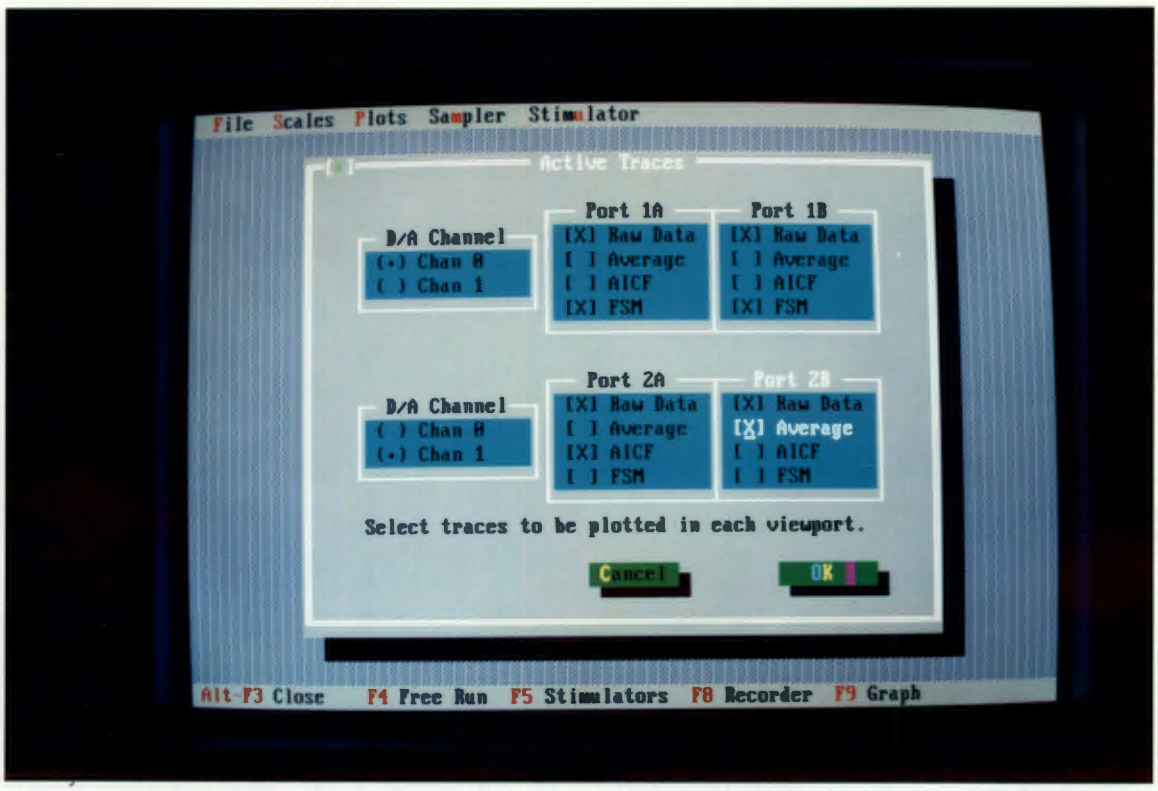

Figure 3-8: Photograph of EPES display showing a dialogue box with check boxes and radio buttons.

boxes consist of a box [ ] followed by an item which can either be turned ON or OFF. When a check box is selected, an X appears in the box to show that it is ON: **[X]**. **Radio buttons** consist of a box ( ) followed by an item that can be selected or not. If an item is selected then a dot appears in that box: **(•)**. Radio buttons always appear in

groups (two or more options) and only one radio button can be ON in a group at any one time. **Input boxes** allows the user to enter values for certain parameter settings such as trigger delay time. The dialogue box has two standard **action buttons**: OK and CANCEL. If OK is chosen then the settings made in that dialogue box is accepted. If CANCEL is chosen, then no changes are made to the settings that were current when the dialogue box was opened.

Graphical plotting screen:

The **graphical plotting screen** shown in Figure 3-9 provides four windows in which either the current extracted EP signal estimates or the raw unprocessed signals may be displayed.

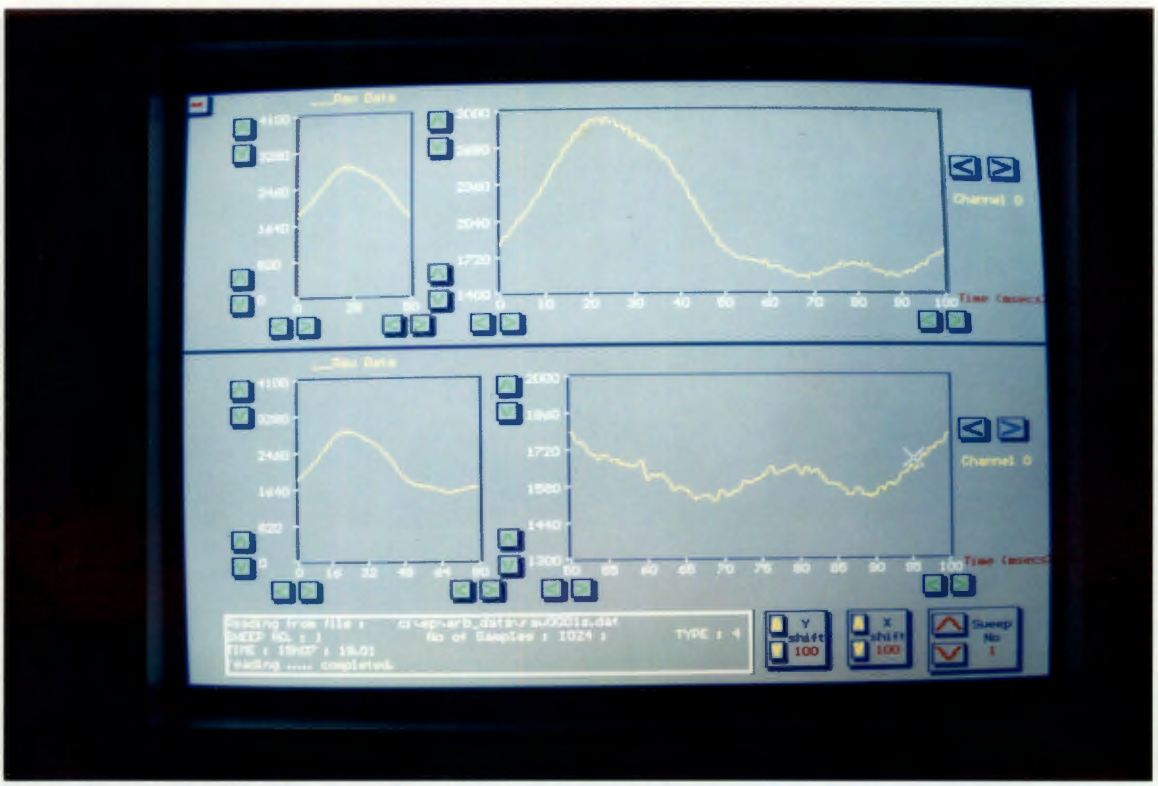

Figure 3-9: Photograph of EPES display showing the graphical plotting screen.

The plotting area is split into a top and bottom section. The windows in each section may be sized relative to each other in the horizontal plane. Up to 4 signals can be plotted in each window. These include the raw unprocessed signal and each of the extracted signal estimates from the three different algorithms. The amplitude and time

scales of each window is adjustable using the arrowed buttons located at the minimum and maximum value positions of each axis. All buttons are activated using the mouse cursor. A status window at the bottom of the screen indicates various parameters such as the trial (sweep) number, time of capturing and filename.

3.2.3 Sources of Clinical Data

Most of the clinical data was obtained in the Department of Neurology at Groote Schuur Hospital using the CEPMS. Raw analogue signals together with the associated trigger signals were recorded onto magnetic tape using the data recorder. These signals were later processed off-line using the EPES. These sets of data represented EP signals that were assumed to be stationary and did not change with time.

Differential amplifiers are used to record the voltage differences between electrodes on the scalp. The electrode configuration chosen for a given application depends on what area of the cortex is being examined and what information is being sought. Bipolar as well as monopolar electrode configurations were used. Bipolar electrode configurations require that each recording channel is connected to a pair of electrodes and the potential difference between these electrodes is recorded as the raw signal. In the monopolar electrode configuration, each channel records the potential difference between an active scalp electrode and an "indifferent" or reference electrode usually located on the chin, forehead, neck or ear.

The typical recording configuration for the extraction of the SSEP signals is illustrated in Figure 3-10. The plus (+) and minus (-) signs indicate the terminals that were used with a bipolar electrode configuration while the reference electrode refers to the "indifferent" electrode used in the monopolar electrode configuration. These configurations were used in the case where the stimulus was in the form of a 10 to 20 mA electric current to the left median nerve. The scalp electrodes were placed on the contralateral (right) side relative to the stimulus (left side) because of the crossover of these sensory pathways. Figure 3-11 illustrates the typical positions of electrodes used during the extraction of the AEP signals. "Clicks" with levels sufficiently above the threshold so as to elicit an adequate

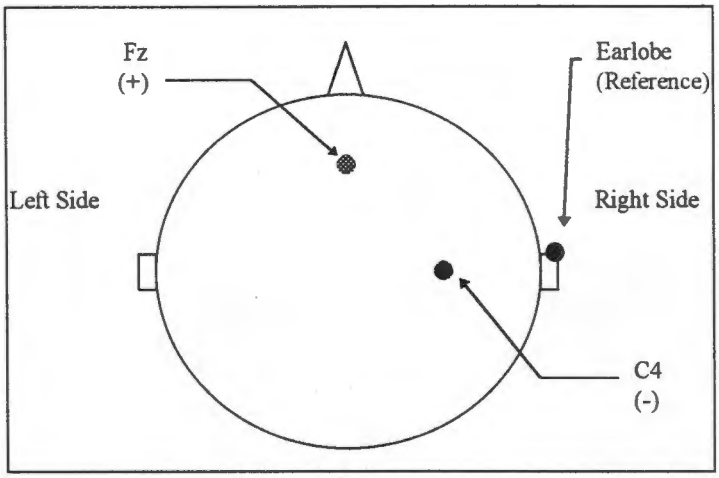

Figure 3-10: Electrode configuration for the extraction of SSEP signals.

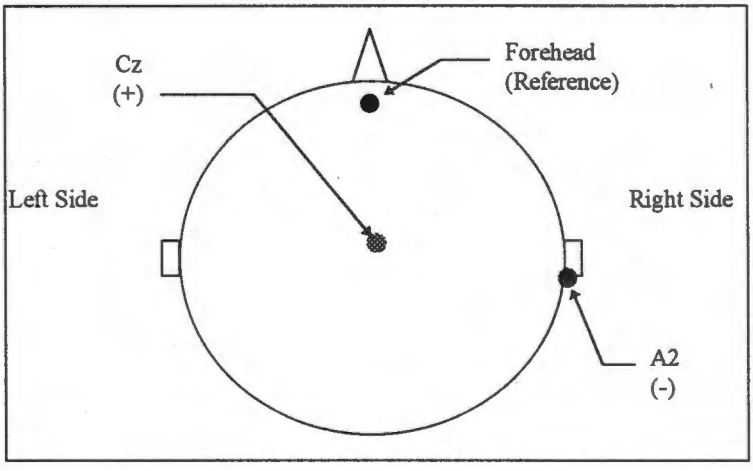

Figure 3-11: Electrode configuration for the extraction of AEP signals.

response were presented to the left ear. A white noise mask was sent to the opposite ear. Again the recording scalp electrodes were placed contralaterally to the stimulus.

3.3 Simulation Study

The use of EP signals for DOA monitoring requires that the EP extraction algorithms are able to extract the time-varying EP signals rapidly enough to detect changes as well as track any changes in these signals. This study was aimed at comparing the performance of the various algorithms in extracting EP signals as well as ascertaining how well they are able to track changes in the EP signal. The algorithms were tested using various circumstances

which included different types of noise or interference (hereafter referred to as *interference*) as well as different levels of this interference. Relative performance of the algorithms was measured by comparing SNR-related parameters and subjecting these to statistical analysis. The simulations were performed using MATLAB (Mathworks Incorporated, USA), a mathematical and matrix manipulation package.

3.3.1 Algorithms Evaluated

EP signals are extracted by processing the trials. These trials are all of equal length and time-locked to their respective stimuli (see last section of Appendix C). EP signals are extracted by processing the trials in succession. Signals corresponding to each trial were digitised and served as the input signals to the algorithms tested. An estimated signal was made available after the processing of each successive trial.

The aim of the study was to evaluate the EP extraction performance of the AICF as proposed by Laguna *(1992)* and the FSM as proposed by Vaz (*1989*). The AVE technique was also implemented as a control. The AICF and FSM algorithms are adaptive algorithms and are directed at extracting time-varying signals. Both use the LMS algorithm to perform the adaptive process which is discussed in greater detail in appendix E. The AVE, AICF and FSM algorithms are discussed in greater detail in Appendices D, F and G. The FSM algorithm was implemented with a model order of 10. According to Thakor *(1991)*, the signal reconstructed from 10 harmonics (i.e. model order of 10) captures 99.1% of the energy in the actual signal and visual observation confirms that 10 harmonics reconstruct the signal with adequate detail.

Associated with adaptive algorithms is a parameter called the **convergence factor** (μ). This factor determines how quickly the adaptive algorithm adapts to changes in the incoming signal. The algorithms remain stable for $0 < \mu < 1$. Three μ values for each of the AICF and FSM algorithms were selected. These were chosen based on those quoted in the literature as well as those tested empirically in a pre-trial.

Table 3-1 lists the convergence factors used for the AICF algorithm. These are named AICF1 to AICF3 and correspond to increasing values of the convergence factor.

Table 3-1: Convergence factors used for the AICF algorithm.

Name	convergence factor (μ)
AICF1	$1x10^{-6}$
AICF2	$5x10^{-6}$
AICF3	$1x10^{-5}$

Table 3-2 lists the convergence factors for the FSM algorithm. Each algorithm has its own set of convergence factor values because the relationship between convergence factor value and performance is algorithm-specific.

Table 3-2: Convergence factors used for the FSM algorithm.

Name	convergence factor (μ)
FSM1	$1x10^{-5}$
FSM2	$5x10^{-5}$
FSM3	$1x10^{-4}$

3.3.2 Simulation Design

The study required the generation of representative EP signals and interference signals. These signals were combined in various ways to produce sets of data. Figure 3-12 illustrates the summation of a SSEP signal and an EEG interference signal. The performance of the various algorithms in extracting the original EP signal from the summated signal was then evaluated.

Both AEP and SSEP signals were used. Each was constructed as a stationary and non-stationary signal.

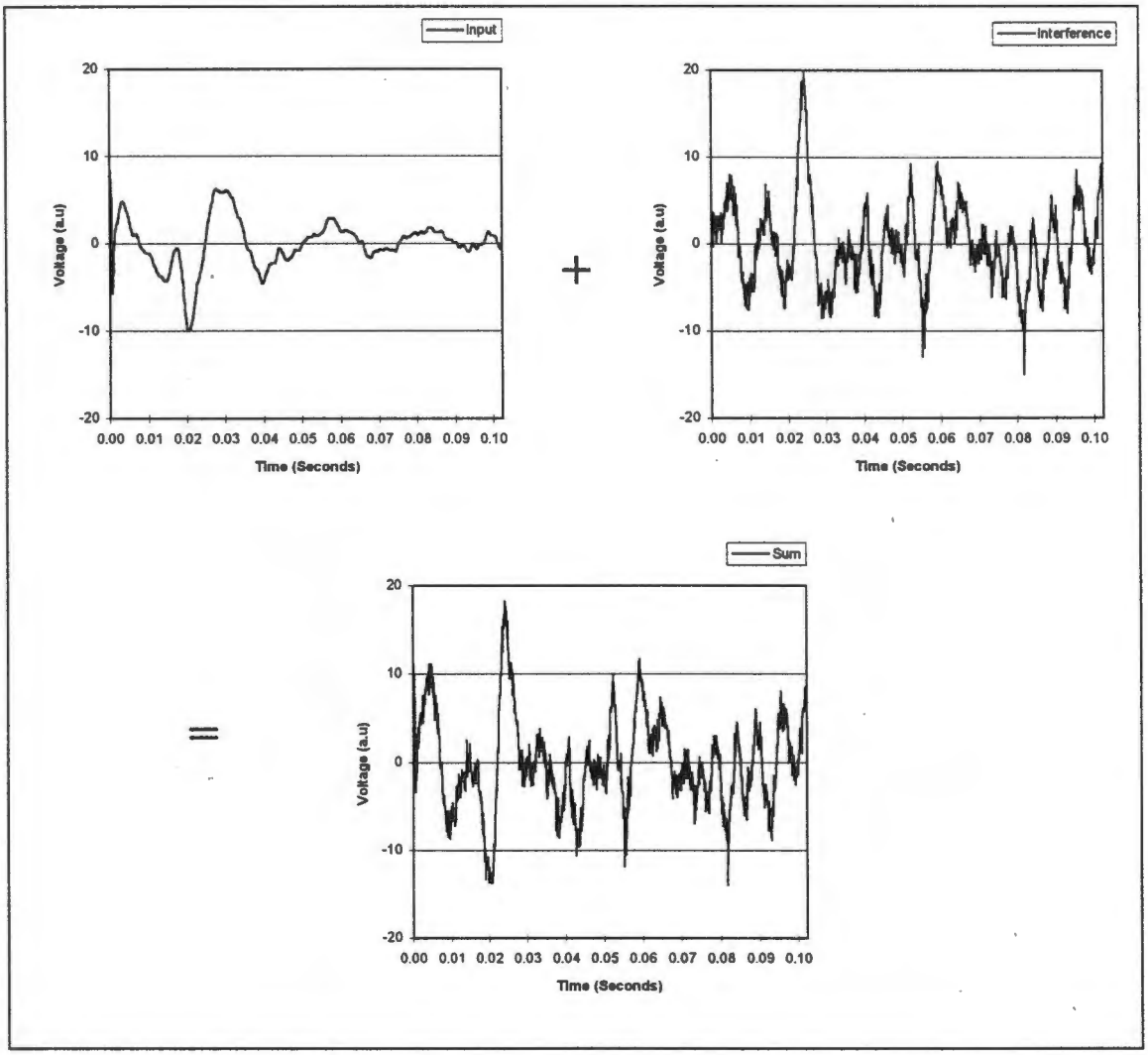

Figure 3-12: Summation of a SSEP signal and EEG interference signal.

The interference signals included:

- spontaneous EEG
- band-limited random interference
- 50-Hz mains interference
- a combination of band-limited random and 50-Hz mains interference.

For each of the interference signals we defined three graded amplitude levels:

- low
- medium
- high.

The EP signals were combined with the interference signals in all the possible permutations and produced a number of test data sets such as:

◊ stationary AEP + random interference (low/medium/high levels)

◊ stationary AEP + EEG interference (low/medium/high levels)

◊ stationary AEP + 50-Hz interference (low/medium/high levels)

◊ stationary AEP + combined band-limited random and 50-Hz interference (low/medium/high levels)

etc.

This produced 48 different permutations of evoked potential-interference signal combinations as shown below:

2 (EP signals: SSEP, AEP)
x 2 (types: stationary, non-stationary)
x 4 (interference types)
x 3 (graded amplitude levels of interference)
= 48 test data sets

These test data sets were used to evaluate the performance of the extraction algorithms, viz.:

- adaptive impulse correlated filter (3 convergence factors)
- Fourier series model (3 convergence factors)
- synchronous time averaging.

Each of the different convergence factors were treated separately giving a total of 7 algorithms for evaluation. This resulted in the execution of 336 simulation runs as calculated below:

48 (test data sets)
x 7 (algorithms)
= 336 simulations.

In this study, 1000 trials were used for each of the 336 individual simulations. The extracted signals as well as parameters such as SNR were recorded after each trial. This information was used for further comparative and statistical analysis.

In order to obtain results that would be comparable between algorithms, a custom unit of voltage or amplitude was defined. This unit was called the **au** (*arbitrary unit*). The typical spontaneous EEG signal has higher amplitude levels than the EP's with the typical SSEP having higher amplitude levels than the typical AEP. This study assumed that the peak amplitudes of the spontaneous EEG, the SSEP and the AEP signals were in the ratio 100:10:1. Using this assumption, the peak amplitude of a typical AEP signal was specified to be 1 au, and that for a typical SSEP signal equalled 10 au. The interference signals were also scaled accordingly and are discussed later in this section.

Peak amplitude was used as the criterion for defining the amplitude levels of the signals so as to contain outlying peaks or spikes that may exist in the interference signals. These peaks or spikes could detrimentally affect the performance of the algorithms. If mean amplitude was used instead, single outlying peaks would not increase the mean amplitude of an epoch of interference by much but the spike would affect the performance of the algorithms under test. The use of peak amplitudes also eased the computation complexity and decreased the simulation execution time.

3.3.3 Generation of EP Signals

The EP signals used during the simulation study were extracted from the recorded raw signals obtained with the CEPMS. These signals were digitised at a sampling rate of 10 kHz and the EP signals were extracted using the EPES. The length of a trial equalled 102.4 msecs and corresponded to 1024 samples per trial. The amplitudes of the EP signals were set according to the convention discussed in the previous section: EP's were scaled such that the peak amplitudes were 1 au for AEP's and 10 au for SSEP's.

Signals AEP_A and SEP_A illustrated in Figure 3-13(i) and Figure 3-14(i) respectively were used as the stationary EP signals.

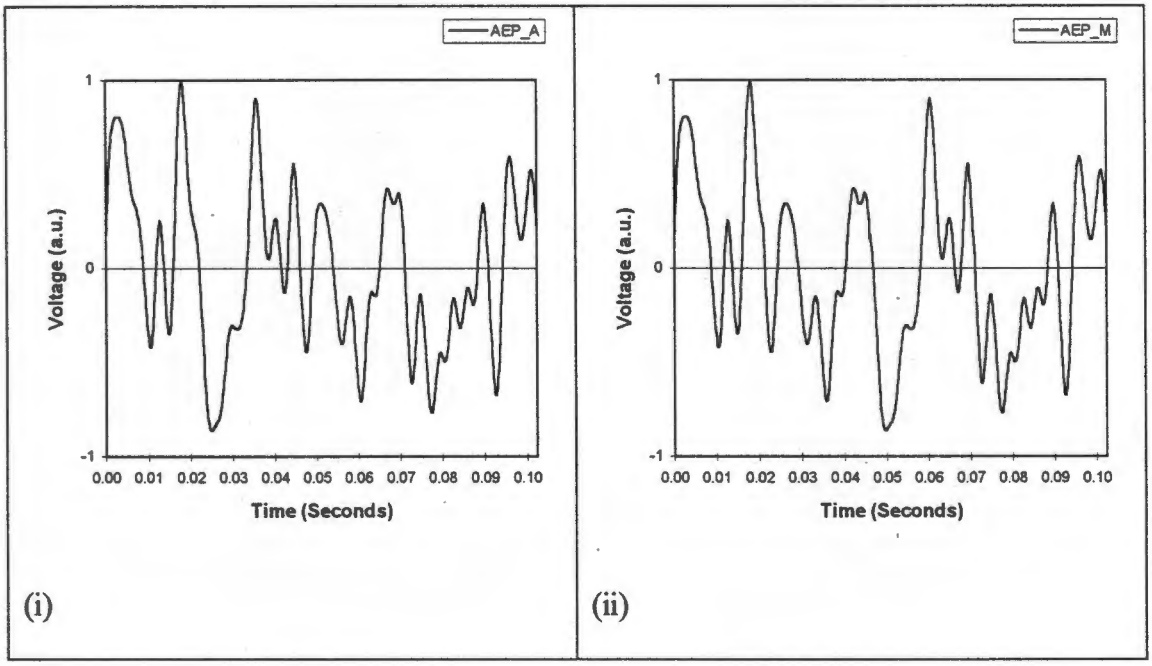

Figure 3-13: Time domain plots of the AEP signals.

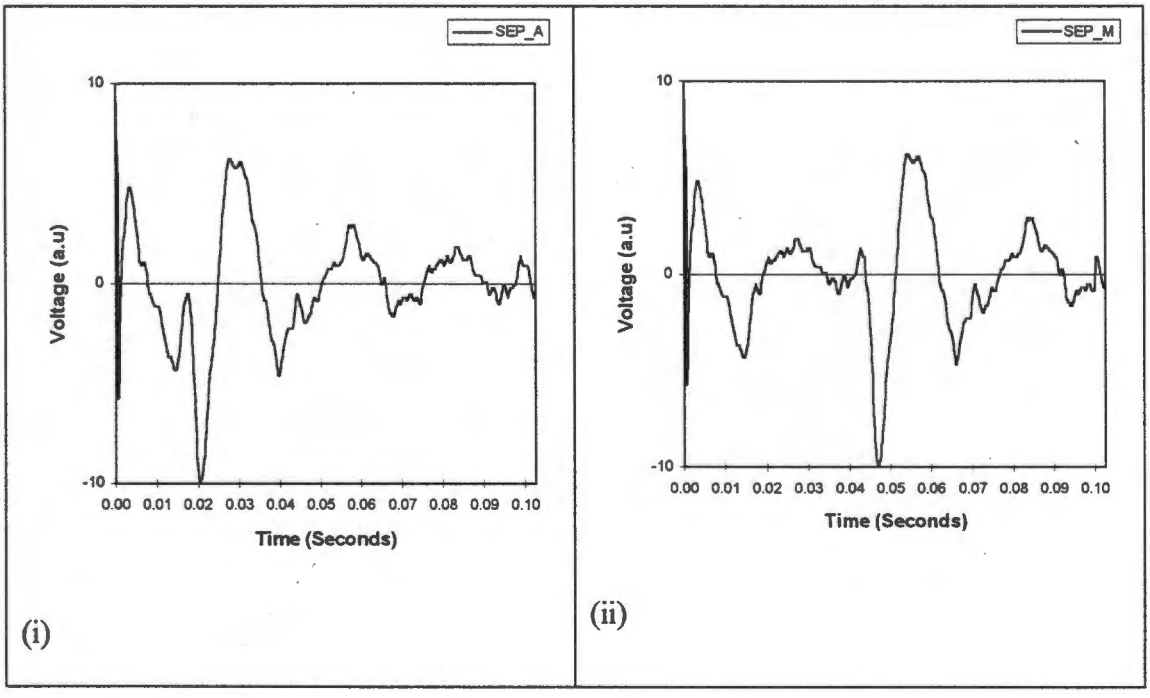

Figure 3-14: Time domain plots of the SSEP signals.

For the simulation of stationary EP signals, the same EP signal was used for each successive trial. During this period the interference signals were changing with each successive trial.

The non-stationary EP signal simulations required that a change in the EP signal occurred. This was achieved by changing the AEP signal from AEP_A to AEP_M in Figure 3-13(ii). Similarly the SSEP signal was changed from SEP_A to SEP_M as illustrated in Figure 3-14(ii). These changes were initiated at trial 100 in both cases. The altered EP signals (AEP_M and SEP_M) were generated by modifying the original EP signals: sections of the signals (AEP_A and SEP_A) were delayed in the time domain.

3.3.4 Generation of Interference Signal

(a) Types of Interference Signals

Four types of interference signals with the same temporal length as the EP signals were generated, viz. band-limited random noise (hereafter also referred to as *random interference*), 50-Hz interference, combined band-limited random interference and 50-Hz interference (hereafter also referred to as *combined interference*) and spontaneous EEG (hereafter also referred to as *EEG interference*). Time domain plots of typical interference signals are illustrated in Figure 3-15.

The random interference signals were generated using the random number generator supplied with the MATLAB package. In order to have emulated the effects of filtering, these random interference signals were band-limited to between 100 Hz and 2500 Hz using a third order Butterworth bandpass filter. Because no standard bandwidth limits were found in the literature, values were chosen which fall within the limits of those values more commonly quoted. The 50-Hz interference signals were generated using cosine waveforms. Signals for consecutive trials had a random phase shift, also generated using the random number generator supplied with the MATLAB package.

The combined interference was derived by combining the random interference signal with the 50-Hz interference. The spontaneous EEG signals were derived from real data that was recorded in the clinical environment and digitised using the EPES.

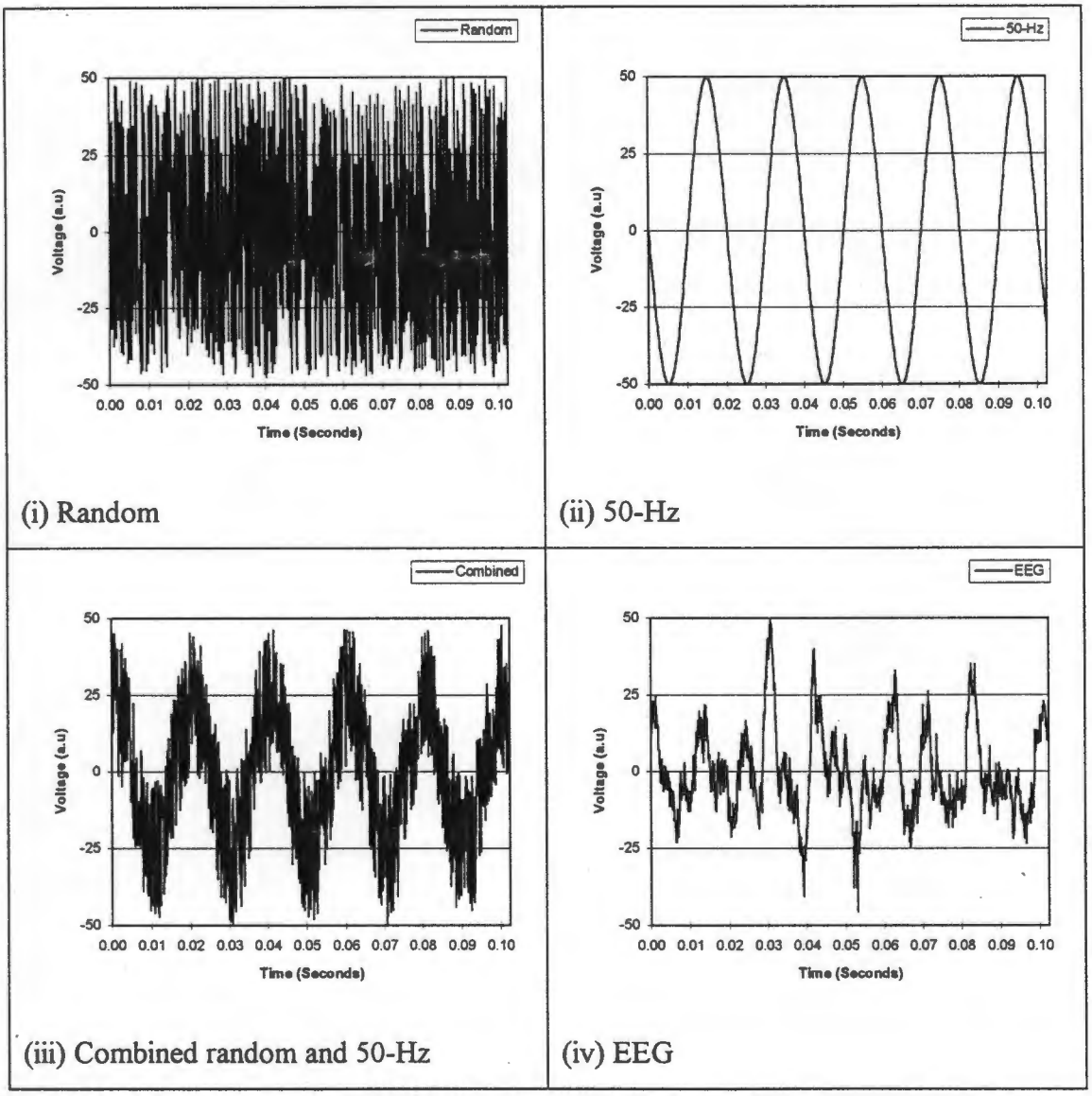

Figure 3-15: Time domain plots of typical interference signals.

Figure 3-16 illustrates the accumulated power spectral density distribution for each of the different interference types. These were obtained by summing the power spectra for each of the 1000 successive trials of interference signals. These spectra were normalised such that the maximum peak was equal to unity. Figure 3-16(i) clearly

indicates the band-limiting that was introduced to the random interference signals. Both the 50-Hz and combined interferences have prominent 50 hertz components.

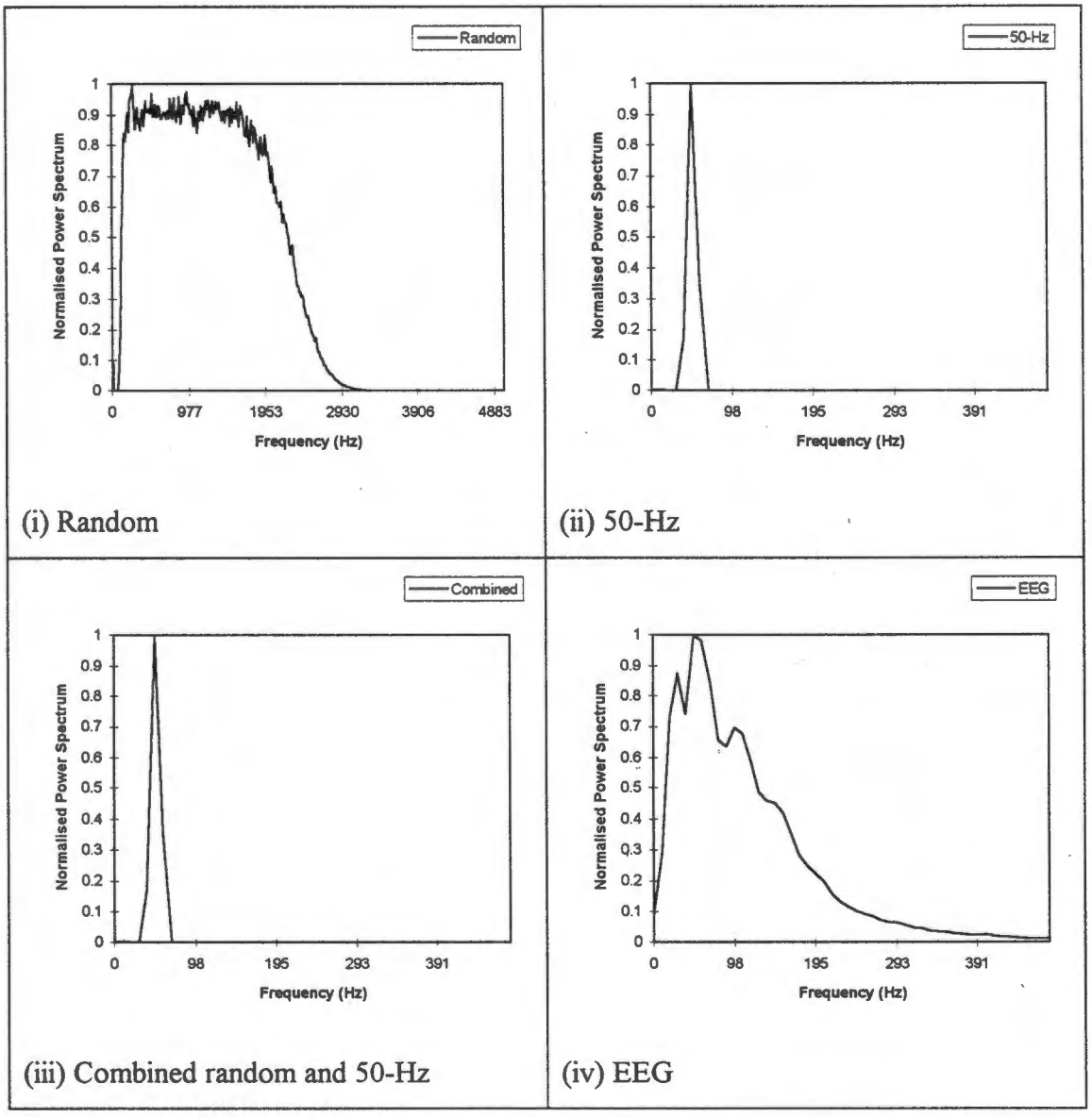

Figure 3-16: Accumulated power spectral density of typical interference signals.

(b) Levels of Interference

The interference signals were scaled to three discrete amplitude levels called low, medium and high. The levels were defined in terms of their peak amplitudes as shown in Table 3-3.

Table 3-3: Nomenclature for interference amplitude levels and corresponding maximum amplitude values.

Level	Peak amplitude (au)
low	20
medium	50
high	100

Figure 3-17 shows 50-Hz interference signals representing the low, medium and high levels of interference.

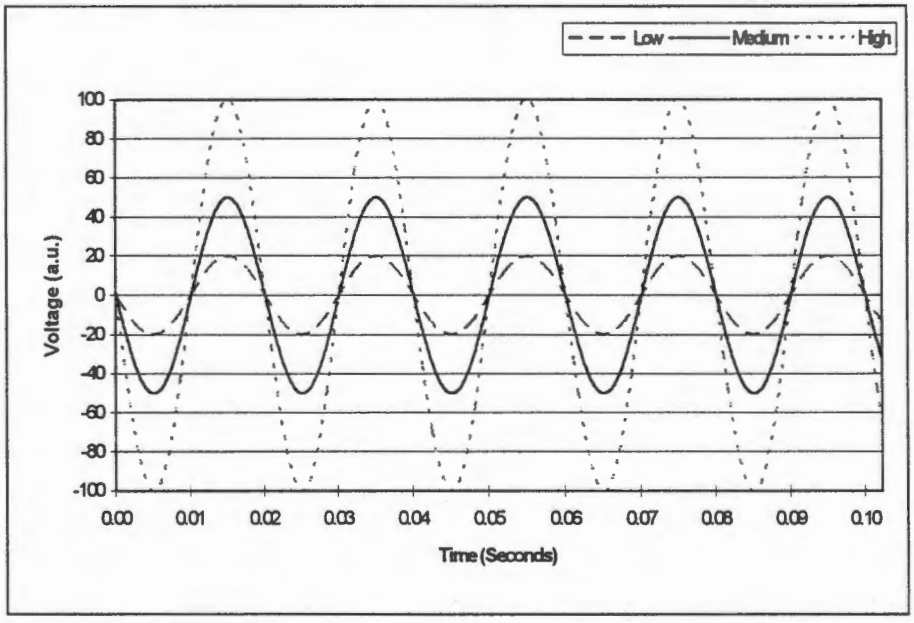

Figure 3-17: Plot of 50-Hz interference signals illustrating low, medium and high amplitude levels.

3.3.5 Figures of Merit

The primary figure of merit or performance measure used to compare the algorithms was the SNR which gives a quantitative measure of the relationship between the

extracted signal and the true signal. The SNR is measured in decibel (dB) and is defined as follows for sampled data signals:

$$SNR = 10 * \log \frac{\sum_{i=1}^{N} [S_i]^2}{\sum_{i=1}^{N} [S_i - R_i]^2}$$

where

S = true EP signal sample

R = current estimated signal samples (during extraction)

N = total number of samples

i = sample number

This definition is based on one used by Thakor (*1993*). The SNR values were calculated after each of the 1000 trials during each of the 336 simulation sets. This resulted in a total of 336 000 SNR values that were stored for later analysis. This included the plotting of SNR versus trial number responses for each of the algorithms as well as statistical analysis that could provide some quantitative measures of the performances of the algorithms.

The other figure of merit, **ΔSNR**, was used to determine the rates of change in the SNR response as a function of trial number. This parameter was used in the case of the non-stationary EP simulations where a change in the EP signal was introduced after trial 100. This was obtained from the SNR data by calculating the differences in SNR as follows:

- SNR(at trial 150) - SNR(at trial 100)
- SNR(at trial 200) - SNR(at trial 100).

3.3.6 Statistical Analysis

Analysis of Variance (ANOVA) was used to analyse the results of this study. The statistical analysis was performed using Statgraphics version 6.0 (Manugistics, USA). ANOVA and how it relates to this study is described in slightly greater detail in Appendix H.

The analysis was performed on the SNR results described in the previous section. Because of the large amount of SNR values recorded (336 000), a limited number of values could be used for statistical analysis and interpretation. The analysis for the stationary simulations was thus restricted to the evaluation of SNR values after 100, 200 and 400 trials for the SSEP and 100, 200, 400 and 1000 trials for the AEP. For the non-stationary simulations, the values evaluated were the ΔSNR values derived from the differences in SNR between trial 100 and 150 and between trial 100 and 200. This resulted in a total of 924 (84x7 + 84x2x2) values used for statistical analysis.

CHAPTER 4

RESULTS

The results obtained during the simulation study are presented in this chapter. Some typical time domain signals and SNR responses are presented first. An overview of the simulation study results and how the statistical analysis is incorporated into the study is then presented. The actual statistical results obtained from the simulations studies using the AEP and SSEP signals are finally presented separately.

4.1 Typical Results

This section presents some typical responses obtained during the simulation study. It illustrates a few of the general trends exhibited by the algorithms as well as the differences between the algorithms.

4.1.1 Typical Extracted Time Domain Signals

The time domain plots in Figure 4-1 illustrate a typical progression of the extraction process. The figure displays time domain plots of the extracted EP signals after

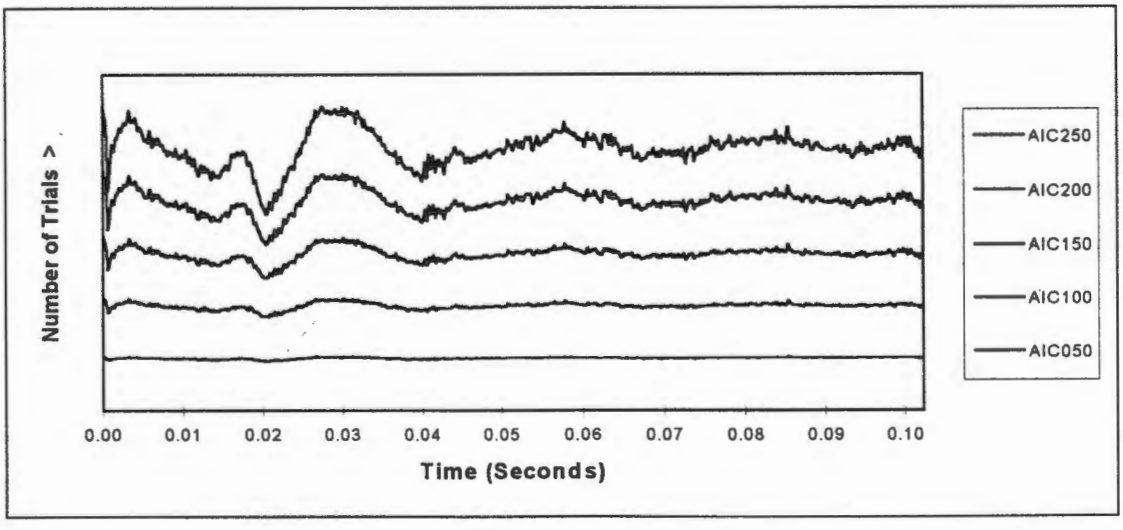

Figure 4-1: Time domain plots of extracted SSEP signals against increasing trial number (AICF2 algorithm with low level random interference).

increasing numbers of trials from 50 (bottom) to 250 (top). These signals were obtained using the AICF2 algorithm on the SSEP signal with random interference (low level).

Figure 4-2 illustrates time domain plots of extracted SSEP signals for each of the different algorithms investigated. These signals were extracted from low level random interference after 400 trials. The original SSEP signal is plotted at the top.

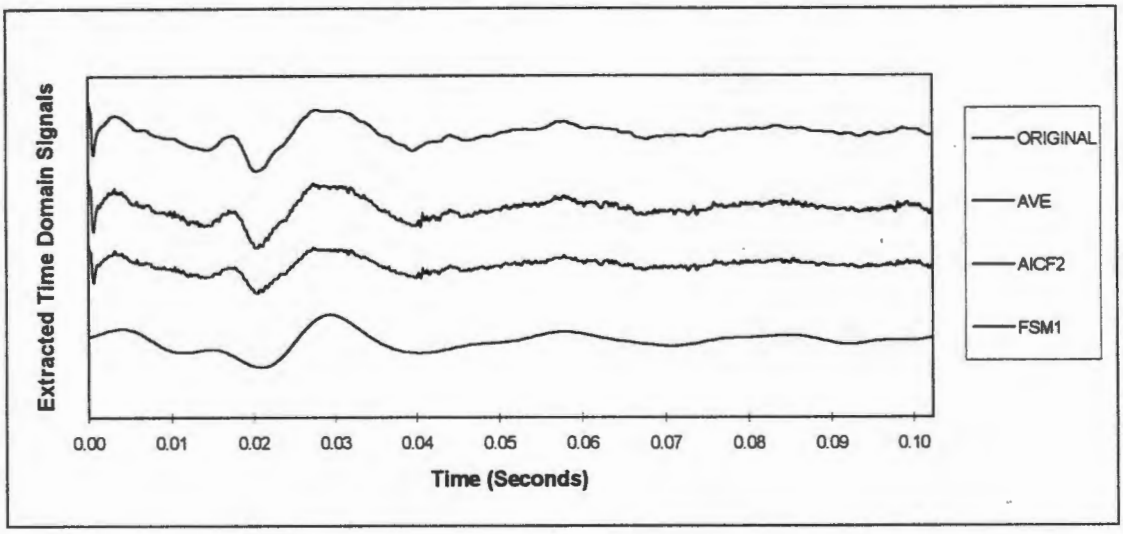

Figure 4-2: Time domain plots of extracted SSEP signals after 400 trials from low level random interference using the AVE, AICF2 and FSM1 algorithms.

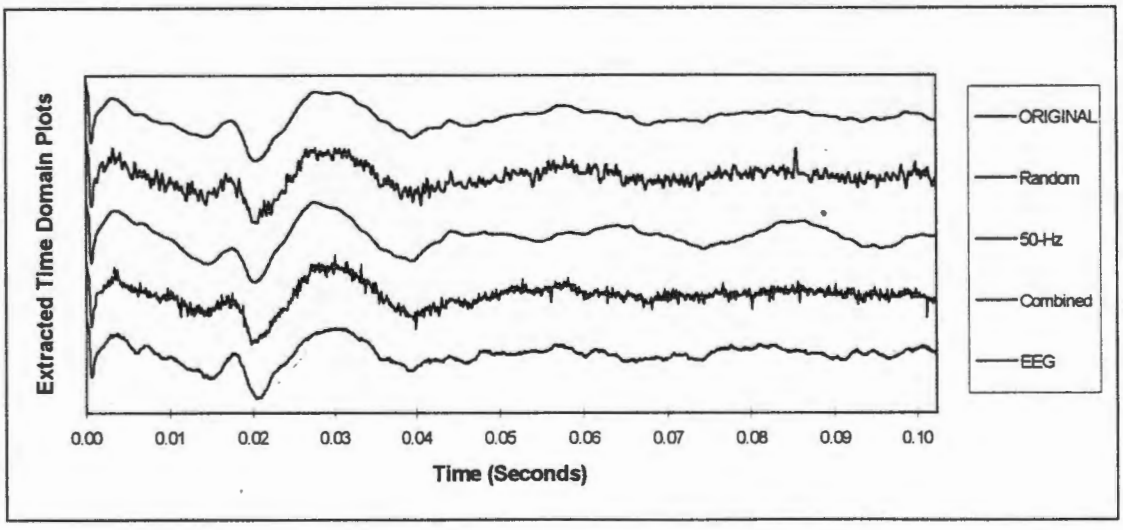

Figure 4-3: Time domain plots of extracted SSEP signals after 100 trials from different types of interference using the AVE algorithm.

Figure 4-3 illustrates time domain plots of the extracted SSEP signals from each of the interference types. The original SSEP signal is plotted at the top. The extracted signals were extracted after 100 trials from low levels of interference using the AVE algorithm.

Figure 4-4 illustrates time domain plots of extracted SSEP time domain plots from low, medium and high levels of random interference. These signals were each extracted after 100 trials. The original SSEP signal is plotted at the top. Similar time domain plots for EEG interference are illustrated in Figure 4-5.

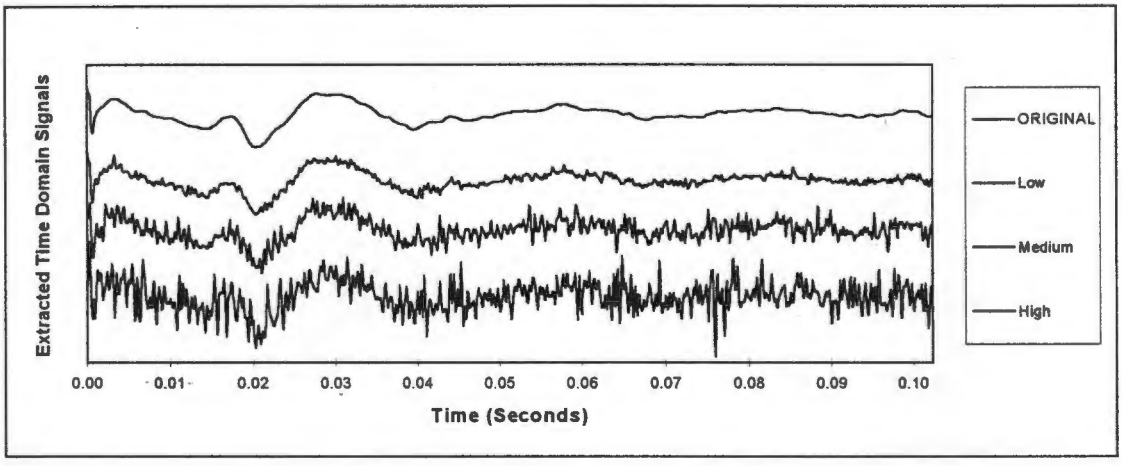

Figure 4-4: Time domain plots of extracted SSEP signals after 100 trials (AVE) from low, medium and high levels of interference (random interference).

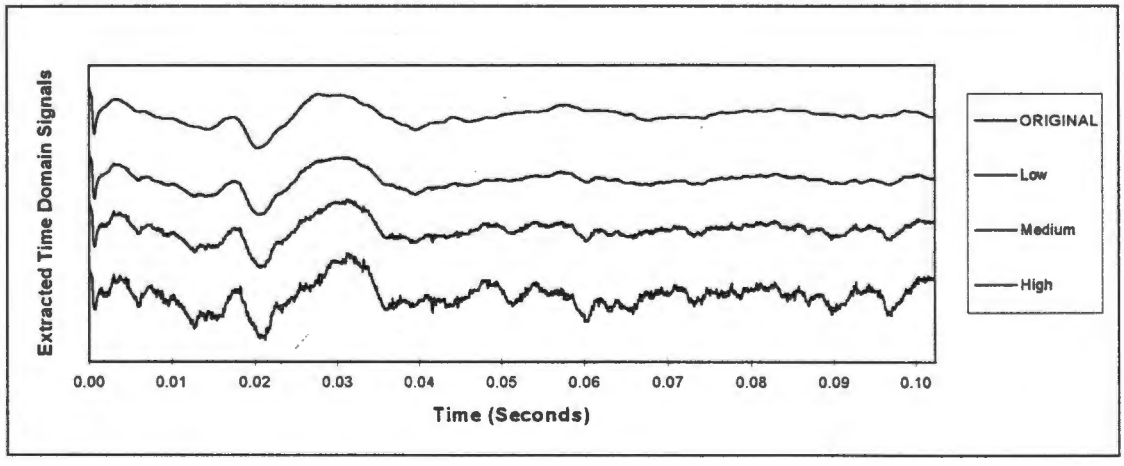

Figure 4-5: Time domain plots of extracted SSEP signals after 100 trials (AVE) from low, medium and high levels of interference (EEG interference).

4.1.2 Typical SNR Responses

Figure 4-6 illustrates typical SNR responses of the AVE, AICF and FSM algorithms. These responses were derived from simulation sets with the *stationary* SSEP signal extracted from random interference (medium level). The convergence factors used for the AICF and FSM algorithms were $5x10^{-6}$ and $1x10^{-5}$ respectively. The AICF algorithm has a characteristic decline in the SNR levels after it reaches maximum at about 500 trials.

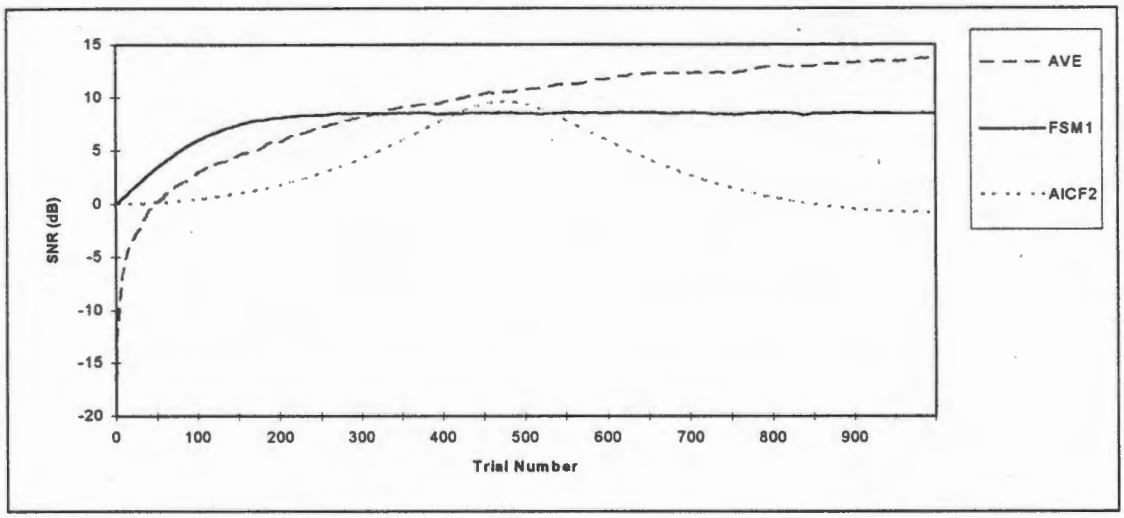

Figure 4-6: Plots of typical SNR responses of the AVE, AICF and FSM algorithms (*stationary* SSEP with medium level random interference).

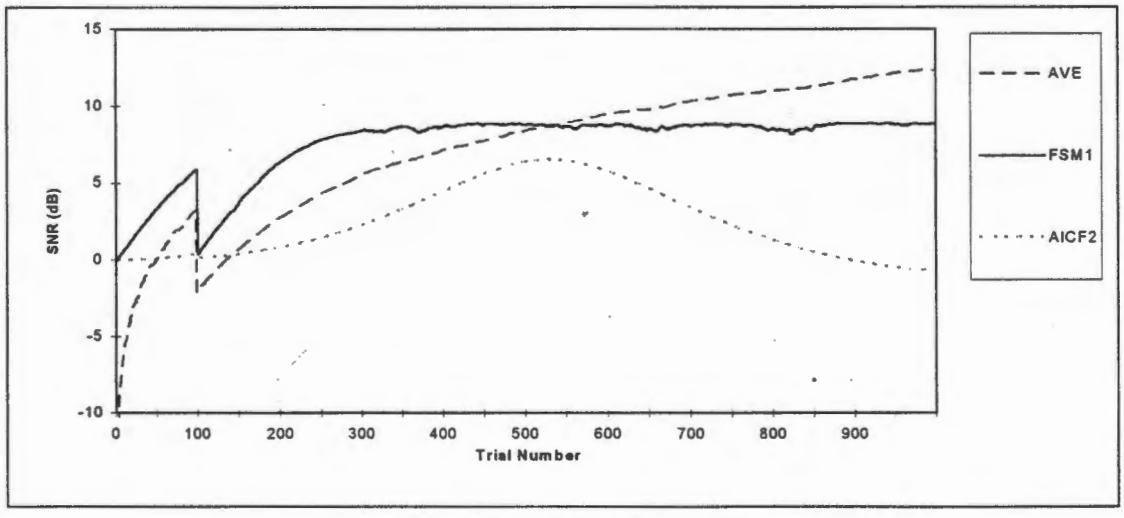

Figure 4-7: Plots of typical SNR responses of the AVE, AICF and FSM algorithms (*non-stationary* SSEP with medium level random interference).

Figure 4-7 illustrates the same responses but for a *non-stationary* SSEP. The transition in the original EP signal is clearly visible at trial 100 where there is a sudden decrease in SNR values.

Figure 4-8 illustrates the SNR responses of the AICF algorithm for the three different AICF convergence factors under consideration. AICF1, AICF2 and AICF3 show the

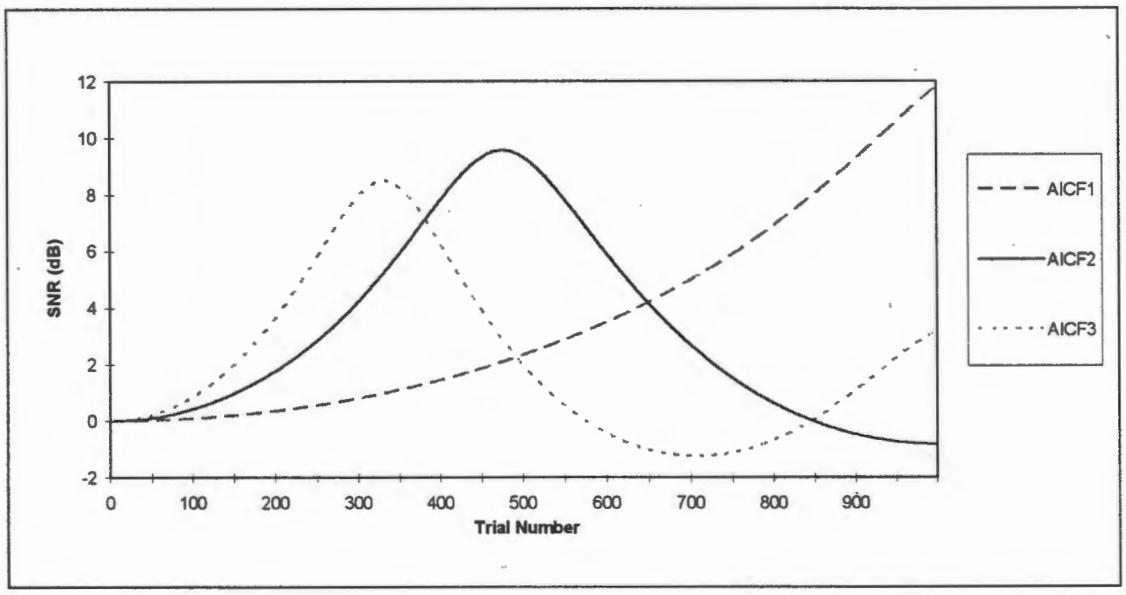

Figure 4-8: Plots of the AICF SNR response for three values of μ. (SSEP with medium random interference).

responses for increasing values of convergence factor, viz. $1x10^{-6}$, $5x10^{-6}$ and $1x10^{-5}$ respectively. As expected, AICF3 shows the most rapid increase in SNR whilst AICF1 shows the slowest rate of increase. This satisfies one of the criterion for adaptive algorithms (see Appendix E) that a larger convergence factor value results in a more rapid attempt to converge to the MMSE solution value but with greater instability in the response. This instability can be seen in the oscillatory response of AICF3 compared to AICF1 which shows a steady increase in SNR but at a much slower rate.

The convergence factor also determines the performance of the FSM algorithm which also uses the LMS algorithm for the adaptive process. The SNR responses for the FSM algorithm with three different convergence factors are illustrated in Figure 4-9.

FSM1, FSM2 and FSM3 represent the different SNR responses for increasing values of FSM convergence factor, viz. $1x10^{-5}$, $5x10^{-5}$ and $1x10^{-4}$ respectively. These plots

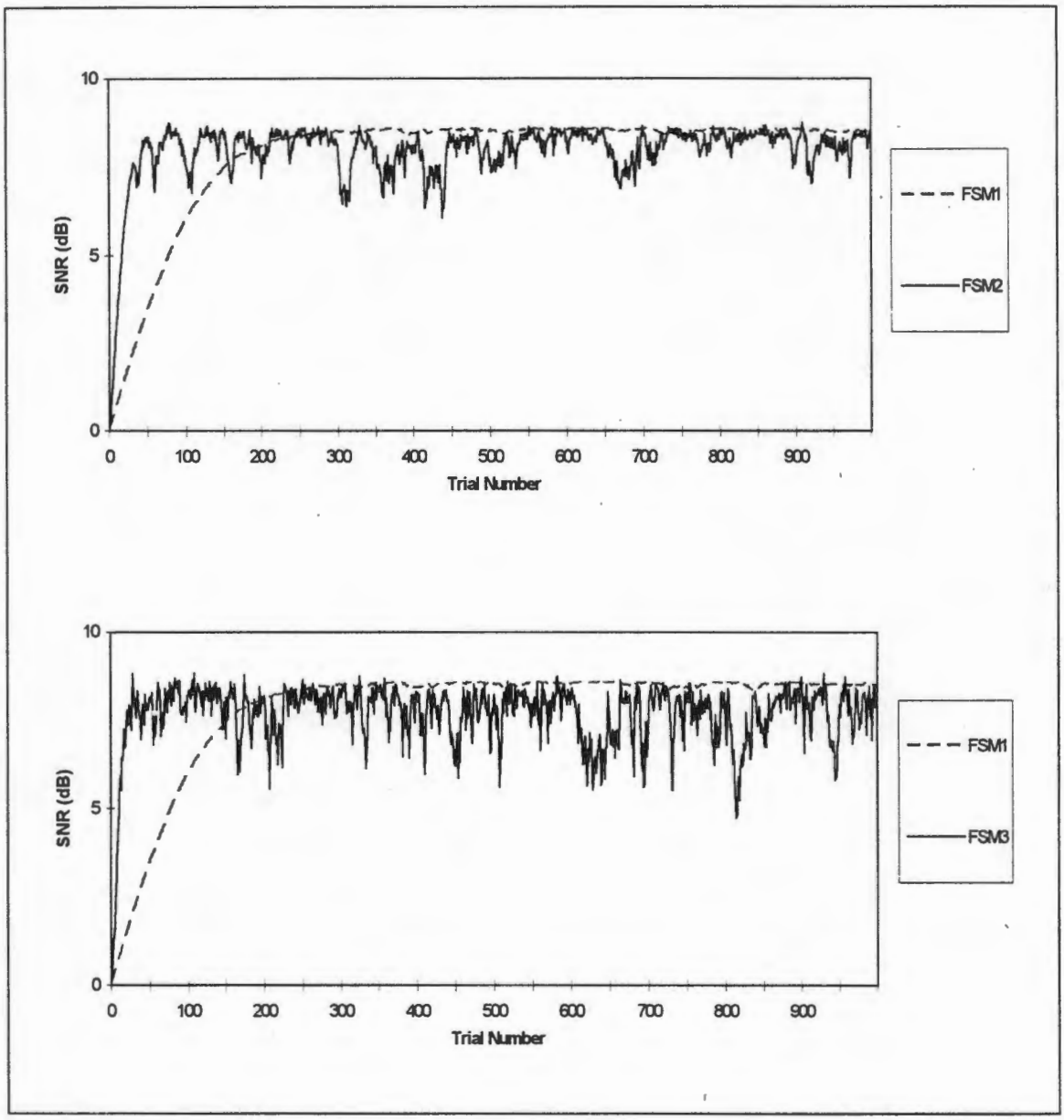

Figure 4-9: Plots of the FSM SNR responses for three values of μ. (SSEP with medium random interference). The responses are shown in two separate plots so as to show a clear distinction between FSM2 and FSM3.

also illustrate the adaptive algorithm criterion (see Appendix E) that a larger convergence factor results in a more rapid response but with greater instability in the response. This is quite clear observing FSM3. It shows a rapid increase in the SNR level until a steady level is reached. The response is however rather unstable and

oscillates around this steady level. This is in contrast to FSM1 (lower convergence factor value), where there is a slower rise to the steady SNR level but with a much greater stability in maintaining the level.

4.2 Results of Study

Results obtained for the AEP and the SSEP are presented individually. These results are from both the stationary and non-stationary EP simulations. Each of these sets is further subdivided into four sets corresponding to the type of interference added to the original EP signal. The four types of interference are:

- band-limited random interference
- 50-Hz interference
- combined band-limited random interference plus 50-Hz interference
- spontaneous EEG.

Each interference set is further subdivided into three graded amplitude levels:

- high
- medium
- low.

Results for the graded levels are however not shown individually but are lumped together into a single index by the statistical analysis.

Results are shown for each of the different combinations of the above for the AVE, AICF and FSM algorithms. The AICF and FSM algorithm results are further subdivided (three different values of convergence factor) to give a total of seven algorithm evaluations.

As indicated in the previous chapter, two parameters are presented for each permutation. The first is the SNR measured at trial numbers of 100, 200, 400 and 1000 for the AEP and 100, 200 and 400 for the SSEP. This data is derived from simulations which use *stationary* EP signals. The second is the ΔSNR derived from simulations

which use *non-stationary* EP signals. The rates of change of SNR are calculated between the transition point at trial number 100 and at trial numbers 150 and 200 respectively. These measures are referred to as ***slope(150)*** and ***slope(200)***.

The figures on the following four pages are selected graphical outputs generated by the ANOVA analysis. Figure 4-10 and Figure 4-11 show the plots of the ANOVA *interactions of interference by algorithm* for the stationary AEP and SSEP simulations after trial 400. The results presented are shown without confidence intervals because the plots would otherwise be congested and difficult to interpret. ANOVA compares the various parameters level by level for each given algorithm to give a single indicator for each type of interference. It thus lumps the graded levels together into a single index per EP type per interference type per algorithm. The unit of the response is dB.

Figure 4-12 and Figure 4-13 show the plots of the ANOVA *interactions of level by algorithm* for the AEP and SSEP simulations after trial 400. These plots are included to show some of the other interaction plots generated by the ANOVA analysis.

The ANOVA *interference by algorithm* results have been analysed and are presented in Section 4.2.1 and Section 4.2.2 as individual bar graphs plotted together for all trial numbers (100, 200, 400 and/or 1000) under investigation. These have been plotted separately for each type of interference in order to ease analysis and interpretation.

The analysis compares both SNR and ΔSNR values for each of the algorithms and indicates whether there are significant differences between the algorithms or not. The values presented in the bar graphs are the average values together with confidence intervals. Confidence intervals of 95% ($p \leq 0.05$), 90% ($p \leq 0.1$) and 80% ($p \leq 0.2$) are indicated depending on what level of confidence is needed to indicate a significant difference between the algorithms.

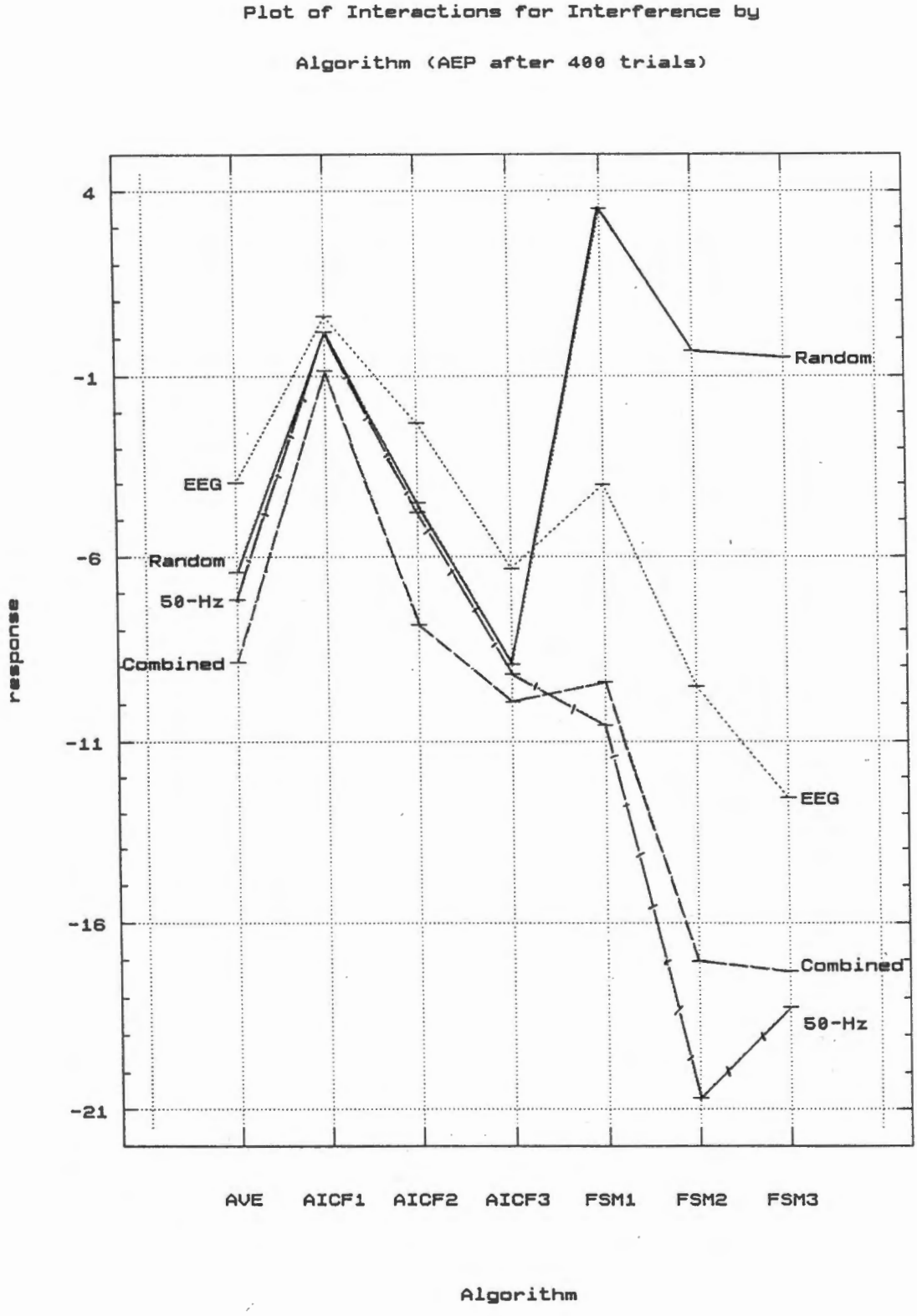

Figure 4-10: ANOVA plot of interactions of interference by algorithm (stationary AEP after 400 trials).

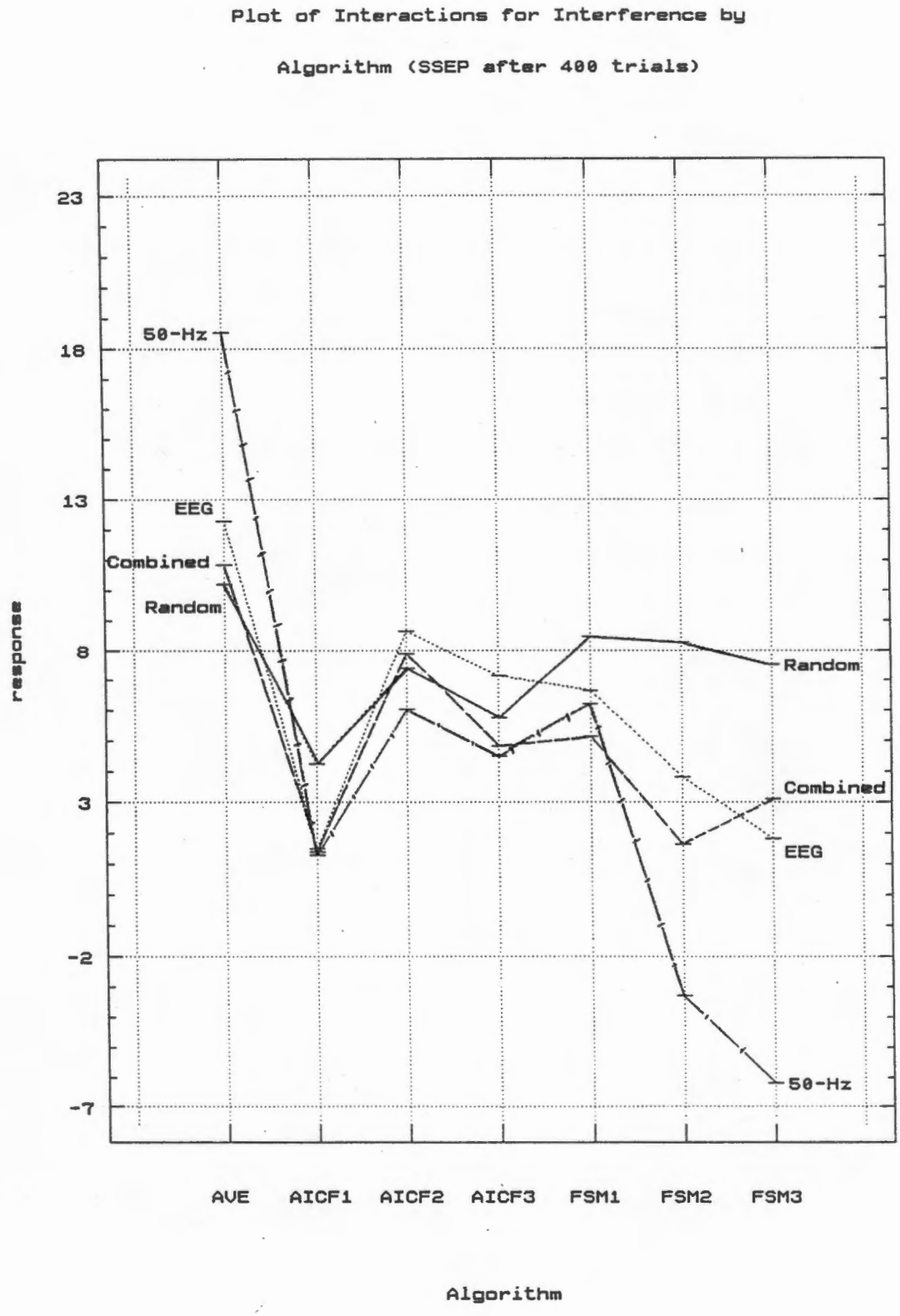

Figure 4-11: ANOVA plot of interactions of interference by algorithm (stationary SSEP after 400 trials).

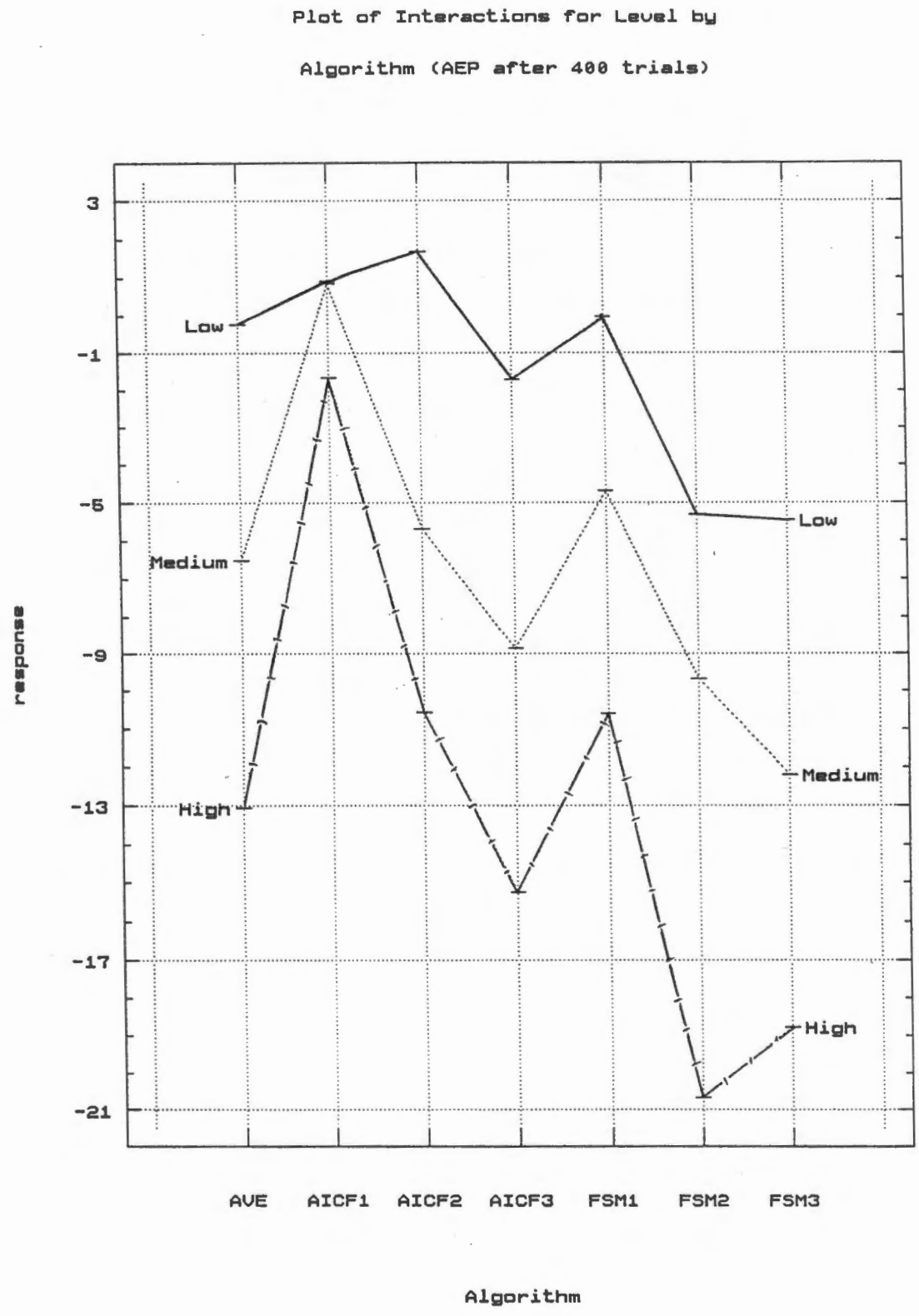

Figure 4-12: ANOVA plot of interactions of level by algorithm (stationary AEP after 400 trials).

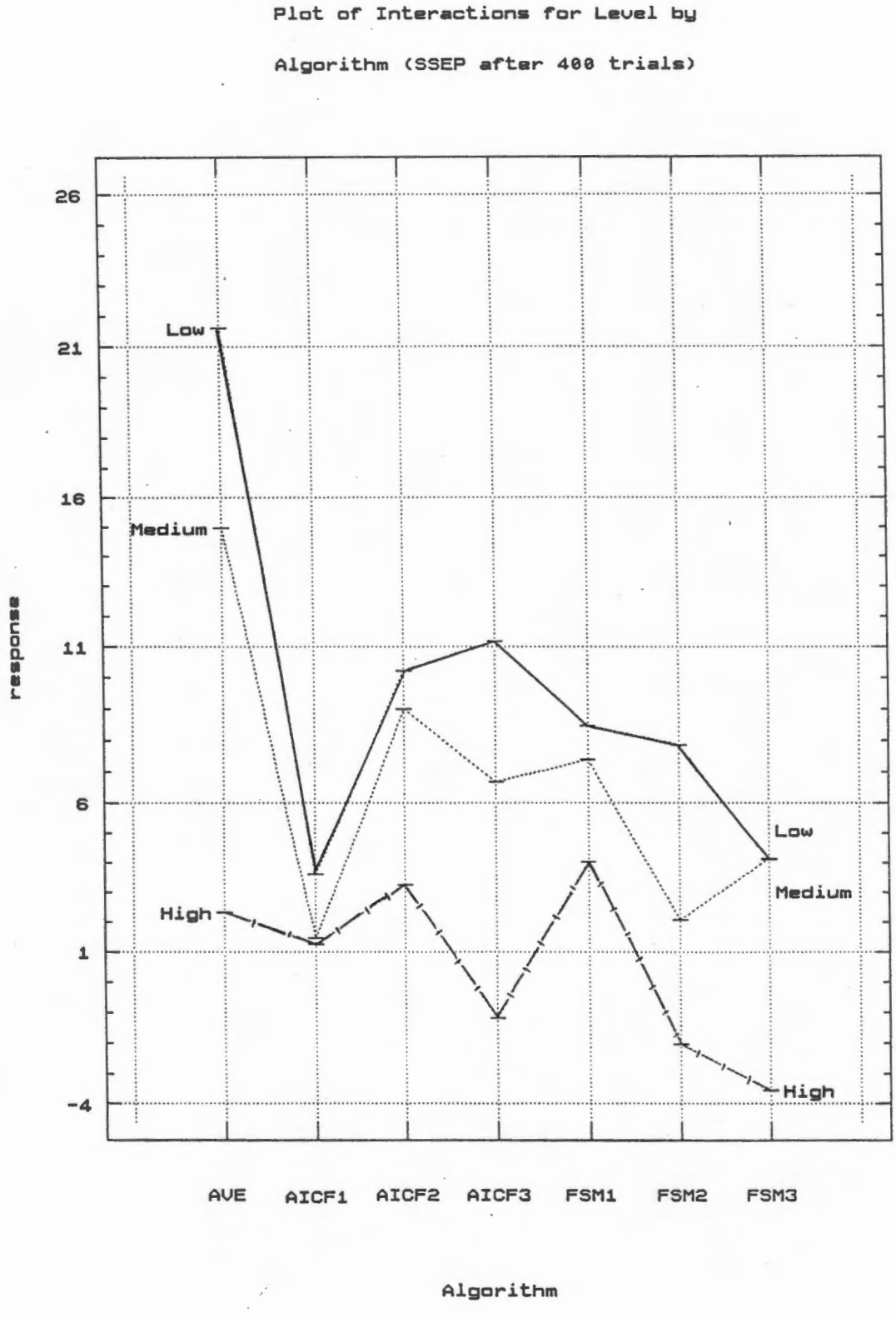

Figure 4-13: ANOVA plot of interactions of level by algorithm (stationary SSEP after 400 trials).

4.2.1 Auditory Evoked Potentials

The results for the simulations using the AEP signal are presented below for the different types of interference used in the study.

4.2.1.1 Band-limited Random Interference (AEP)

In Figure 4-14 FSM1 outperforms all the other algorithms for 100, 200, 400 and 1000 trials. The results however show no significantly dominant performer except that both the AICF and FSM algorithms perform better than the AVE. All the FSM algorithms

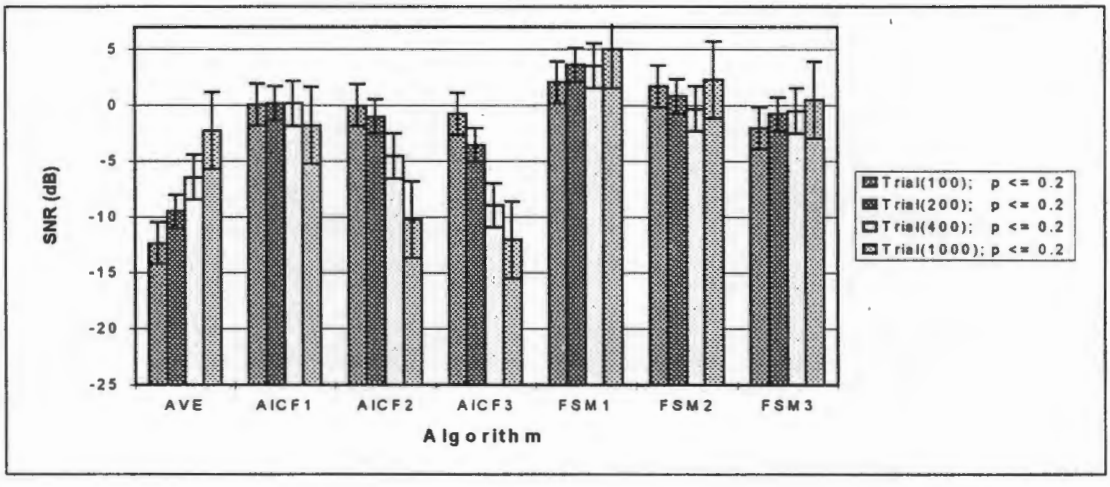

Figure 4-14: SNR - Band-limited random interference (AEP).

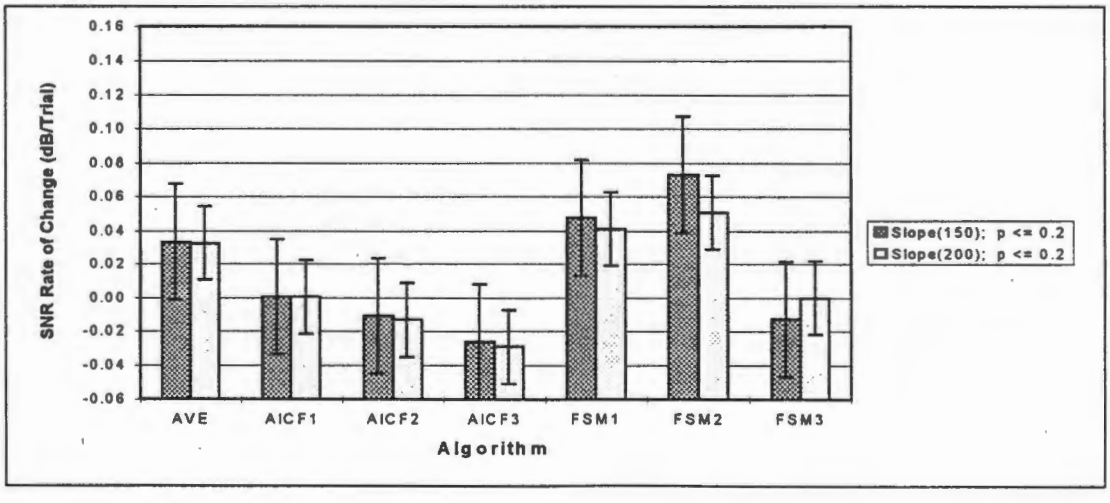

Figure 4-15: ΔSNR - Band-limited random interference (AEP).

perform significantly better than AICF2 and AICF3 after trial 400 and 1000 ($p \leq 0.2$).

In Figure 4-15 the average ΔSNR for FSM1 and FSM2 is higher than for the other algorithms. FSM2 shows significantly better performance than AICF1, AICF2 and AICF3 ($p \leq 0.2$). The AVE results are however comparable to that of FSM1 and FSM2. AICF2, AICF3 and FSM3 perform particularly poorly and have negative ΔSNR values.

4.2.1.2 50-Hz Interference (AEP)

Figure 4-16 shows that the AICF algorithms show significantly higher average SNR values than the AVE and FSM algorithms after 100 and 200 trials ($p \leq 0.05$).

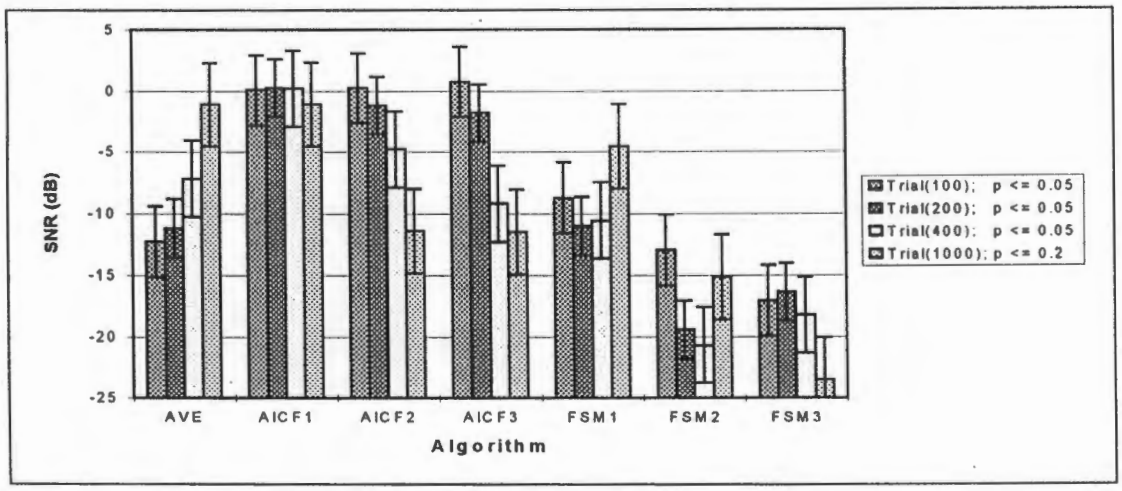

Figure 4-16: SNR - 50-Hz interference (AEP).

However, only AICF1 showed significantly higher average SNR levels than all the FSM and AVE algorithms after 400 trials ($p \leq 0.05$). By 1000 trials AVE, AICF1 and FSM1 are comparable and show significantly higher SNR values than the other algorithms ($p \leq 0.2$).

Using the more conservative slope(200) measure in Figure 4-17, FSM3 shows a significantly higher ΔSNR value than AICF1, AICF2 and AICF3 ($p \leq 0.05$). AVE also

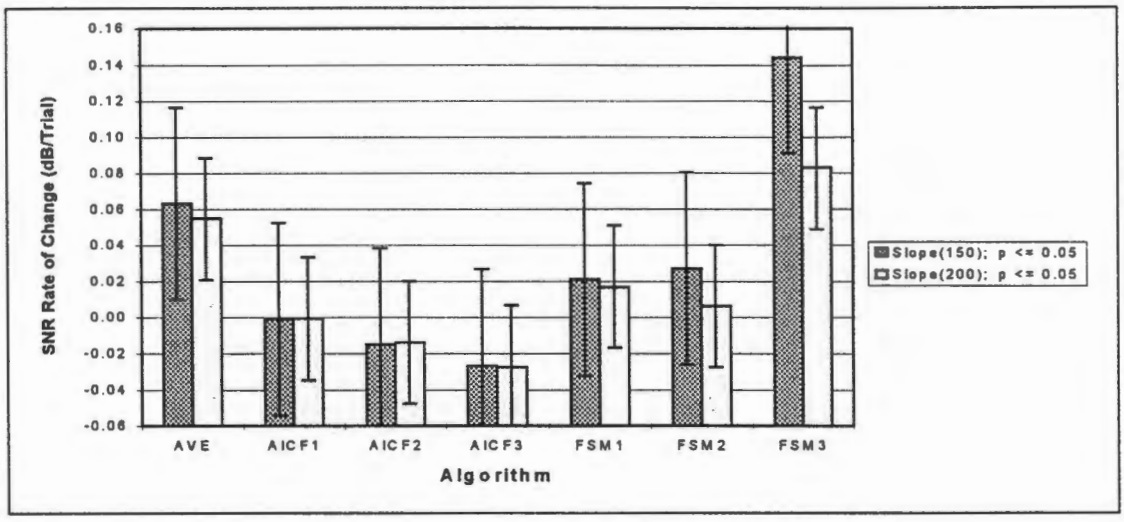

Figure 4-17: ΔSNR - 50-Hz interference (AEP).

shows a higher average ΔSNR than all FSM1, FSM2 and all the AICF algorithms. The AVE is however comparable to FSM3.

4.2.1.3 Combined Band-limited Random and 50-Hz Interference (AEP)

In Figure 4-18 all AICF algorithms perform significantly better than all the others after 100 and 200 trials ($p \leq 0.05$). AICF2 and AICF3 show SNR levels comparable to FSM1 and AVE while AICF1 significantly outperforms all the other algorithms after trail 400 ($p \leq 0.05$). After 400 trials all the other algorithms still show significantly higher SNR levels than FSM2 and FSM3 ($p \leq 0.05$).

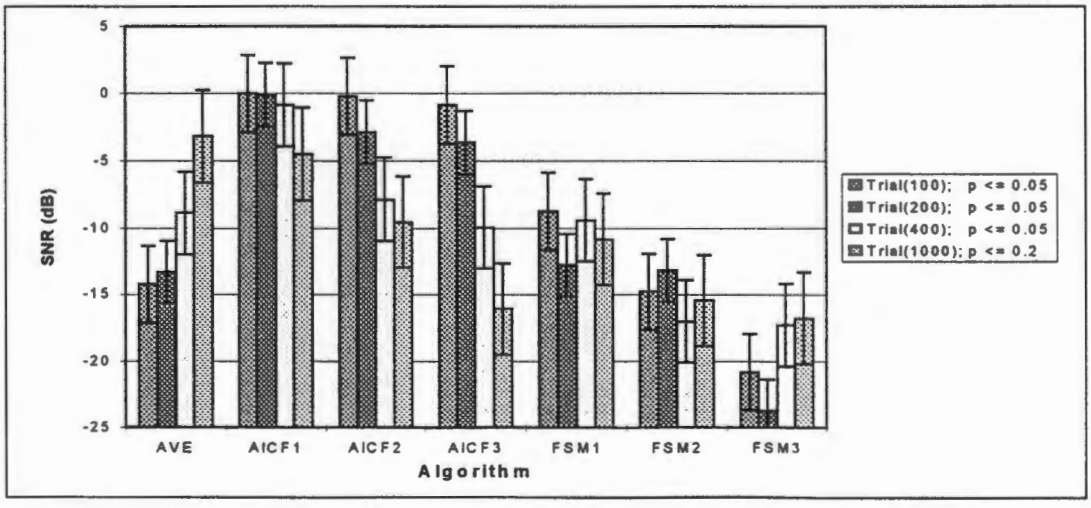

Figure 4-18: SNR - Combined band-limited random interference and 50-Hz interference (AEP).

In Figure 4-19 AVE and FSM2 show significantly higher values of slope(200) than AICF3, FSM1 and FSM3 ($p \leq 0.1$). The AICF1 and AICF2 values are not significantly

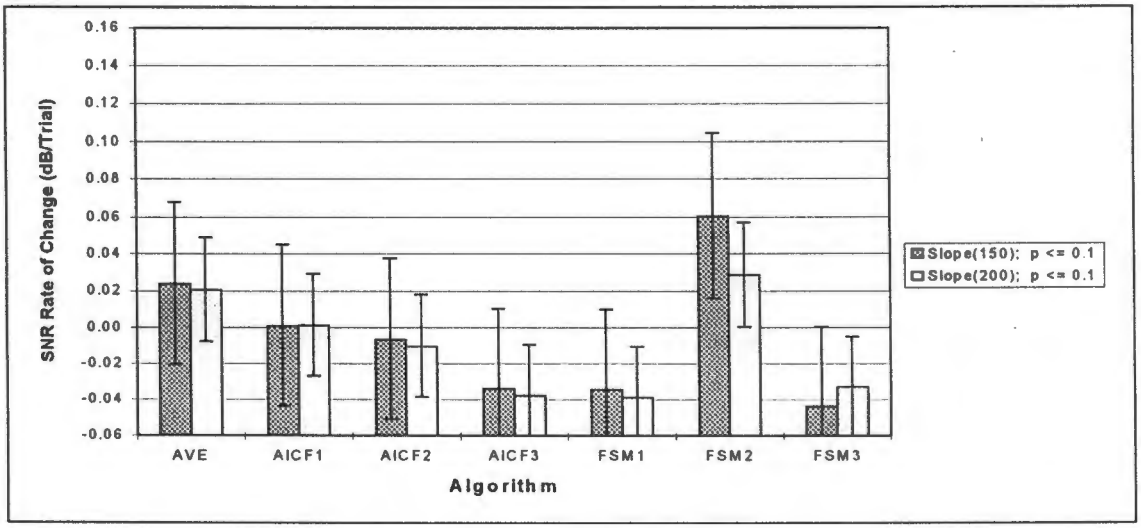

Figure 4-19: ΔSNR - Combined band-limited random and 50-Hz interference (AEP).

lower or higher than any of the other algorithms ($p \leq 0.1$). Note that the average ΔSNR of AICF2, AICF3, FSM1 and FSM3 are negative thus indicating poor performance.

4.2.1.4 EEG Interference (AEP)

In Figure 4-20 AICF1, AICF2 and AICF3 have significantly higher SNR levels than

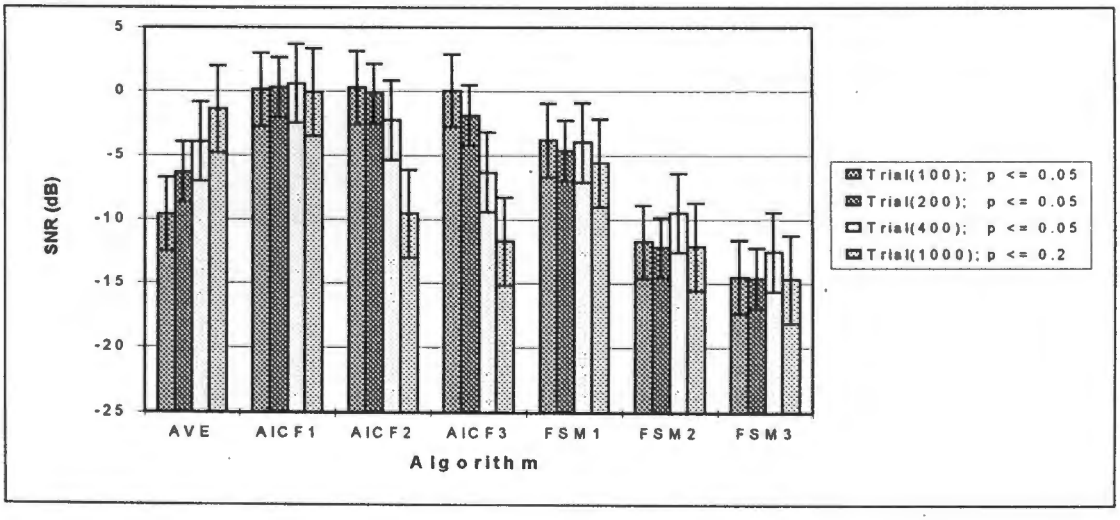

Figure 4-20: SNR - EEG interference (AEP).

FSM2, FSM3 and AVE after 100 and 200 trials ($p \leq 0.05$) (except for AICF3 and AVE after 200 trials). There is no significant difference between FSM1 and the AICF algorithms after 100, 200, 400 ($p \leq 0.05$) and 1000 trials ($p \leq 0.2$). The overall poorest performers are FSM2 and FSM3. However, AICF2 and AICF3 show decreasing SNR levels with increasing trials.

Figure 4-21 shows that the average ΔSNR values for all the AICF algorithms are negative. There are no clear significantly better performers for this measure except for AVE and FSM2 that significantly outperform AICF2 and AICF3 ($p \leq 0.2$).

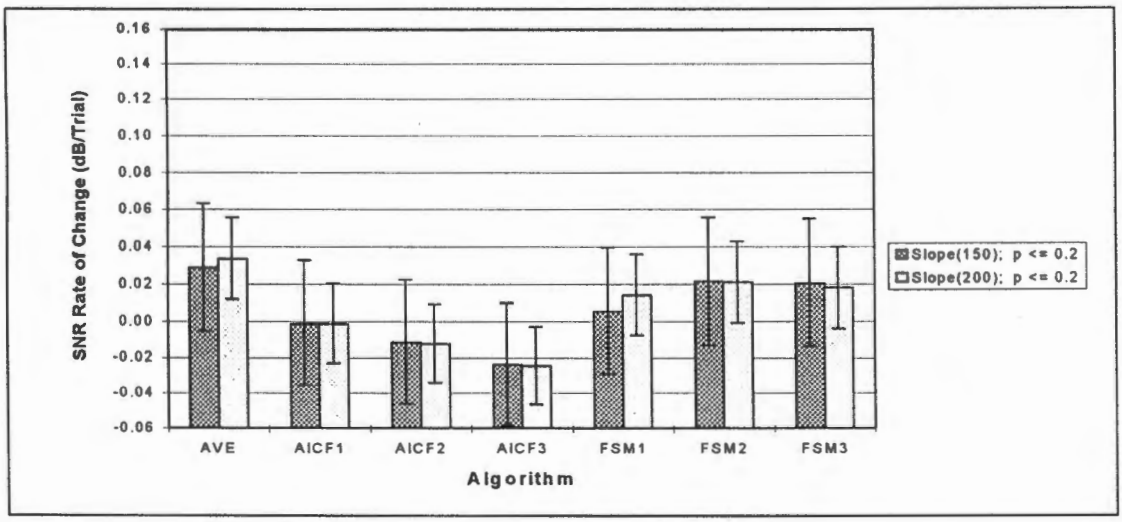

Figure 4-21: ΔSNR - EEG interference (AEP).

4.2.2 Somatosensory Evoked Potentials

The results for the simulations using the SSEP signal are presented below for the different types of interference used in the study.

4.2.2.1 Band-limited Random Interference (SSEP)

In Figure 4-22 FSM1, FSM2 and FSM3 show significantly higher SNR values than all the AICF algorithms after 100 and 200 trials ($p \leq 0.05$). By trial 400, the AICF SNR

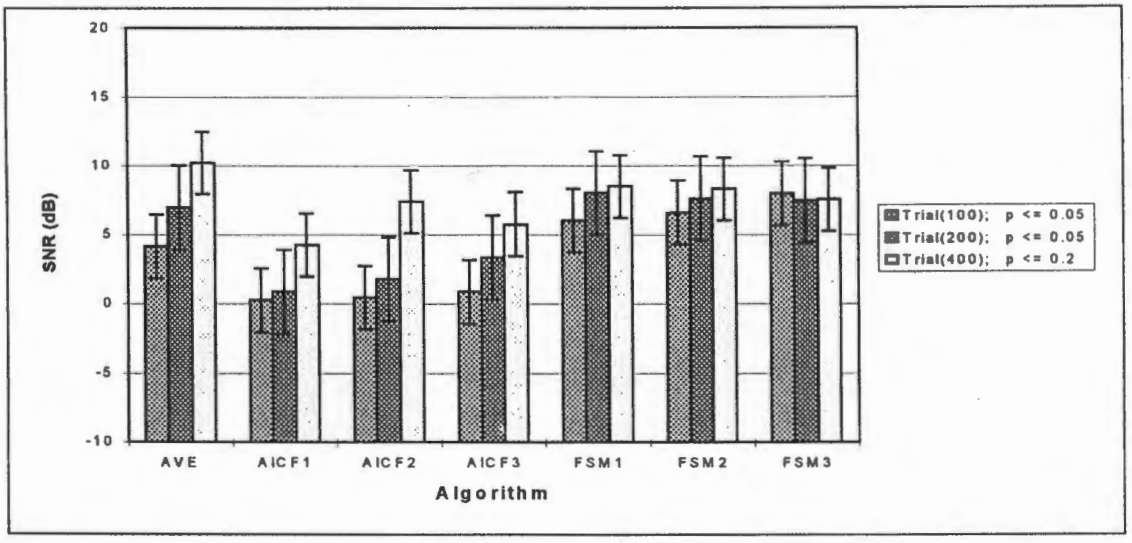

Figure 4-22: SNR - Band-limited random interference (SSEP).

values have improved to comparable levels to that of the FSM algorithms. The AVE algorithm's average SNR improves steadily with an increase in the number of trials and eventually produces the highest SNR after trial 400. All the algorithms (except FSM3) show a graded increase in the SNR with increasing number of trials.

FSM2 and FSM3 in Figure 4-23 show significantly higher values of slope(200) than all the AICF algorithms ($p \leq 0.05$). The FSM1 and AVE algorithms show ΔSNR values between the highest and lowest ΔSNR values.

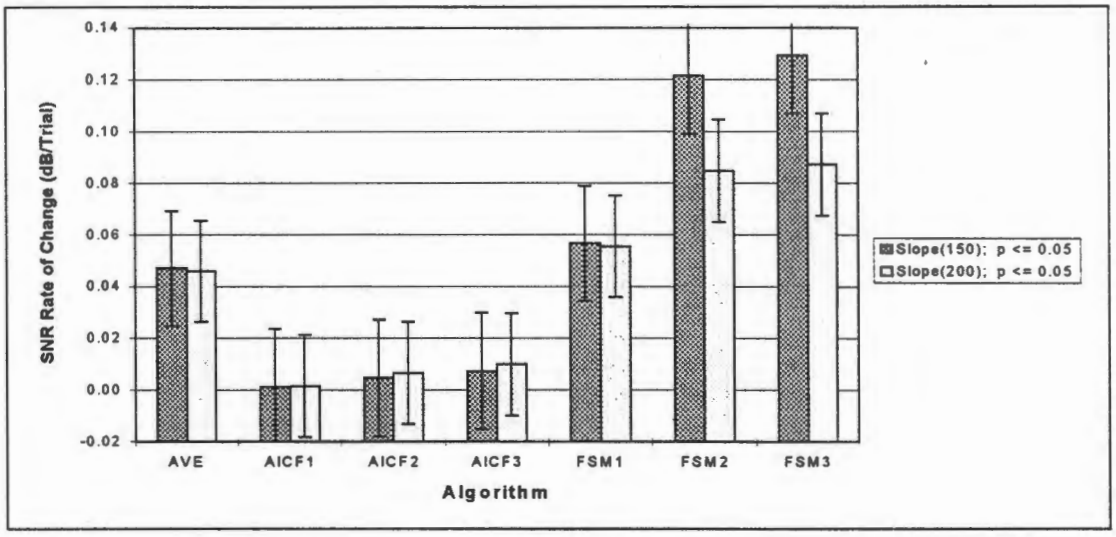

Figure 4-23: ΔSNR - Band-limited random interference (SSEP).

4.2.2.2 50-Hz Interference (SSEP)

Figure 4-24 shows the AVE algorithm performing better than all the AICF and FSM algorithms for all trial number measurements ($p \leq 0.1$). The poorest performers are FSM2 and FSM3. FSM1 performs at about the same level as the AICF algorithms.

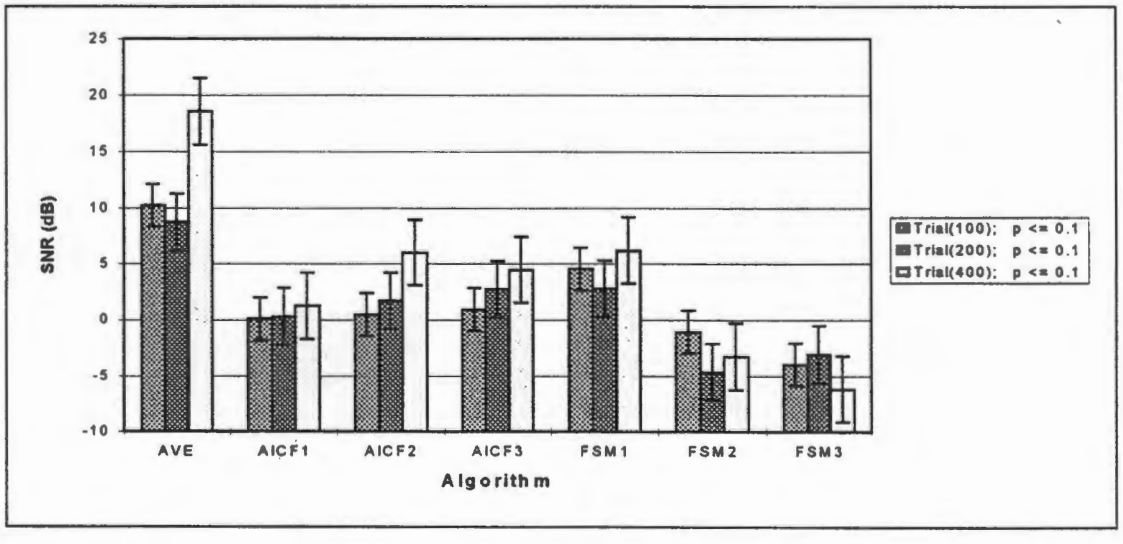

Figure 4-24: SNR - 50-Hz interference (SSEP).

AVE, FSM1 and FSM3 in Figure 4-25 show significantly higher slope(200) values than all the AICF and FSM2 algorithms ($p \leq 0.2$). All the algorithms except FSM2 show positive slope(200) values.

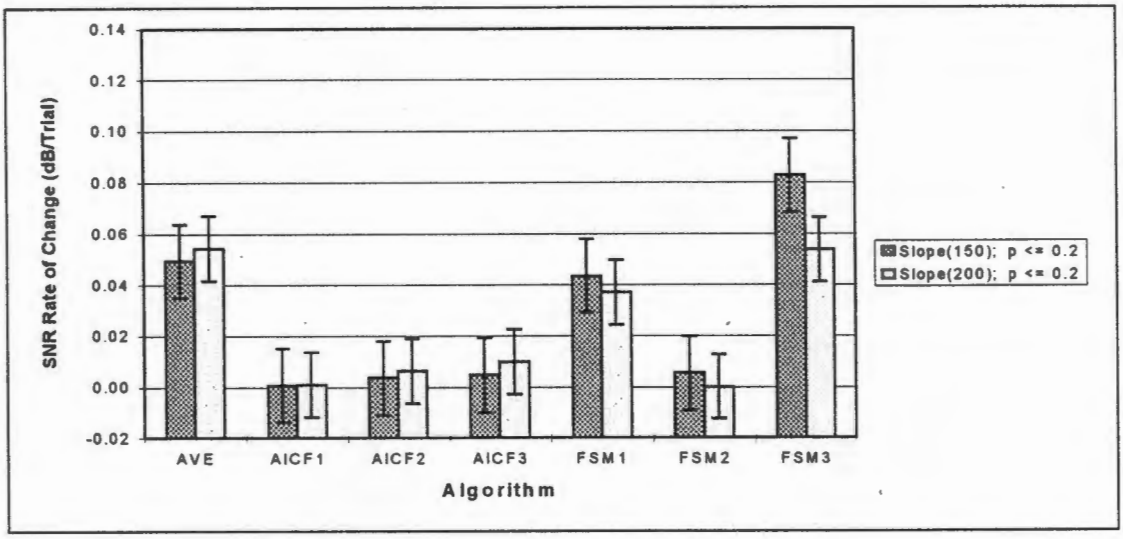

Figure 4-25: ΔSNR - 50-Hz interference (SSEP).

4.2.2.3 Combined Band-limited and 50-Hz Interference (SSEP)

In Figure 4-26 the AVE and FSM1 algorithms show significantly higher SNR values than all the AICF algorithms after 100 and 200 trials ($p \leq 0.2$). AICF1 and AICF2 only show comparable levels after trial 400. FSM1 performs better than the other FSM algorithms.

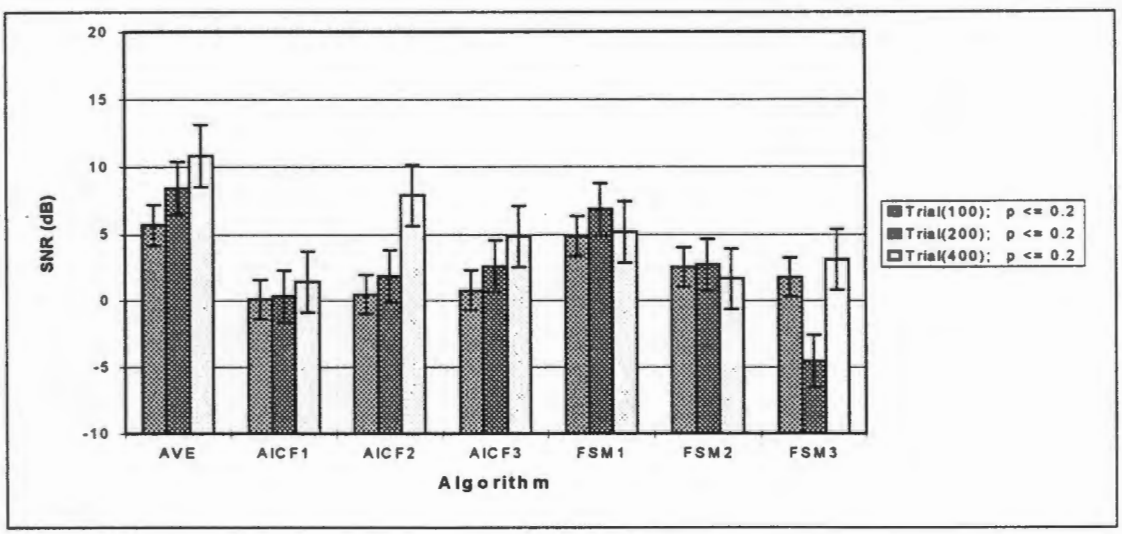

Figure 4-26: SNR - Combined band-limited and 50-Hz interference (SSEP).

The more conservative slope(200) ΔSNR measurement in Figure 4-27 shows that the AVE and FSM1 algorithms have significantly higher ΔSNR values than all the AICF and FSM3 algorithms ($p \leq 0.2$). FSM2 performs with ΔSNR values somewhere between the highest and lowest values.

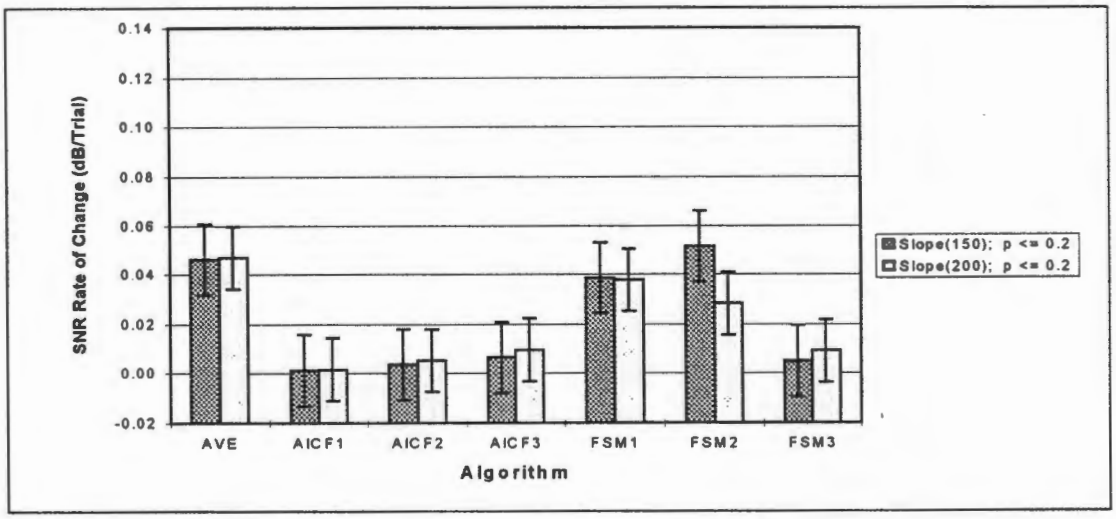

Figure 4-27: ΔSNR - Combined band-limited and 50-Hz interference (SSEP).

4.2.2.4 EEG Interference (SSEP)

The AVE and FSM1 algorithms in Figure 4-28 show significantly higher SNR values

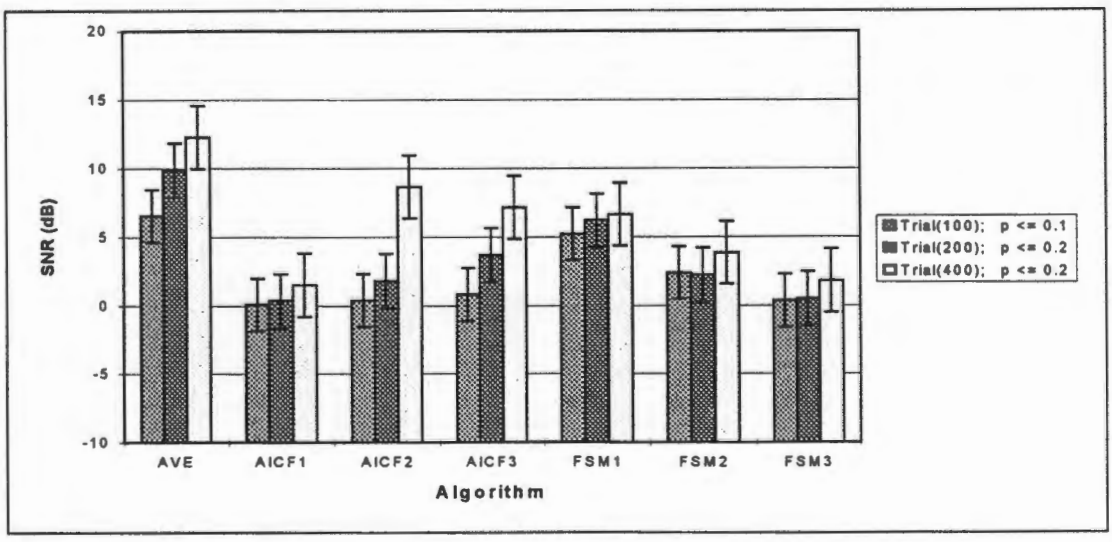

Figure 4-28: SNR - EEG interference (SSEP).

than all the AICF algorithms after trial 100 ($p \leq 0.1$). The SNR of FSM1 is significantly higher than AICF1 and AICF2 after trial 200 ($p \leq 0.2$). The SNR levels for the AICF and FSM algorithms show no significant difference after trial 400. The AVE however outperforms both the AICF and FSM algorithms after trial 400.

The AVE and FSM algorithms in Figure 4-29 show greater values of slope(200) than all the AICF algorithms ($p \leq 0.05$). The AVE and FSM algorithms perform at about the same higher level, while the AICF algorithms perform at about the same low level.

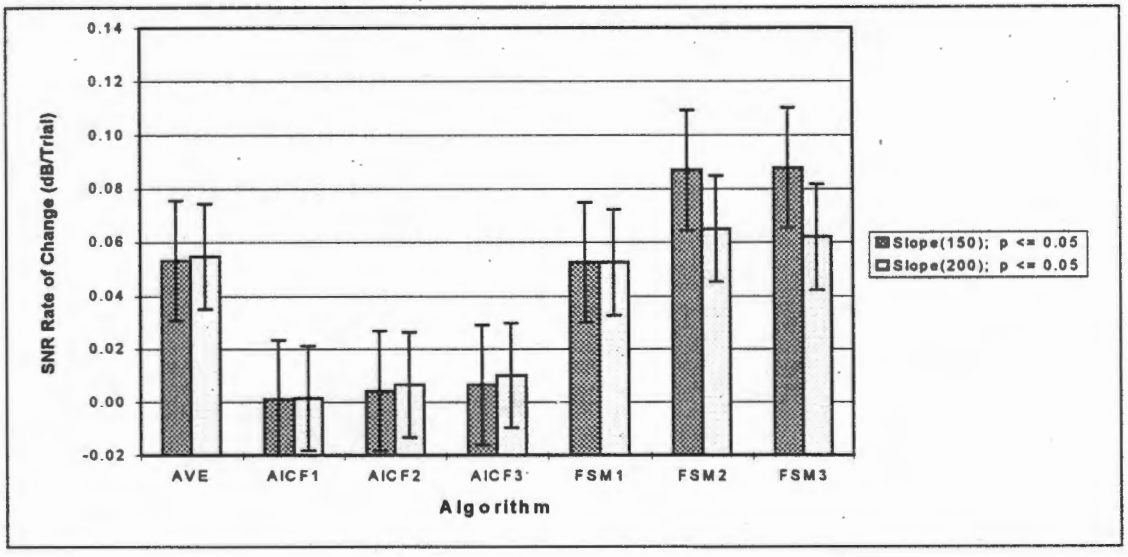

Figure 4-29: ΔSNR - EEG interference (SSEP).

CHAPTER 5

DISCUSSION

5.1 Evoked Potential Extraction System

The EPES was used to extract the EP signals from the composite EEG/EP ("raw") signal recorded in a controlled environment. The raw signals were acquired using the CEPMS and recorded onto magnetic tape for off-line analysis. The raw signals were digitised and processed by the EPES off-line. The EPES used each of the three algorithms under investigation and allowed the user to compare the extracted EP signal estimates.

The EP signals extracted using the EPES compared well with those extracted by the CEPMS, by visual inspection. These extracted EP signals were used in the simulation stage of this project. The EPES system was also used to acquire the EEG signals which were used as interference signals in the simulation study.

The front-end patient data was intended to be used in a pilot study to test the EPES under conditions of surgical anaesthesia in real-time and on-line. This could not be done because of problems experienced with the front-end. The original front-end, which was designed to be used as a general purpose biosignal amplifier unit, was modified to be used with the EPES. This modification included the extension of the original bandwidth. The front-end configuration was tested but did not perform satisfactorily for the purposes of testing the EPES under conditions of surgical anaesthesia. Because of the very large gain required, problems were experienced with saturation of the amplifiers. When the amplifiers saturated, they had very long recovery periods. The extension of the front-end bandwidth also resulted in the introduction of high level high frequency oscillations in the amplifier and filter system. The simulator buffer unit is physically part of the same printed circuit board as the channel amplifier and filters units. This resulted in a certain amount of crosstalk between the high level

stimulation triggers and the low level analogue input channels. Problems with excessive amounts of 50-Hz interference were also experienced.

Since on-line signal acquisition was not the focus of this project, it was decided to accept that these difficulties would require considerable resources to correct and it is recommended that the front-end be redesigned specifically for EP extraction. The problems discussed above should be addressed. The EPES system may then be tested in the surgical environment using the redesigned front-end.

The EPES menu-driven and mouse supported user interface allows for ease of operation. All options are readily available within the software shell. The software was designed such that more options or features may be added to the menu system relatively easily.

A feature-tracking facility should be included in the software. This should allow the user to mark particular peaks or troughs which the software should then be able to track. There should be a continuous numerical display of the latencies and relative amplitude values of each of the peaks being tracked. A facility to plot these feature data sets while the extraction process is taking place should also be provided. In addition to this, the feature data should also be logged to a file for later analysis.

A patient information facility should also be included. This should allow the user to enter patient data as well as information about significant incidents that occurred during the execution of the procedure.

The present system allows for artefact handling in the form of a simple threshold detector but the user is not explicitly warned as to when the automatic artefact rejection facility is discarding trials. A facility that warns the user when artefacts are being detected should be included in the system. This would provide the user with an indication of whether the signal levels are too high over a continuous period of time allowing the user to make the necessary signal level adjustments.

A facility allowing for the calibration of signal levels should also be included. At present the amplitudes are indicated in terms of arbitrary units. A calibration routine should allow for the setting of amplitude levels using a calibration signal with a known amplitude prior to starting an extraction sequence. This information should be saved with each trial file.

The system runs under the MS-DOS operating system which has a 640 KB limit in terms of space available for the code and data. This sets a limit on the temporal size of the signals being extracted. The use of an operating system such as OS/2 would be worth considering since it uses a flat memory model and the code and data space is only limited by the physical memory available. The speed of operation and extraction can be improved by the use of DSP technology. A DSP device could perform all the "number-crunching" associated with the extraction algorithms while the PC is free to manage the user-interface and display the results.

5.2 Simulation Study

This discussion is based on the results obtained from the simulation study and statistical analysis.

5.2.1 Relative Performance of Algorithms

The performance of the algorithms for each of the AEP and SSEP signals in relation to each type of interference is discussed in this section.

(a) Auditory Evoked Potentials

Band-limited Random Interference

FSM1 performs significantly better than the AVE and AICF algorithms after trial 1000 ($p \leq 0.2$). FSM1 shows an improving SNR response. The AVE algorithm shows an increasing SNR response as well but the SNR values are significantly lower than those

of FSM1 for all trials ($p \leq 0.2$). All the AICF algorithms show a declining SNR response. This could be explained by the very low level of the underlying AEP signal with the algorithm seemingly unable to extract this signal.

50-Hz Interference

Again the AICF algorithms, particularly AICF2 and AICF3, show declining SNR responses and there are no signs of improvement even after trial 1000, despite starting at SNR levels significantly higher than the other algorithms ($p \leq 0.05$). This decline is confirmed by the negative ΔSNR values for the AICF algorithms. FSM1 and AVE have comparable SNR levels but it seems as if the FSM algorithms had difficulty in extracting the underlying signal and drifted at low SNR levels. The AVE algorithm does show an improving SNR response with an increasing number of trials while FSM1 only shows an increasing SNR response from trials 400 to 1000.

Combined Band-limited Random and 50-Hz Interference

The AVE algorithm shows an improving SNR response with increasing number of trials while the AICF algorithms show decreasing SNR responses. Again the AICF algorithms start at significantly higher SNR values compared to the AVE and FSM algorithms after trials 100 and 200 ($p \leq 0.05$).The FSM algorithms show no significant changes and again show oscillating SNR responses at low levels.

EEG Interference

The FSM algorithms show no significant changes in the SNR response. They however show higher starting levels which are comparable to those of the AICF algorithms. There are no significant differences between AICF1 and FSM1 after 100, 200, 400 and 1000 trials. AICF1 shows a slight improving SNR response but starts to decline after trial 400. AICF2 and AICF3 again show declining responses from the start. The AVE algorithm shows an increasing SNR response and the SNR levels become comparable to those of FSM1 and AICF1 after trial 1000.

(b) Somatosensory Evoked Potentials

Band-limited Random Interference

The FSM algorithms perform better in terms of SNR than the AICF algorithms up to trial 100 ($p \leq 0.05$). The SNR responses of the FSM algorithms increase rapidly and reach a plateau. The AICF algorithms show a steady increase in SNR but these values only become comparable to those of the FSM algorithms after trial 400. The FSM algorithms show significantly higher ΔSNR values than AICF ($p \leq 0.05$) and this would be expected looking at the previous observation. The AVE algorithms shows a steady increase in the SNR, but does not show as high a ΔSNR as those of the FSM algorithms ($p \leq 0.05$). It would therefore seem that the FSM algorithms generally outperform the AICF algorithms because of their fast initial response.

50-Hz Interference

Generally the FSM algorithms, particularly those with the higher convergence factors (FSM2 and FSM3), perform poorly in extracting the EP signal from the 50-Hz interference. The significantly higher ΔSNR value for FSM3 is indicative of the higher convergence factor used for this algorithm ($p \leq 0.2$). Higher convergence factors are usually associated with a fast initial response but accompanied by instability in tracking the underlying signal (see Appendix E). This is confirmed by the lower SNR values of FSM2 and FSM3 compared to FSM1 ($p \leq 0.1$). These results confirm the findings by Thakor et al. *(1993)* that the FSM algorithm cannot adequately handle dominant periodic signals such as 50-Hz mains interference. The AICF algorithms show a steady increase in SNR with the FSM1 algorithm showing SNR values comparable to the AICF algorithms. When experiencing transients in the EP signal, FSM1 shows good ΔSNR values which are comparable to that of the AVE algorithm. The AVE algorithm handles 50-Hz interference well with significantly higher SNR levels than the other algorithms after trials 100, 200 and 400 ($p \leq 0.1$).

Combined Band-limited Random and 50-Hz Interference

FSM1 shows a significantly higher SNR than all the AICF algorithms after 100 and 200 trials ($p \leq 0.2$). AICF 2 and AICF3 only start showing comparable levels after trial 400. The FSM1 values are comparable to those of the AVE algorithm after trial 100 and 200 thus showing an improvement in FSM algorithm performance compared to that for only 50-Hz interference. FSM1 and FSM2 also show ΔSNR values comparable to that of the AVE algorithm and these are significantly higher than the AICF values ($p \leq 0.2$). This result is expected because the AICF algorithms show a slow initial response and only start showing a rapid increase in SNR after trial 200. As expected, the AVE algorithm shows an increasing SNR and attains the highest SNR after trial 400 ($p \leq 0.2$).

EEG Interference

The FSM1 algorithm reaches a higher SNR than all the AICF algorithms after trial 100 ($p \leq 0.1$). After trial 400, there are however no significant differences in SNR between the FSM1 and AICF algorithms. As before, the AICF algorithms show a rapid increase in SNR after a larger number of trials. The slow initial responses of the AICF algorithms are confirmed by the significantly lower ΔSNR values recorded ($p \leq 0.05$). After trial 400, all the algorithms seem to have comparable SNR values.

5.2.2 Use of the FSM and AICF in DOA Monitoring

The AEP simulations are representative of situations where the underlying signal has levels very much lower than the interference. The results tend to suggest that the AICF algorithms cannot extract the underlying signal at the signal and interference amplitude levels used. They consistently perform poorly with increasing number of trials. The FSM algorithms generally oscillate and seem to attempt to extract the underlying signal. They perform particularly badly under conditions where the interference is dominated by a periodic interference such as 50-Hz. The AVE algorithm shows a steady improvement in SNR response but the SNR levels are still very low compared to the SSEP results.

The SSEP simulation results are representative of situations where the EP signal is of a suitable level in comparison to the levels of interference. The SSEP used in the study has an amplitude 10 times that of the AEP signal. When compared to the AEP simulation results we see that all the algorithms perform much better and provide more acceptable results. The FSM algorithms perform well from the start and generally reach adequate SNR levels after 100 trials. The AICF algorithm has a very unusual SNR response. The decrease in SNR level after a peak is a characteristic of this algorithm. However, it is able to reach high SNR levels. This feature may be harnessed because it could be predicted when a maximum SNR is reached. The occurrence of this peak SNR seems to be a function of the convergence factor value. The larger the value of the convergence factor, the earlier the peak SNR occurs.

Algorithms that respond quickly to changes in the EP signal as well extracting the signal within the fewest number of trials are most suitable for DOA monitoring. In this regard the FSM seems to be a more suitable algorithm to use. Even though the SNR levels of the FSM algorithm are not as high as the AVE algorithm levels (after 400 trials), the FSM algorithm is able to respond more rapidly to changes in the underlying EP signal. One limitation of the FSM algorithms is that they are unable to deal with a periodic signal as a primary component of the interference. A notch filter may be useful in removing periodic signals prior to attempting the EP extraction.

The convergence factors used by the AICF and FSM algorithms present a trade-off between the rate at which an optimal SNR level (MMSE solution) is reached and the stability with which this level is maintained. An increased convergence factor will result in a more rapid approach of the optimal SNR level but with poorer stability performance. The converse also holds true. The optimum convergence factor is one that provides rapid enough approach of the optimal SNR level with satisfactory maintenance of this level.

CHAPTER 6

CONCLUSIONS AND RECOMMENDATIONS

6.1 Conclusions

1) A literature review was performed. Three algorithms, viz. an *adaptive impulse correlated filter*, a *Fourier series model* and the *synchronous time averaging* algorithm were selected for extraction of EP signals for DOA monitoring.

2) A PC-based *evoked potential extraction system* was implemented which could be used to track EP signals. The system provides a user-friendly interface and allows for the extraction, display and storage of EP data. The design and implementation consisted of software development using the C++ programming language.

3) The system was used to extract EP signals off-line from data recorded in a quiet and controlled environment.

4) A simulation study was performed in which the three algorithms were tested using different types of interference combined with stationary and non-stationary AEP and SSEP signals. A total of 1000 trials were executed in each case. SNR results were compared at 100, 200 and 400 trials for the AEP and 100, 200, 400 and 1000 trials for the SSEP. ΔSNR values were also determined for the non-stationary EP signals.

5) The simulations using the lower level AEP signal indicate that the AICF algorithm shows a declining SNR response while the FSM algorithm tends to drift at low levels attempting to extract the signal. It seems to suggest that if the underlying signal amplitudes are very low in comparison to the interference (the

peak amplitudes having a ratio of 1:100 in the worst case), then the AICF and FSM algorithms may be unable to extract the EP signals.

6) The results of the higher level SSEP (10 times higher amplitude than the AEP) simulations lead to the following conclusions. The FSM algorithm tends to provide faster initial extraction of the underlying EP signal compared to the AICF algorithm. The FSM algorithm exhibits a greater ability to adapt to changes and track theses changes. However, the FSM algorithm is sensitive to dominant periodic signals (50-Hz mains interference).

7) The FSM algorithm has a SNR response that generally levels out at a value which could be regarded as adequate for EP monitoring. This is unlike the AVE algorithm which exhibits a SNR response which could theoretically improve to infinity as the number of trials increase.

8) The AICF algorithm shows a particularly predefined SNR response which appears to be unaffected by the nature of the interference. It typically has a bell-shaped SNR response and thus shows a decline in the SNR after a certain number of trials. The occurrence of the maximum SNR seems to be a function of the convergence factor chosen. The larger the convergence factor, the earlier the maximum occurs.

6.2 Recommendations for Future Development

The following recommendations are made:

1) A front-end amplifier customised for monitoring EP signals in the surgical environment needs to be designed and implemented. This unit should consist of two parts, housing the data acquisition hardware and the stimulation triggering hardware separately.

2) A feature tracking facility allowing for the tracking of specific peaks or troughs of the EP signals should be added to the *evoked potential extraction system* software. The recording of patient information, artefact rejection indicators and calibration facilities should also be incorporated into the software.

3) Note should be taken of the types of interference present during EP monitoring and the extraction algorithms should be chosen accordingly.

4) When using the FSM algorithm, it would be useful to remove periodic interference such as 50-Hz mains interference prior to the extraction of the EP signal. This could be achieved using a simple FIR filter with "zeros" at 50 Hz or timing the stimulation pulses taking into account the phase of the 50-Hz cycle (e.g. alternating stimulation pulses during positive and negative slopes).

5) When using the adaptive FSM or AICF algorithms, the convergence factors must be adjusted to provide adequately fast initial extraction but still maintaining the necessary stability as the number of trials increase.

6) The extraction algorithms should be implemented using embedded DSP technology if they are to be used on-line during surgery. This would speed up the extraction time.

7) Future studies should consider the implementation of single trial extraction methods such as segmented matched filters as proposed by Lange et al. *(1995)*.

REFERENCES

AL-NASHI H
1986
A maximum likelihood method for estimating EEG evoked potentials.
IEEE Transactions on Biomedical Engineering, BME-33(12): 1087-1095

AUNON JI, SENCAJ RW
1978
Comparison of different techniques for processing evoked potentials.
Medical and Biological Engineering and Computing, 16: 642-650

BANKMAN I, GATH I
1987
Feature extraction and clustering of EEG during anaesthesia.
Medical and Biological Engineering and Computing, 25: 474-477

BLITT CD
1985
A philosophy of monitoring.
pp 1-4 In: Monitoring in Anesthesia and Critical Care Medicine, Blitt CD (ed), New York: Churchill Livingstone

BRONZINO JD
1984
Quantitative analysis of the EEG - General concepts and animal studies.
IEEE Transactions on Biomedical Engineering, BME-31(12): 850-856

CERUTTI S, CHIARENZA G, LIBERATI D, MASCELLANI P, PAVESI G
1988
A parametric method of identification of single-trial event-related potentials in the brain.
IEEE Transactions on Biomedical Engineering, 35(9): 701-711

CHIAPPA KH
1990
Advanced techniques of evoked potential acquisition and processing.
pp 609-629 In: Evoked Potentials in Clinical Medicine 2nd ed, Chiappa KH (ed), New York: Raven Press

CHILDERS DG
1988
Evoked potentials.
pp 1245-1254 In: Encyclopaedia of Medical Devices and Instrumentation, Webster JG (ed), New York: John Wiley & Sons

CLARSON VH, LIANG JJ
1989
Mathematical classification of evoked potential waveforms.
IEEE Transactions on Systems, Man, and Cybernetics, 19(1): 68-73

COHEN A
1986
Biomedical signal processing. Volume 1: Time and frequency domains analysis.
Florida: CRC Press

DAVILA CE, MOBIN MS
1992
Weighted averaging of evoked potentials.
IEEE Transactions on Biomedical Engineering, 39(4): 338-345

DONEGAN JH
1985
The electroencephalogram.
pp 323-343 In: Monitoring in Anesthesia and Critical Care Medicine, Blitt CD (ed),
New York: Churchill Livingstone

DUMERMUTH G
1973
Numerical spectral analysis of the electroencephalogram.
pp 5A33-5A53 In: Handbook of Electroencephalography and Clinical
Neurophysiology, vol 5, part A, Remond A (ed), Amsterdam: Elsevier

DZWONCZYK R, HOWIE MB, McDONALD JS
1995
A comparison between Walsh and Fourier analysis of the electroencephalogram for tracking the effects of anesthesia.
IEEE Transactions on Biomedical Engineering, 42(3): 317-321

FURST M, BLAU A
1991.
Optimal a posteriori time domain filter for average evoked potentials.
IEEE Transactions on Biomedical Engineering, 38(9): 827-833

GEVA AB, PRATT H
1994
Unsupervised clustering of evoked potentials by waveform.
Medical and Biological Engineering and Computing, 32: 543-550

GEVINS AS, AMINOFF MJ
1988
Electroencephalography: brain electrical activity.
pp 1084-1107 In: Encyclopaedia of Medical Devices and Instrumentation, Webster JG (ed), New York: John Wiley & Sons

GLARIA AP, MURRAY A
1983
Development of dynamic display for cerebral function analysis and its use during open heart surgery.
Clinical Physics and Physiological Measurement, 4(4): 455-459

GRANTHAM CD, HAMEROFF SR
1985
Monitoring anesthetic depth.
pp 427-440 In: Monitoring in Anesthesia and Critical Care Medicine, Blitt CD (ed), New York: Churchill Livingstone

GRUNDY BL
1985
Evoked potential monitoring.
pp 345-411 In: Monitoring in Anesthesia and Critical Care Medicine, Blitt CD (ed), New York: Churchill Livingstone

GUO X, THAKOR NV
1990
Adaptive Walsh estimation of time-varying evoked potential signals.
Annual International Conference of the IEEE Engineering in Medicine and Biology Society, 12(2): 0866-0867

HENEGHAN CPH, THORNTON C, NAVARATNARAJAH M, JONES JG
1987
Effect of isoflurane on the auditory evoked response in man.
British Journal of Anaesthesia, 59: 277-282

JACOBSON B, WEBSTER JG
1977
Surgery.
pp 505 - 519 In: Medicine and Clinical Engineering, New Jersey: Prentice-Hall

JONES JGJ
1988
Awareness under anaesthesia.
Anaesthesia Rounds, Number 21, England: ICI Pharmaceuticals

KEIRN ZA, AUNON JI
1990
The bimodal evoked potential and a simple additive model.
Annual International Conference of the IEEE Engineering in Medicine and Biology Society, 12(2): 0862-0863

LAGUNA P, JANÉ R, MESTE O, POON PW, CAMINAL P, RIX H, THAKOR NV
1992
Adaptive filter for event-related bioelectric signals using an impulse correlated reference input: comparison with signal averaging techniques.
IEEE Transactions on Biomedical Engineering, 39(10): 1032-1043

LANGE DH, PRATT H, INBAR GF
1995
Segmented matched filtering of single event related evoked potentials.
IEEE Transactions on Biomedical Engineering, 42(3): 317-321

LIBERATI D, BEDARIDA L, BRANDAZZA P, CERUTTI S
1991
A model for the cortico-cortical neural interaction in multisensory evoked potentials.
IEEE Transactions on Biomedical Engineering, 38(9): 879-890

LOPES DA SILVA F
1993
Event-related potentials: methodology and quantification.
pp 877-886 In: Electroencephalography: Basic Principles, Clinical Applications, and Related Fields 3rd ed., Niedermeyer E, Lopes Da Silva F (eds), Baltimore: Williams & Wilkins

MAGATANI K, TAKASE T, KIMURA Y, et al.
1985
Monitoring anesthesia using auditory brainstem response.
Medical and Biological Engineering and Computing, 23 Suppl (Pt 1): 735-736

McGILLEM CD, AUNON JI
1977
Measurement of signal components in single visually evoked brain potentials.
IEEE Transactions on Biomedical Engineering, BME-24(3): 232-241

MOORE DS, McCABE GP
1993
Introduction to the practice of statistics, 2nd edition.
New York: W. H. Freeman and Company

NETER J, WASSERMAN W, WHITMORE GA
1993
Applied statistics, 4th edition.
Boston: Allyn and Bacon

NUWER MR
1986
Evoked potential monitoring in the operating room.
New York: Raven Press

PAYNE JP, INGRAM GS
1979
Anaesthetics and the EEG.
Anaesthesia Rounds, Number 13, England: Ayerst Pharmacological Products

PFURTSCHELLER G, COOPER R
1975
Selective averaging of the intracerebral click evoked response in man: an improved method of measuring latencies and amplitudes.
Electroencephalography and Clinical Neurophysiology, 38: 187-190

PFURTSCHELLER G, SCHWARZ G, SCHROETTNER O, et al.
1987
Continuous and simultaneous monitoring of EEG spectra and brainstem auditory and somatosensory evoked potentials in the intensive care unit and the operating room.
Journal of Clinical Neurophysiology, 4(4): 389-396

RAMPIL IJ, LASTER MJ
1992
No correlation between quantitative electroencephalographic measurements and movement response to noxious stimuli during isoflurane anesthesia in rats.
Anesthesiology, 77(5): 920-925

SEBEL PS, FLYNN PJ, INGRAM DA
1984
Effect of nitrous oxide on visual, auditory and somatosensory evoked potentials.
British Journal of Anaesthesia, 56: 1403-1407

SEBEL PS, HENEGHAN CP, INGRAM DA
1985
Evoked responses - a neurophysiological indicator of depth of anaesthesia (editorial).
British Journal of Anaesthesia, 57(9): 841-842

SEBEL PS, INGRAM DA, FLYNN PJ, RUTHERFOORD CF, ROGERS H
1986
Evoked potentials during isoflurane anaesthesia.
British Journal of Anaesthesia, 58: 580-585

SEBEL PS, GLASS P, NEVILLE WK
1988a
Do evoked potentials measure depth of anaesthesia?
International Journal of Clinical Monitoring and Computing, 5: 163-166

SEBEL PS, WITHINGTON PS, RUTHERFOORD CF, MARKHAM K
1988b
The effect of tracheal intubation and surgical stimulation on median nerve somatosensory evoked potentials during anaesthesia.
Anaesthesia, 43: 857-860

SGRO JA, EMERSON RG
1985
Phase synchronised triggering: a method for coherent noise elimination in evoked potential recording.
Electroencephalography and Clinical Neurophysiology, 60: 464-468

SGRO JA, EMERSON RG, STANTON PC
1990
Advanced techniques of evoked potential acquisition and processing.
pp 609-629 In: Evoked Potentials in Clinical Medicine 2nd ed, Chiappa KH (ed), New York: Raven Press

SILBERT BS, KOUMOUNDOROS E, DAVIES MJ, CRONIN KD
1989
The use of aperiodic analysis of the EEG during carotid artery surgery.
Anaesthesia and Intensive Care, 17(1): 16-23

SNYDER EJ
1990
The electroencephalogram.
Biomedical Instrumentation and Technology, July/August, pp 296-298

STEARNS SD, DAVID RA
1988
Signal processing algorithms.
New Jersey: Prentice-Hall

STRACKEE J, PEPER A
1992
Effects of mains interference on time coherent averaging.
Medical and Biological Engineering and Computing, 30: 491-494

THAKOR NV
1987
Adaptive filtering of evoked potentials.
IEEE Transactions on Biomedical Engineering, BME-43(1): 6-12

THAKOR NV, VAZ CA, McPHERSON RW, HANLEY DF
1991
Adaptive Fourier series modelling of time-varying evoked potentials: study of human somatosensory evoked response to etomidate anesthetic.
Electroencephalography and Clinical Neurophysiology, 80: 108-118

THAKOR NV, XING-RONG G, VAZ CA, et al.
1993
Orthonormal (Fourier and Walsh) models of time-varying evoked potentials in neurological injury.
IEEE Transactions on Biomedical Engineering, 40(3): 213-221

THOMSEN CE, ROSENFALCK A, NØRREGAARD CHRISTENSEN K
1991
Assessment of anaesthetic depth by clustering analysis and autoregressive modelling of electroencephalograms.
Computer Methods and Programs in Biomedicine, 34: 125-138

THORNTON C, KONIECZKO K, JONES JG, JORDAN C, DORÉ CJ, HENEGHAN CPH
1988
Effect of surgical stimulation on the auditory evoked response.
British Journal of Anaesthesia, 60: 372-378

VANDAM LD
1985
The senses as monitors.
pp 5 - 27 In: Monitoring in Anesthesia and Critical Care Medicine, Blitt CD (ed), New York: Churchill Livingstone

VAZ VA, THAKOR NV
1989
Adaptive Fourier estimation of time-varying evoked potentials.
IEEE Transactions on Biomedical Engineering, 36(4): 448-455

WARK KJ, SEBEL PS, VERGHESE C, MAYNARD DE, EVANS SJW
1986
The effect of halothane on cerebral electrical activity - an assessment using the cerebral function analysing monitor.
Anaesthesia, 41: 390-394

WIDROW B, STEARNS SD
1985
Adaptive signal processing.
New Jersey: Prentice-Hall

YU K, McGILLEM CD
1983
Optimum filters for estimating evoked potential waveforms.
IEEE Transactions on Biomedical Engineering, BME-30(11): 730-737

SELECTED BIBLIOGRAPHY

Important classical papers include the following:

PRONK et al.
1975
The use of the EEG for patient monitoring during open heart surgery.
Proc. Comp. Cardiology, Rotterdam, 77-81

WALTER DO
1968
A posteriori "Wiener Filtering" of averaged EPs.
EEG Clin. Neurophysiol. Suppl. 27: 61-70

WOODY CD
1967
Characterisation of an adaptive filter for the analysis of variable latency neuroelectric signals.
Med. Biol. Engng. 5: 539-553

APPENDICES

APPENDIX A

CLINICAL SIGNS AS INDICATORS OF DOA

With the advent of the use of ether, it became useful to delineate "stages" in the continuum of anaesthetic administration from the awake state to respiratory paralysis, cardiovascular collapse, and in worst cases, death. In 1847, John Snow was the first to describe five empirical stages through which a patient anaesthetised with ether progresses from consciousness to respiratory paralysis.

In 1920, Arthur Geudel published codified stages and signs of anaesthesia. Geudel predicated his stages on clear physical signs involving somatic muscle tone, respiratory pattern, and ocular signs. He enumerated four stages: stage of analgesia, stage of delirium, surgical stage (subdivided into four planes), and stage of respiratory paralysis. Others have added another stage, anaesthetic overdose; characterised by extreme anoxia, convulsions, and imminent death *(Grantham and Hameroff, 1985)*.

Both general and regional anaesthesia are neurologic phenomena, yet quantitative evaluation of the state of anaesthesia has been slow to evolve. Although pertaining mainly to ether anaesthesia, the signs and stages of anaesthesia still offer a reasonable guide to depth and to prediction of recovery *(Vandam, 1985)*.

Assessment of anaesthetic depth has traditionally always relied on the monitoring of physical signs. At present anaesthetists still rely on these physical signs to determine whether a patient is adequately anaesthetised *(Grantham and Hameroff, 1985)*.

When increasing amounts of anaesthetics are administered, the DOA steadily increases. This is carefully followed by observing a number of reflexes, which weaken and disappear at different depths of anaesthesia *(Jacobson and Webster, 1977)*.

The typical observed levels of anaesthesia are shown in Figure A-1.

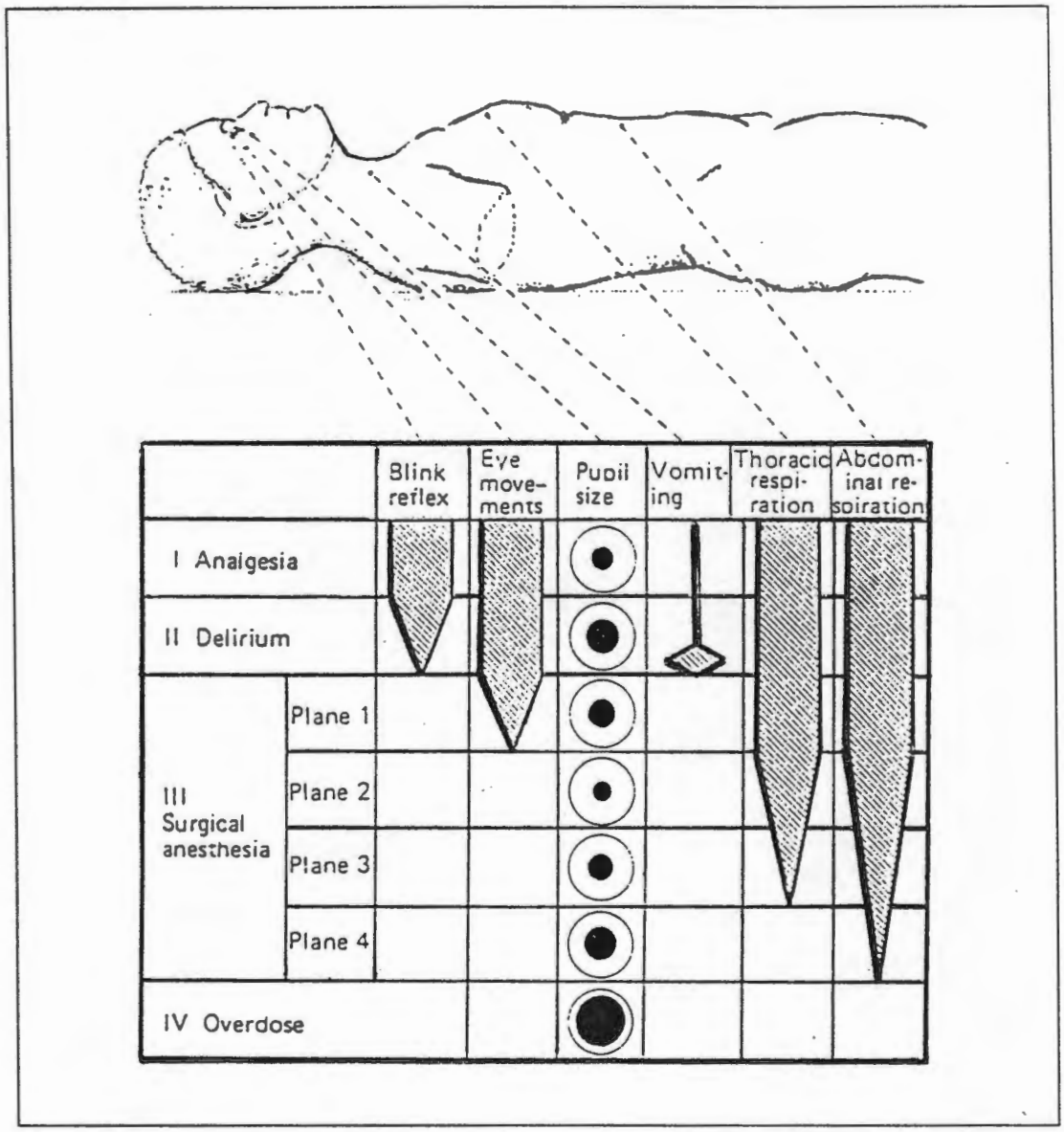

Figure A-1: The stages of anaesthesia by observing whether certain natural reflexes are abolished. The stages indicated here are typical of anaesthesia induced with diethyl ether. (Reproduced from *Jacobson and Webster, 1977*).

A description of these stages is as follows:

Analgesia stage: Consciousness is retained, but there is an alleviation of pain (which is analgesia). The respiration is unchanged and the reflexes are slightly hyperactive.

Delirium stage: Loss of consciousness begins, but at the same time a number of motor reflexes are elicited so that involuntary muscular movements and jerking movements

appear. The pupils are relatively wide. No operations are performed in the delirium stage.

Stage of surgical anaesthesia: As the DOA gradually increases, the reflexes weaken and are abolished and the eye movements cease. The pupils first diminish in size and then, at a greater DOA, they widen again. Respiration involves first both the chest and abdomen - thoracic and abdominal respiration - in very deep anaesthesia only abdominal respiration is present. In this third stage of anaesthesia, four planes are distinguished. The four planes represent different depths of anaesthesia. On each occasion that anaesthesia is induced, a suitable plane is chosen according to the type of surgical operation. An attempt is made to keep the DOA as shallow as possible.

Overdose stage: If the dose of anaesthetic is excessive, total respiratory paralysis results and all vital reflex mechanisms that are important for maintaining life are depressed. Unless resuscitation is performed with controlled (artificial) ventilation, death follows from asphyxia (suffocation and circulatory collapse).

When emerging from the anaesthetised state, the patient passes through all the stages in the reverse order. The patient is carefully watched until reflexes are normal and consciousness returns *(Jacobson and Webster, 1977; Grantham and Hameroff, 1985)*.

With modifications, this description remained useful until the advent of neuromuscular blockers. Although these stages are still used today, they are less applicable to current anaesthetic practice with its many pharmacological adjuncts. However, this description is still historically and conceptually important *(Grantham and Hameroff, 1985)*.

APPENDIX B

DEFINITION AND ORIGIN OF THE EEG

The EEG is a record representing the potential differences derived from scalp electrodes after suitable amplification, filtration and processing of the spontaneously occurring electrical potentials generated in the underlying cortex of the brain *(Payne and Ingram, 1979)*. It is thought that potentials recorded from the scalp of healthy people and representing this "so-called" background activity are largely attributed to postsynaptic potentials of the cell body and large dendrites of vertically orientated pyramidal cells in cortical layers three and five of the cerebral cortex. The EEG is not derived from summated neuronal action potentials (depolarisation and depolarisation of individual axons), but from graded dendritic potentials. The columnar structure of the cerebral cortex facilitates a large degree of summation rather than mutual cancellation. The signals are attenuated by the intervening tissue layers of the dura, skull, and scalp, as well as by the fact that they are spatially smeared over a larger area than the cortical signal. It is thought that the standard waking EEG is a combination of the activity of a number of small cortical zones and that its amplitude reflects the degree of synchronisation of the underlying cortical activity *(Bronzino, 1984; Gevins and Aminoff, 1988)*.

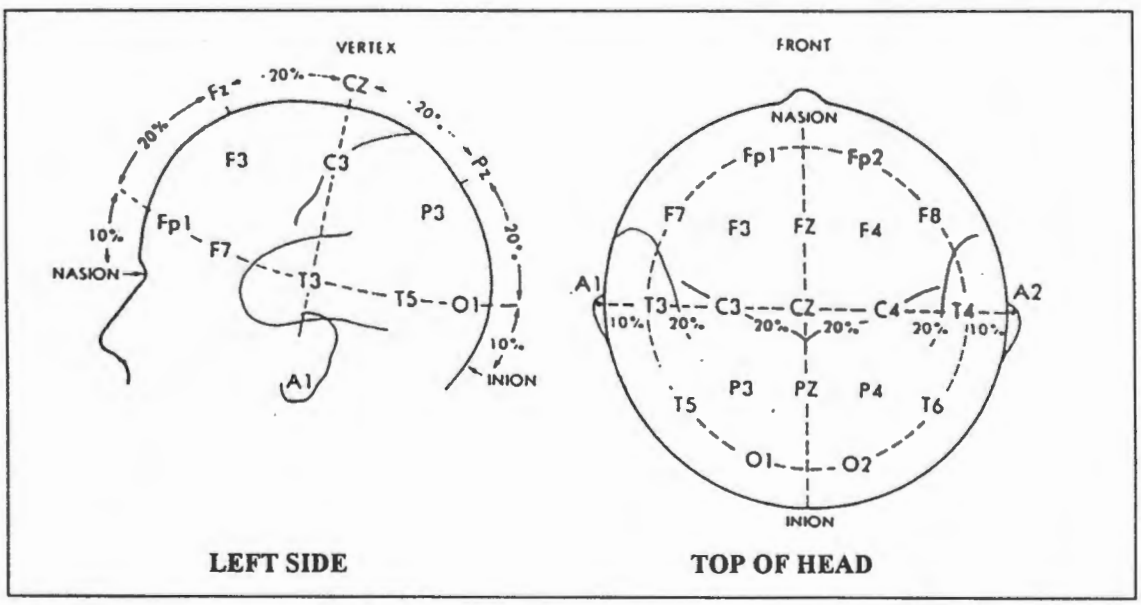

Figure B-1: Diagrammatic representation of the International 10-20 system for electrode placement on the scalp. (Reproduced from *Gevins and Aminoff, 1988*)..

To systematically record the EEG from different regions of the scalp, bio-potential electrodes are placed in predetermined patterns called montages. The electrodes are normally placed in accordance with the International 10-20 system (see Figure B-1) as proposed by Jasper *([Jasper, 1958] cited by Gevins and Aminoff , 1988).*

The rhythmic activity of the brain is generally characterised by its frequency. The harmonic composition of the EEG is usually complex and only occasionally approaches sinusoidal form. In a normal, awake adult, the scalp-recorded EEG amplitude ranges from a few microvolt to about 75 microvolt. It has a frequency spectrum of 0.5 Hz to 70 Hz. The frequency spectrum has been arbitrarily divided into four bands: delta (0.5 - 3 Hz); theta (4 - 7 Hz); alpha (8 - 13 Hz); and beta (above 13 Hz) *(Gevins and Aminoff, 1988).* Activity in each of these bands generally occurs under known certain conditions and in various areas of the cortex as depicted in Figure B-2 *(Snyder, 1990).*

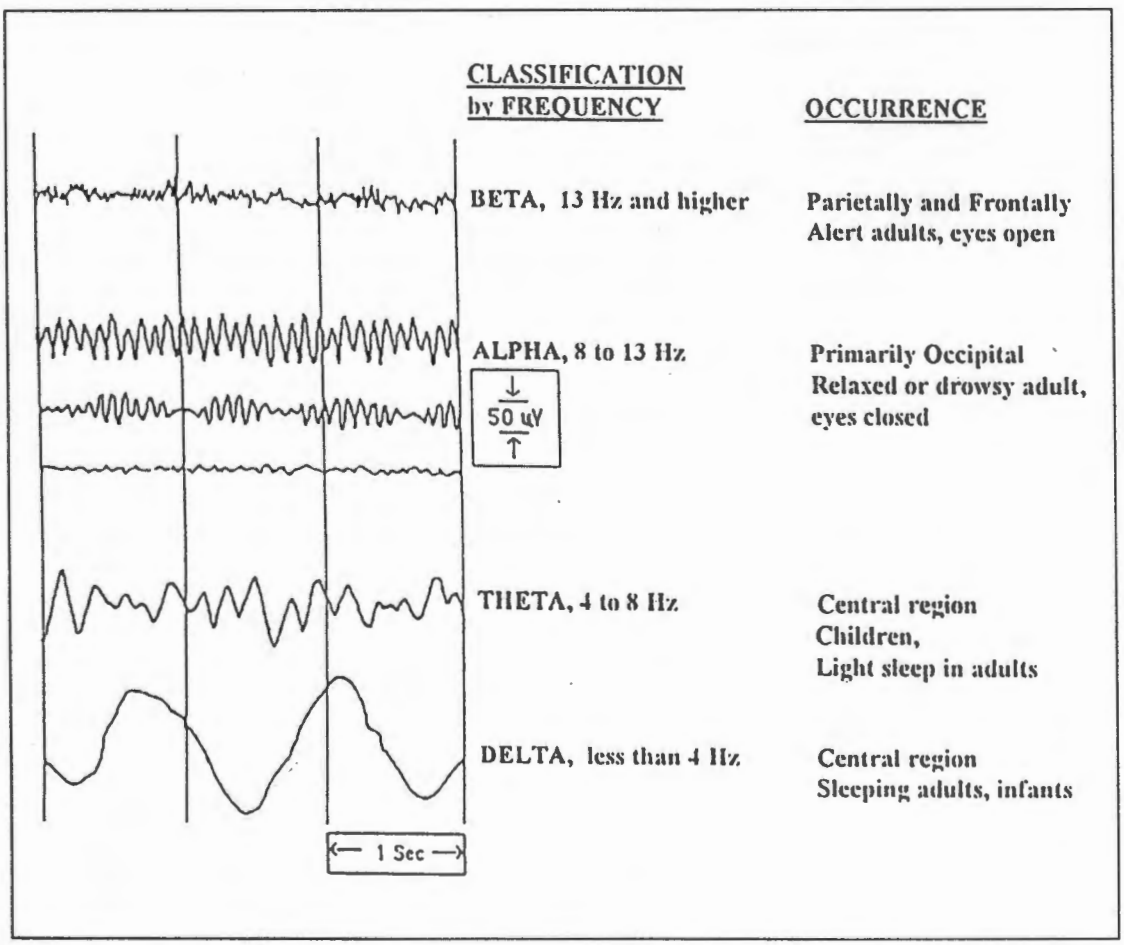

Figure B-2: Time domain EEG activity of different frequency bands of EEG. (Reproduced from *Snyder, 1990*).

APPENDIX C

DEFINITION AND ORIGIN OF EVOKED POTENTIALS

Richard Caton reported his observations concerning brain waves recorded from the exposed surface of the brain of rabbits and monkeys in 1875. He was also the first to distinguish the two forms of brain electrical activity: the first being the spontaneous or "background" EEG, and the second now known as the evoked potential or evoked response potential *(Childers, 1988)*.

The EEG represents spontaneous electrical potentials generated by the cerebral cortex. These potentials occur during all of the many varied behavioural states possible in humans. However, the nervous system can also give rise to specific electrical potentials evoked by discrete stimuli *(Nuwer, 1986)*.

EP's are usually defined in the time domain as the electrical activity that is triggered by the occurrence of particular events or stimuli. Most EP's cannot be seen in routine EEG recordings. This is because of their low amplitudes (0.1 - 20 microvolts) and their combining with normal background EEG activity and various artefacts that together are from twenty to several hundred microvolts in amplitude. The basic problem of analysis is thus detecting EP activity within this often much larger background activity. *(Chiappa, 1990; Lopes da Silva, 1993)*.

In 1951, Dawson attempted to solve this problem using the photographic superposition of a number of time-locked responses. This method has the advantage of enhancing the response in contrast to the ongoing activity and, at the same time, providing an indication of response variability. It is however, difficult to quantify the results in this way. Since the introduction of the averaging technique (see Appendix D) and the development of digital computer techniques, EP's are obtained using special computerised algorithms and expressed as time-varying functions *(Lopes da Silva, 1993)*.

Evoked Potential Generation:

EP's can be generated by a number of different types of stimuli, and are usually defined in terms of the mode of sensory stimulation *(Grundy, 1985)*. This appendix considers only some of these modes. For example visual evoked potentials (VEP's) can be generated by flashes of light or by changes in a patterned visual stimulus, AEP's occur following presentations of brief clicks or tones, and SSEP's are usually generated by brief electrical stimuli applied to the median nerve or other peripheral nerves *(Nuwer, 1986)*. A typical recording paradigm is illustrated in Figure C-1 which depicts the recording of a SSEP.

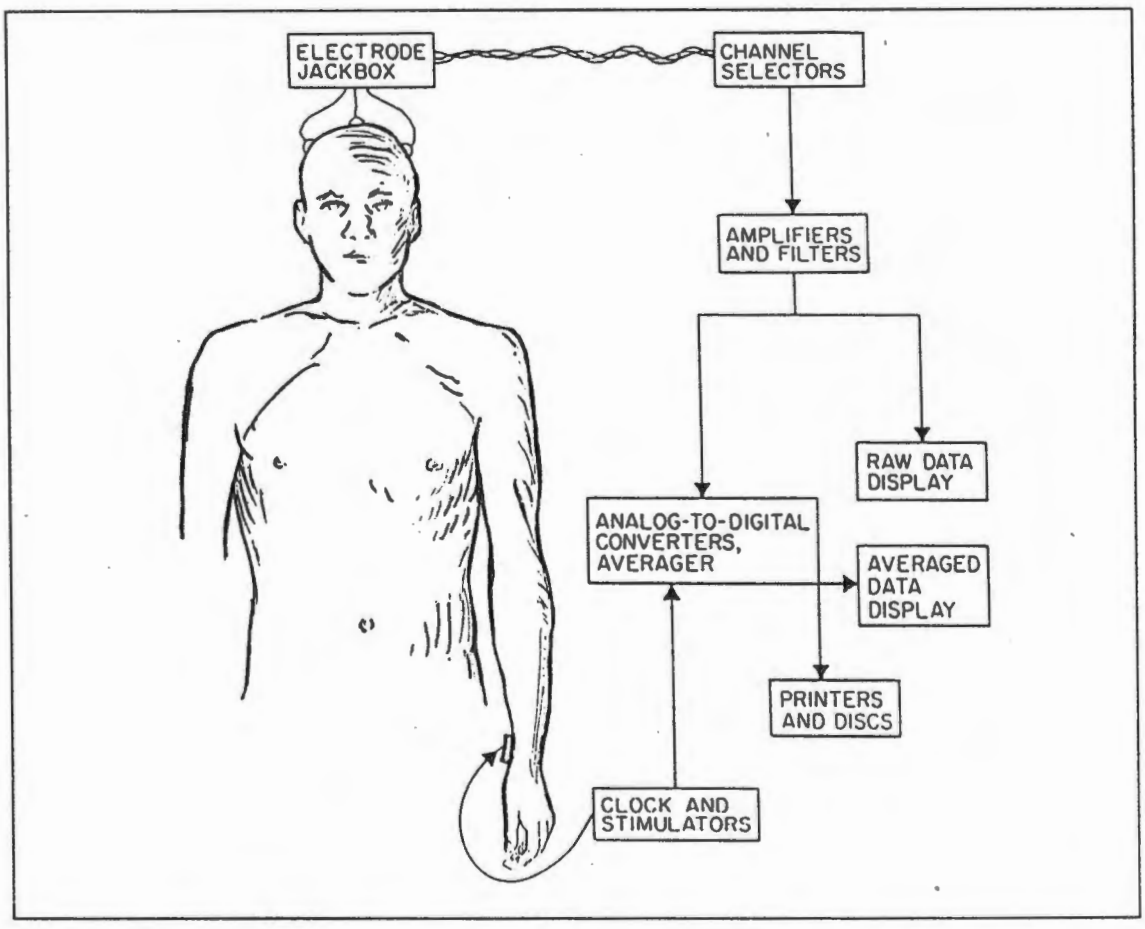

Figure C-1: Illustration of EP recording paradigm for the SSEP. (Reproduced from *Nuwer, 1986*).

The EP signal is often discussed in terms of its "components" or peaks and troughs. The EP's are individually characterised by the amplitudes and post-stimulus *latencies* of these components.

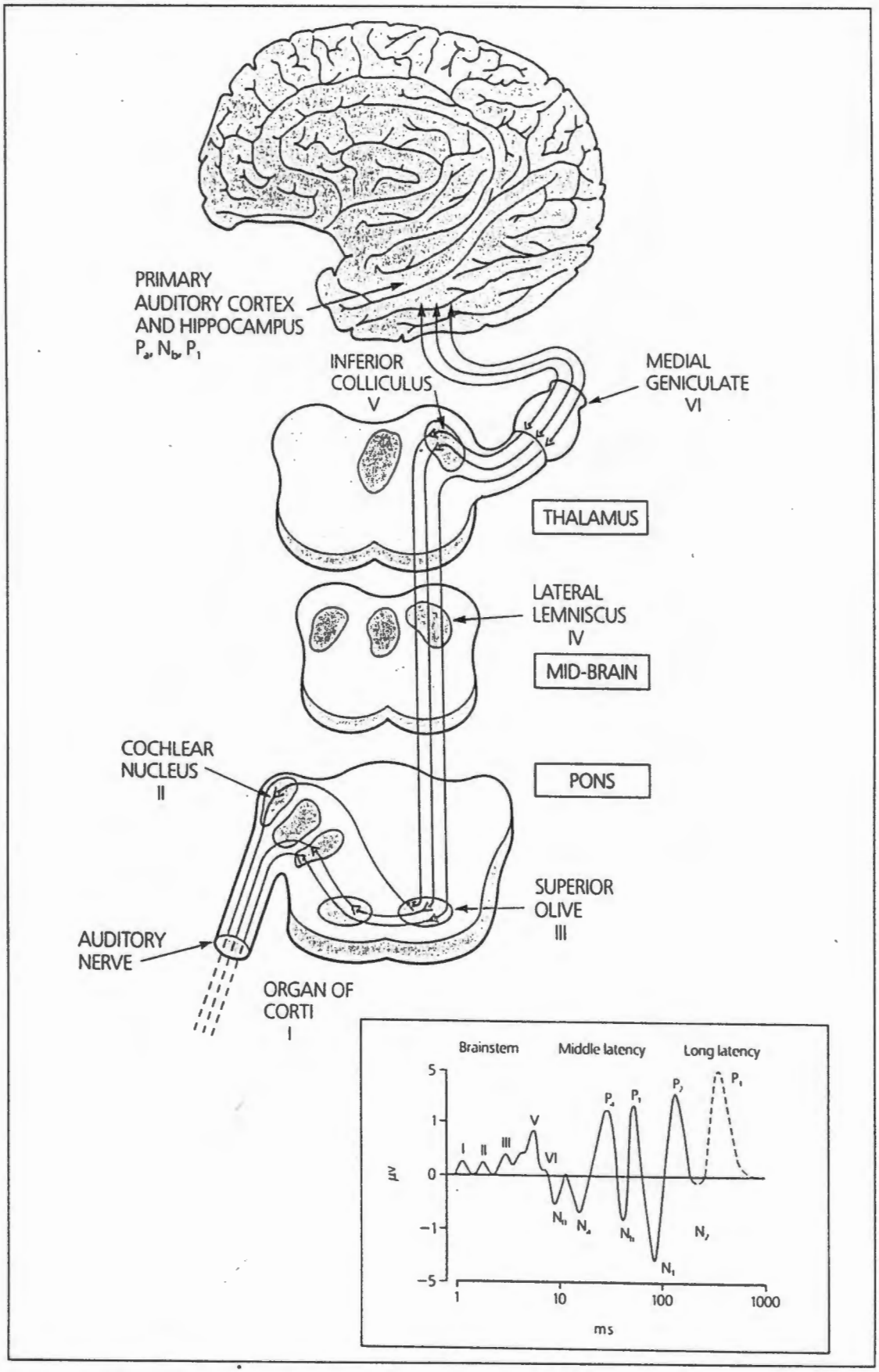

Figure C-2: The brain stem pathway of the auditory signal. Waves I-VI in the AEP are thought to arise in the relay stations shown. The middle latency waves arise in the primary auditory cortex and longer latency waves in other cortical association areas.(Reproduced from *Jones, 1988*).

Latencies:

The term latency most commonly refers to the time interval between the onset of the stimulus and a specific point on the EP waveform typically a peak (local maximum) or trough (local minimum). Latency is usually measured in milliseconds *(Grundy, 1985; Childers, 1988; Chiappa, 1990)*.

Latencies are loosely subdivided into short (less than 40 msecs), intermediate (40 to 120 msecs), and long (120 to 500 msecs). Clinically important characteristics are related to these poststimulus latencies *(Grundy, 1985)*.

Figure C-2 illustrates the relationship between various structures along the auditory sensory pathway and the corresponding peak or trough in the AEP signal.

Amplitudes:

Amplitudes are measured in microvolts: from peak to peak, from an average zero baseline prior to stimulus, from the zero point at the onset of the recording, or from a designated point in the waveform. Each method of amplitude referencing has advantages and disadvantages, and no general agreement exists at present as to the most appropriate method *(Grundy, 1985)*.

Peak Naming Conventions:

Peaks and troughs are named according to their polarity and temporal location (latency) following the stimulus presentation *([Picton and Stuss, 1980] cited by Childers, 1988)*.

Waveform nomenclature is most commonly derived from either of two methods as illustrated in Figure C-3: (1) the components are numbered in sequence by polarity, for example, Na, Nb, P1, P2, Pa, etc.; or (2) the components are labelled according to their polarity and mean latency in normal subjects, for example, P100, N20 *(Chiappa, 1990)*. Thus, P45 would be the label for a positive component at 45 msecs following the stimulus onset time. The temporal location of these components is liberally interpreted by investigators; for example, P45 may occur from about 40 to 50 msecs

(Childers, 1988). Most publications use the convention of signal positivity displayed upward; however, in some publications waveforms are plotted using the opposite convention *(Childers, 1988).*

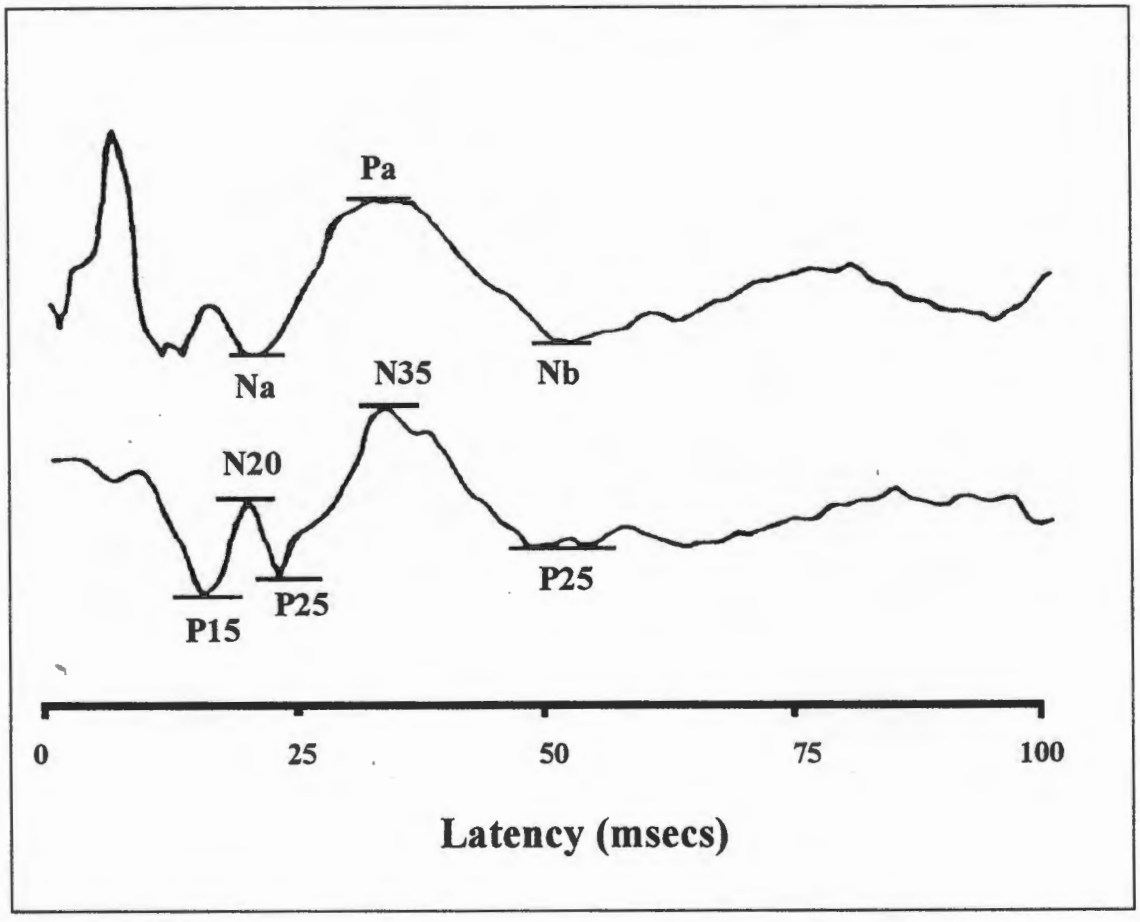

Figure C-3: Two forms of nomenclature used to name peaks and troughs of EP signals. An AEP is shown on the top with a SSEP below.

Other Considerations:

Characterisation of EP waveforms depends upon other qualitative and quantitative methods. First the overall configuration and reproducibility of waveforms, as shown by superimposition of replicated records, are examined. Then measurements are made of the poststimulus latencies and amplitudes of individual peaks and troughs. The human brain recognises patterns more accurately than any computer programs so far devised, and peaks must be identified by a trained observer before definitive measurements are taken. Thus we see the absolute need for qualitative characterisation of EP waveforms.

Once the points of interest in the waveform are identified using qualitative techniques, quantitative methods are used to describe the waveform more precisely.

Secondary measurements may be derived from the absolute values of amplitudes and poststimulus latencies. Inter-peak or inter-trough latencies and ratios between the amplitudes of different peaks are clinically useful. One of these secondary measurements is central conduction time. This is calculated by subtracting the latencies of early subcortical peaks from the latencies of later peaks that arise in the midbrain or cerebral cortex. Central conduction times are particularly useful for distinguishing those EP alterations due to brain dysfunction from EP changes related to failure of sensory input, abnormalities of sensory receptors, or normal differences among subjects such as difference in height that affect absolute latencies of SSEP's *(Grundy, 1985).*

Short-latency EP's arise closer to the site of the sensory stimulation than do potentials of intermediate and long latency. Relatively few synapses have been crossed in the transmission of these impulses, and the effects of anaesthetic agents and other drugs on these potentials are minimal. When recorded from scalp electrodes, short-latency EP's are of lower amplitude than the spontaneous EEG. Sensory EP's of intermediate poststimulus latency arise in the cerebral cortex. These potentials are considered to be fairly well localised to specific sensory areas of the cortex. They are altered by anaesthetic agents and other drugs as well as by physiological influences such as hyperventilation. Sensory EP's of long poststimulus latency are thought to arise in the association areas of the cerebral cortex. They are generally abolished by general anaesthesia and are markedly affected by factors such as attention, expectancy, drowsiness and emotional state *(Grundy, 1985).*

EP Extraction:

EP responses are generally elicited by stimulating one or other sensory pathway. This response when recorded with scalp electrodes is not discernible as an EP signal since it is swamped by ongoing electrical activity of the cerebral cortex. The most common way of extracting the EP signal from the surrounding electrical activity is to repeatedly

send a large number of stimuli in succession. After each stimulus is sent, a fixed time period of the signal is recorded or captured as illustrated by the dashed boxes in Figure C-4. These fixed periods are called trials or sweeps (herein referred to as *trials*) and are all of equal length and time-locked to their respective stimuli. The start of the recorded trial always occurs with exactly the same delay after each stimulus. In this example trials 1,2 and 3 all commence when the stimuli occur and are all of equal

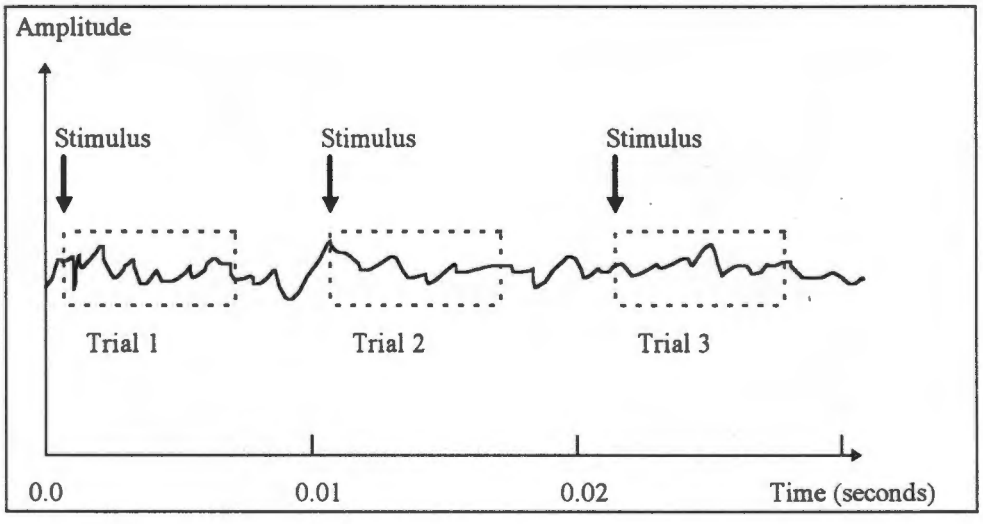

Figure C-4: Extraction of EP's using repeated stimuli.

temporal length. The EP signal is extracted by processing the trials in succession.

APPENDIX D

SYNCHRONOUS TIME AVERAGING

Synchronous time averaging of EP signals begins with two basic assumptions: that

1. the electrical response evoked from the brain is invariably fixed relative to the stimulus and
2. the ongoing EEG activity is a zero mean random process, statistically independent of the evoked responses.

In this way, the EP can be considered a signal s(k) corrupted by additive noise n(k), the ongoing EEG activity, assuming that the signals are sampled with k as the discrete time variable. EP detection then reduces to the task of improving the SNR. Usually one assumes a *simple additive model* (random variables are underlined). The observed and recorded random signal $\underline{x}(k)$ is given as a sum of two terms:

$$\underline{x}(k) = s(k) + \underline{n}(k)$$

The expected value of $\underline{n}(k)$ is zero. The average of $\underline{x}(k)$ over N realisations (trials) is then defined as:

$$\bar{\underline{x}}(k) = \frac{1}{N}\sum_{i=1}^{N}\underline{x}_i(k)$$

The expected value of the average is given as:

$$E[\bar{\underline{x}}(k)] = E\left[\frac{1}{N}\sum_{i=1}^{N}\underline{x}_i(k)\right] = s(k)$$

since $E[(\underline{n}(k)] = 0$, the variance of $\bar{\underline{x}}(k)$ is as follows:

$$\mathrm{var}[\bar{\underline{x}}(k)] = E\left[\left(\frac{1}{N}\sum_{i=1}^{N}\underline{n}_i(k)\right)^2\right] = \frac{1}{N}\mathrm{var}[\underline{n}(k)]$$

since s(k) is assumed to be invariant. Therefore the SNR in terms of amplitude improves proportionally to $\sqrt{N}$. In more general terms, however, it should be assumed that the signal s(k) is a random signal, so that the first expression should be reformulated as follows:

$$\underline{x}(k) = \underline{s}(k) + \underline{n}(k)$$

The importance of this apparently small difference lies in the fact that the model given by the above expression implies that the EP is not fully described by the mean value of $\underline{x}(k)$, but also by higher statistical moments, as for instance the variance. In most practical cases, the latter model gives a better account of reality. The former model is valid only for anaesthetised preparations and possibly for the short latency components of the EP that mainly reflect sensory processes; this is, however, not the case for long latency components.

If the responses are statistically independent, then the improvement in SNR is independent of the SNR of the observation x(k). For EP's, the responses can be assumed to be statistically independent if the number of stimuli, N, is such that the influence of learning and fatigue can be neglected ($N \leq N_{max}$). If the responses are samples of the same random process (totally dependent responses), the improvement in SNR depends on the SNR of the observation. The improvement in SNR is always greater than 1. For very noisy observations, the improvement approaches N *(Cohen, 1986; Lopes da Silva, 1993)*.

APPENDIX E

ADAPTIVE ALGORITHMS AND THE LMS ALGORITHM

Adaptive signal processing methods are concerned with time-varying digital systems. The general system is illustrated in Figure E-1, where $H_k(z)$ denotes a time-varying transfer function.

The characteristics of the transfer function $H_k(z)$ change, or adapt, according to signal conditions. An adaptive algorithm is the equation or set of equations used to adjust the

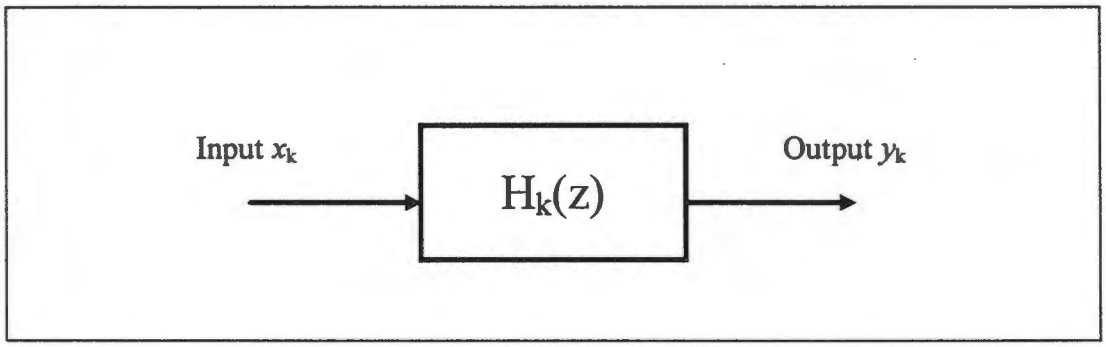

Figure E-1: Block diagram of time-varying digital system.

coefficients of $H_k(z)$. To characterise the digital system in Figure E-1 completely, it would be necessary to analyse its response each time the coefficients are changed. Since we are dealing with algorithms that update the coefficients during every sample interval, a complete characterisation in the conventional sense is impractical.

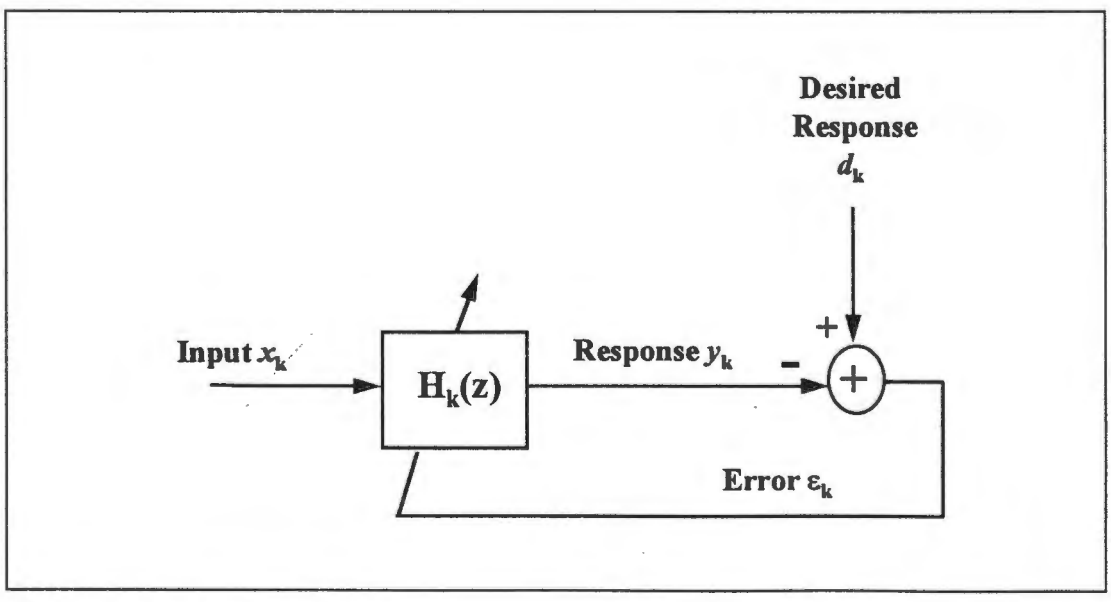

Figure E-2: Elements of the basic adaptive system.

The basic elements of an adaptive system are illustrated in Figure E-2. There is the usual input and output sequences $[x_k]$ and $[y_k]$, but the transfer function describing their relationship is now the time-varying $H_k(z)$. A desired response sequence $[d_k]$ and an error sequence $[\varepsilon_k]$, which is the difference between the desired response ($\varepsilon_k = d_k - y_k$) is also defined. The arrow through the $H_k(z)$ box indicates that the error sequence is used to control the adaptation of $H_k(z)$. The term desired response is a misnomer in some respects, but it is used in order to maintain compatibility with the literature. Realistically, if we had access to the true desired response, we would not in general need an adaptive system. In fact, the definition of this desired response is application-dependent and is often the most difficult part of adaptive system specification. The error sequence $[\varepsilon_k]$ is used to control the adaptive process. In particular, our goal is to adapt toward the minimum mean square error (MMSE) solution, that is, adjusting the coefficients of $H_k(z)$ in order to minimise the mean or expected value of ε_k^2, $E[\varepsilon_k^2]$.

The Least Mean Square (LMS) Algorithm

The LMS algorithm is the simplest and perhaps the most universally applicable adaptive algorithm in use today. For the LMS algorithm, the $H_k(z)$ transfer function in Figure E-1 and Figure E-2 is a time varying FIR filter. The corresponding input-output relationship is described by

$$y_k = \sum_{n=0}^{L} b_n(k)\, x_{k-n} \qquad (1)$$

where the time-varying character of the filter coefficients is signified by the $b_n(k)$ notation. In other notations $b_n(k)$ is referred to as w_{nk}. When the adaptive filter is realised in the direct form structure, the mean squared error (MSE) performance surface is a quadratic function of the filter coefficients and thus has a single minimum. This is illustrated for the simple one-coefficient case ($L = 0$) in Figure E-3, where $b_0(0)$ denotes the initial condition and b_0^* corresponds to the optimal (or MMSE) solution. In the general case, which is somewhat more difficult to envisage, the surface would be a parabolic function in $(L + 2)$-dimensional space.

The goal of the adaptive process is thus to adjust the filter coefficients in such a way that they move from the initial condition, $b_0(0)$, towards the MMSE solution, b_0^*. The fixed

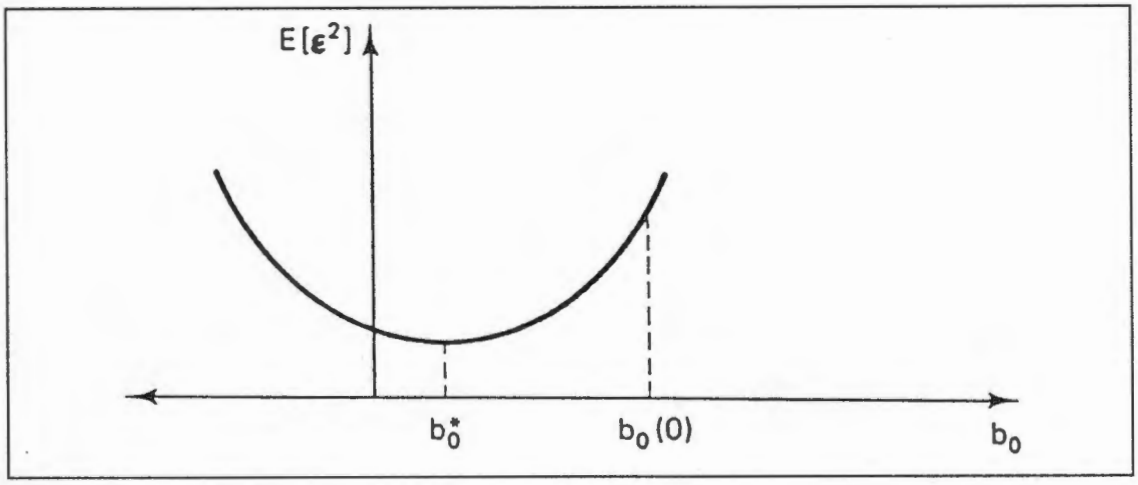

Figure E-3: MSE performance surface for one-coefficient filter.

performance surface just described is rarely dealt with in practical applications. In non-stationary environments, the MMSE solution varies as signal conditions change. Thus, the adaptive process must continually adjust the coefficients in order to track the MMSE solution.

The technique utilised by the LMS algorithm to update filter coefficients is based on the method of steepest descent. This can be described in algorithmic form using vector notation, as follows:

$$\mathbf{B}_{k+1} = \mathbf{B}_k - \mu\nabla_k \qquad (2)$$

where

Coefficient vector: $\mathbf{B}_k = [b_0(k) \ldots b_L(k)]^T$

Gradient vector: $$\nabla_k = \frac{\partial E[\varepsilon_k^2]}{\partial \mathbf{B}_k} = \left[\frac{\partial E[\varepsilon_k^2]}{\partial b_0(k)} \cdots \frac{\partial E[\varepsilon_k^2]}{\partial b_L(k)}\right]^T$$

and μ is a parameter that controls the rate of convergence. Equation 2 shows that the coefficient updates are proportional to the negative gradient ($-\nabla_k$) of the performance surface. Thus when ∇_k is known at each step of the adaptive process, the adjustment

always results in a better filter, that is, the MSE decreases from step k to step k + 1. In addition, once the MMSE solution is found, the gradient reaches zero so the coefficients remain at their optimal values.

In practice, the algorithm as stated in Equation 2 is difficult to implement due to inexact knowledge of the performance surface gradient ∇_k. Various techniques are available for estimating ∇_k. The approach taken in the LMS algorithm is to use a gradient estimate based on the instantaneous square error,

$$\tilde{\nabla}_k = \frac{\partial \varepsilon_k^2}{\partial \mathbf{B}_k} = 2\varepsilon_k \frac{\partial (d_k - y_k)}{\partial \mathbf{B}_k} \qquad (3)$$

where ε_k , d_k, and y_k are as defined in Figure E-2. Since the desired response d_k is independent of the filter coefficients, and the output y_k can be expressed in terms of the filtered input as in Equation 1, Equation 3 can be written as

$$\tilde{\nabla}_k = -2\varepsilon_k \mathbf{X}_k \qquad (4)$$

where $\mathbf{X}_k$ is a vector of input signal values

$$\mathbf{X}_k = [x_k \; x_{k-1} \cdots x_{k-L}]^T$$

Combining Equation 2 and 4, the LMS algorithm is written as follows:

$$\mathbf{B}_{k+1} = \mathbf{B}_k + 2\mu \varepsilon_k \mathbf{X}_k \qquad (5)$$

where μ is the **convergence factor**, ε_k is the error signal from Figure E-2, and $\mathbf{X}_k$ is the input signal vector just defined.

From Equation 5 it is shown that given an input signal x_k and a desired signal d_k, the implementation of the LMS adaptive algorithm requires only the selection of the convergence factor μ. This convergence factor plays an important role in determining the performance of an adaptive system. Recall that the gradient estimate used in the LMS update is based upon the instantaneous error value ε_k^2 rather than the mean value $E[\varepsilon_k^2]$. Although this form of update moves the coefficients toward the MMSE solution, it is apparent that a single update of the **B**-vector could contain a considerable error. Thus a large μ could result in an adaptive process that never

converges to the MMSE solution. Conversely, if μ is too small, the coefficient vector adaptation is very slow and the system may not react rapidly enough to cope with changing signal statistics. To avoid either of these conditions, μ must be neither "too large" or "too small."

The convergence factor (μ) is the gain constant that regulates the speed and stability of adaptation. Since coefficient changes at each iteration are based on imperfect gradient estimates, we would expect the adaptive process to be noisy; that is, it would not follow the true line of steepest descent on the performance surface. No universal solution for picking the best value of μ exists but it has been shown that the stable range of μ is always $0 < \mu < 1$ *(Widrow and Stearns, 1985; Cohen, 1986; Stearns and David, 1988)*.

APPENDIX F

ADAPTIVE IMPULSE CORRELATED FILTER

This filter uses two inputs: the signal d_k (primary input) and an impulse correlated with the deterministic component x_k (reference input) (see Figure F-1). The LMS algorithm is used to adjust the weights of the adaptive filter (see Appendix E).

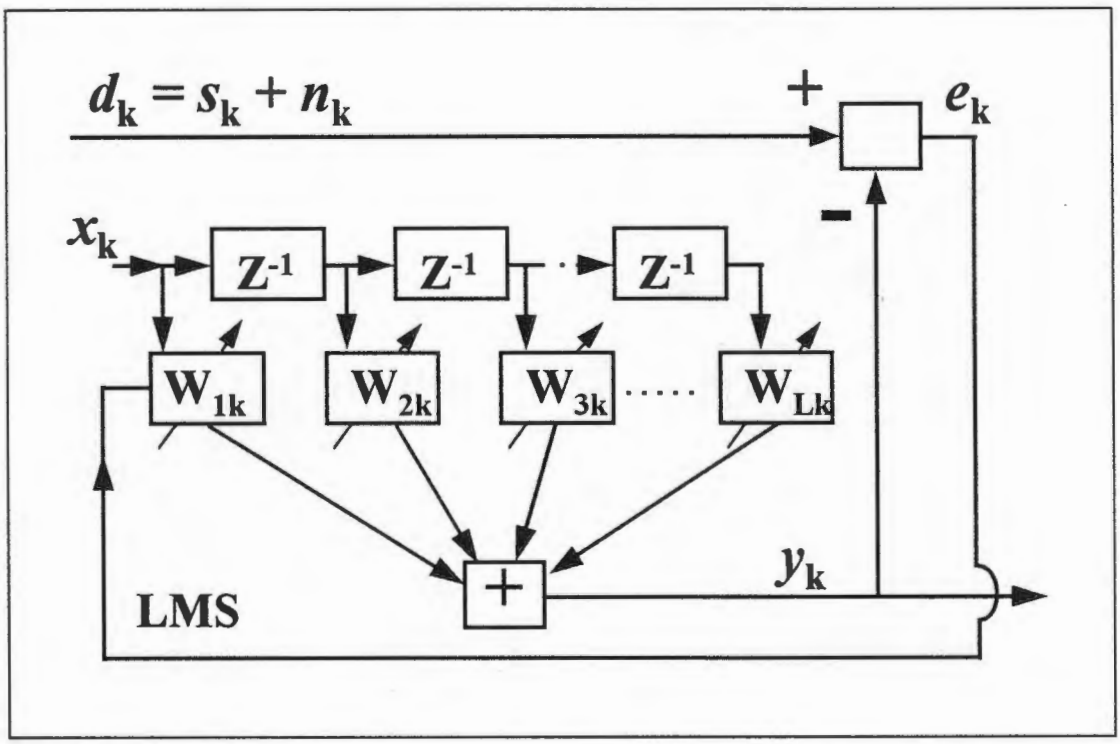

Figure F-1: Block diagram of the adaptive impulse correlated filter. It estimates the deterministic component s_k of a signal d_k, using a nonrecursive adaptive filter. x_k is the impulse correlated with the deterministic signal s_k, n_k is noise uncorrelated with s_k, and y_k is the filter output. (Reproduced from *Laguna et al., 1992*).

The primary input is the consecutive linking of the number of recurrences of the event-related signal to be filtered. The reference input of the adaptive filter is a unit impulse sequence synchronised with the beginning of each recurrence of the primary input. For EP's, the stimulus for the reference signal can easily be derived from the external stimulus of the EP. The additive noise is not correlated with the required signal or the stimulus that generates the EP. The additive noise is thus cancelled. The AICF filter thus estimates the component of the primary input which is event-related to the

stimulus; that is, the EP signal which is of interest. The AICF filter reaches a steady-state improvement of the SNR which depends on the convergence factor of the LMS algorithm *(Laguna et al., 1992)*.

APPENDIX G

FOURIER SERIES MODEL

The noisy EP signal can be decomposed into its Fourier series components, viz. several sine and cosine waveforms (see Figure G-1). The objective of FSM signal estimation is to determine the magnitudes of these sine and cosine waveforms (harmonics) so that the desired signal is adequately reconstructed.

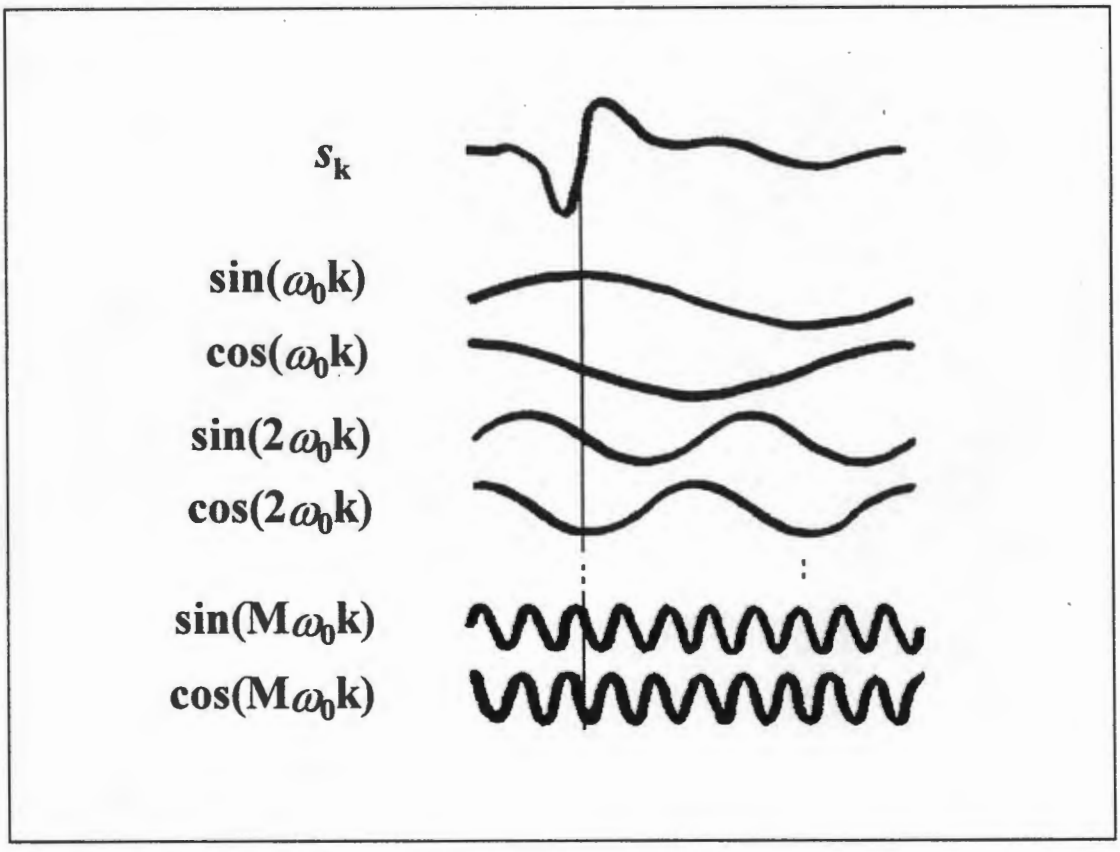

Figure G-1: An adaptive technique to construct the Fourier series model. The objective is to develop a weighted sum of all harmonics to estimate a sample from the EP (adapted from *Thakor et al., 1991*).

The signal to be modelled can be described by a series of weights (see Figure G-2). These weights are expressed mathematically as a vector $\underline{W}_k = [\, w_1, w_2, \ldots w_n \,]$ at time k. The inputs to these weights are the calculated samples from the Fourier series. Let

$\underline{X}_k$ define a vector of samples from the Fourier series (truncated accordingly) which is thus the reference vector. This reference vector can easily be precalculated. A discrete Fourier transform of the EP signal can be obtained during the control period to assess the number of weights or Fourier coefficients required to adequately represent the signal.

The model output is thus

$$\bar{d}_k = \underline{X}^T_k \underline{W}_k$$

The objective is to obtain a weight vector $\underline{W}_k$ that provides the best estimate of the desired EP signal d_k. This is accomplished by adjusting the model weights so that the

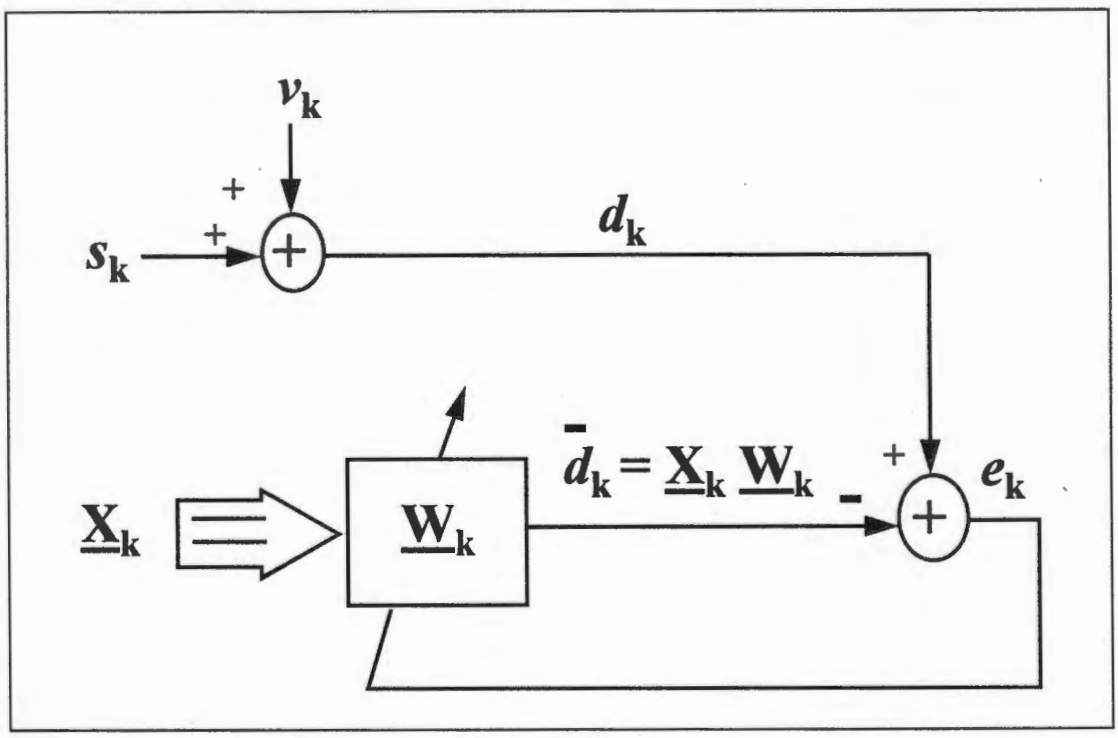

Figure G-2: Block diagram of the adaptive Fourier series modelling algorithm. s_k, actual signal at time k; v_k, noise; d_k, desired signal; $\bar{d}_k$, output of the model; $\underline{X}_k$, Fourier series input to model; e_k, error at time k (Reproduced from *Thakor et al., 1991*).

MSE between the desired EP signal and the model output $\bar{d}_k$ is minimised. Since noise is uncorrelated with both the signal and the filter output, the EP signal can be estimated from noisy (background EEG) EP trials.

In summary , the adaptive FSM appears to be quite suitable for monitoring transient and time-varying EP signals. The adaptive algorithm extracts the EP waveform from the background noise, and at the same time can respond to unpredictable transients. It takes advantage of both recurrence as well as spectral properties of the signal, and consequently provides an improved estimate of the time-varying nature of signal harmonics. The signal estimate is simultaneously available in both time and frequency domains. Either amplitudes and latencies or power in various harmonic bands may be used for diagnosis *(Vaz and Thakor, 1989; Thakor et al., 1991)*.

APPENDIX H

ANALYSIS OF VARIANCE

ANalysis Of VAriance (ANOVA) is a statistical methodology used in comparing means of populations. This appendix gives a very simplified description of ANOVA and how it relates to this study.

A very basic description of ANOVA is as follows:
To assess whether several populations (algorithms) all have the same mean or not, we compare the means of samples drawn from each population (algorithm). The question is whether any observed differences in sample means amongst the groups (algorithms) are just the result of chance variation. Normally we do not expect sample means to be equal even if the population (algorithm) means are all identical.

The purpose of ANOVA is to assess whether the observed differences among sample means are statistically significant or not. In other words, could any large variation in mean sample value between any of the groups (algorithms) be plausible due to chance, or is it good evidence for a difference among the population means. This cannot be determined from the sample mean $\bar{x}$ alone. Because the standard deviation of a sample mean $\bar{x}$ is the population standard deviation σ divided by $\sqrt{n}$ (n = total number of samples), the question of whether the variation is statistically significant depends upon both the variation within the groups of observation (algorithms) and the sizes of the samples. ANOVA uses what is called the F-test which is the ratio of the differences amongst groups (algorithms) and the variation within groups (algorithms):

$$F = \frac{Difference\_Amongst\_Groups}{Variation\_Within\_Groups}$$

A large F value implies that the differences amongst groups are greater than the overall variation within groups. Associated with the F statistic is the p-value which indicates whether the group means are significantly different or not. A small p-values indicates that the group means are significantly different. It however does not indicate which

group means differ. To establish which means differ significantly, we need to inspect plots of the results.

Some terminology associated with ANOVA in terms of this simulation study is described as follows:

factors - An independent variable is called a factor (e.g. algorithm, interference type, interference level);

multifactor study - There are two or more independent variables (e.g. EP signals, algorithm, interference type and interference level);

factor level - A factor level is a particular outcome of the independent variable (e.g. low, medium, high for interference level; AVE, AICF1, AICF2, AICF3, FSM1, FSM2, FSM3 for interference type);

treatments - In multifactor ANOVA studies a treatment is a particular combination of factor levels (e.g. FSM1 algorithm for stationary SSEP with low level 50-Hz interference).

This is a *multifactorial study* where the performance of 7 algorithms are evaluated for 2 specific EP signals each being of 2 types viz. stationary and non-stationary, each combined with 4 types of interference and each type of interference having 3 graded amplitude levels.

The system presented is also a *neat system* whereby changes in the factor levels are uniform and consistent across each of the algorithms being tested. Because of this as well as the large number of permutations being used, we only needed to perform one run of each *treatment*.

The ANOVA model assumes that the populations (algorithms) have a normal distribution and that standard deviations (variances) are all equal. This assumption was taken to be valid after a pre-trial study in which 5 sets of simulations had been repeated for 12 runs each to establish distribution and variance characteristics. ANOVA procedures however are not very sensitive to unequal standard deviations.

A multifactor study in which all combinations of factors are investigated is called a *complete factorial study*. A factorial study in which only a selected subset of all possible treatment combinations is investigated is called a *fractional factorial study*.

ANOVA is an extensive subject which is beyond the scope of this discussion and the reader should refer to Moore et al. *(1993)*, Neter et al. *(1993)* or any other appropriate text on statistics to get a more detailed description of ANOVA and its application.